Scuola Internazionale Superiore di Studi Avanzati – SISSA

Trieste, Italy

Gene expression profiling of prion-infected brains: a novel disease signature for neurodegeneration in non-human primates and in humans

Academic Year 2014/2015

CANDIDATE

Silvia Vanni

SUPERVISOR

Prof. Giuseppe Legname

CO-SUPERVISOR

Dr. Maura Barbisin

to Miranda and Giorgio,
who gave me so much more than life

"Each one of us here today will, at one time in our lives, look upon a loved one who is in need and ask the same question: we are willing to help, Lord, but what, if anything, is needed? For it is true […] it is those we live with and should know who elude us. But we can still love them – we can love completely, without complete understanding."

INDEX

LIST OF ABBREVIATIONS

TSE = transmissible spongiform encephalopathy

PrP^{C} = cellular prion protein

PrP^{Sc} = scrapie prion protein

PRNP = prion protein gene

BSE = bovine spongiform encephalopathy

CJD = Creutzfeldt-Jakob disease

vCJD = variant Creutzfeldt-Jakob disease

sCJD = sporadic Creutzfeldt-Jakob disease

iCJD = iatrogenic Creutzfeldt-Jakob disease

fCJD = familial Creutzfeldt-Jakob disease

AD = Alzheimer's disease

PD = Parkinson's disease

CBD = corticobasal degeneration

RIN = RNA integrity number

RT-qPCR = quantitative reverse transcription polymerase chain reaction

FC = fold change

ORF = open reading frame

GPI = glycophosphatidylinositol

CDS = coding DNA sequence

RBV = red-backed vole

GAPDH = glyceraldehyde-3-phosphate dehydrogenase

ACTB = actin beta

RPL19 = ribosomal protein L19

HBB = hemoglobin beta

HBA2 = hemoglobin alpha2

TTR = transthyretin

APOC1 = apolipoprotein C1

SERPINA3 = serpin peptidase inhibitor clade A

USP16 = ubiquitin specific peptidase 16

NR4A2 = nuclear receptor subfamily 4 group A member 2

ALAS2 = 5'-aminolevulinate synthase 2

RHAG = Rh-associated glycoprotein

PMCA = protein misfolding cyclic amplification

SDS-PAGE = sodium dodecyl sulphate - polyacrylamide gel electrophoresis

CWD = chronic wasting disease

FSE = feline spongiform encephalopathy

EUE = exotic ungulate encephalopathy

GSS = Gerstmann-Sträussler-Scheinker syndrome

FFI = fatal familial insomnia

CAA = cerebral amyloid angiopathy

VPSPr = variably protease-sensitive prionopathy

PK = proteinase K

ALS = amyotrophic lateral sclerosis

SAA = serum amyloid A

HD = Huntington's disease

mHTT = mutant huntingtin

Aβ = amyloid beta

APP = amyloid precursor protein

DLB = dementia with Lewy bodies

MSA = multiple system atrophy

SOD1 = superoxide dismutase 1

TDP-43 = transactive response DNA binding protein 43

FTD = frontotemporal dementia

PSP = supranuclear palsy

AGD = argyrophilic grain disease

MAPT = microtubule-associated protein tau

BASE = atypical BSE

CSF = cerebrospinal fluid

EEG = electroencephalogram

RT-QuIC = real-time quaking induced conversion

DEG = differentially expressed gene

HRP = horseradish peroxidase

cDNA = complementary DNA

FDR = false discovery rate

RT = room temperature

IV = intravenous

IC = intracranially

LXR/RXR = liver X receptor / retinoid X receptor

FAM = fluorescein amidite

GFAP = glial fibrillary acidic protein

TNFSF10 = tumor necrosis factor ligand superfamily member 10

MT-CYTB = mitochondrial cytochrome b

MT-ND4 = mitochondrial NADH dehydrogenase subunit 4

IHC = immunohistochemistry

CNS = central nervous system

VLDL = very low density lipoprotein

EOAD = early onset Alzheimer's disease

WT = wild type

Hb = hemoglobin

HDAC = histone deacetylase

TSA = thricostatin

SN = substantia nigra

ER = endoplasmic reticulum

ABSTRACT

Background: Prion diseases or transmissible spongiform encephalopathies (TSE) are a class of fatal infectious neurodegenerative disorders whose pathogenesis mechanisms are not fully understood. The diseases manifest as sporadic, genetic or acquired. So far, neither specific biomarkers for early diagnosis nor effective therapeutic targets have been identified. The pathological molecular component of the diseases is a misfolded isoform of the prion protein (PrP) denoted as prion. Mounting evidence suggests that in addition to gene coding for the PrP (*PRNP*) other genes may contribute to the genetic susceptibility of TSE. In this context, microarray-based gene expression analyses offer unique tools to approach neurodegenerative disorders. In particular, transcriptome profiling can be used to identify altered transcripts in response to pathogens, and select potential targets for novel therapeutic approaches. Up to date, a number of studies have been carried out in order to investigate the gene expression alterations occurring in prion-infected organisms, but most of them involved animal models such as mice, sheep and cattle, which are not closely related to humans. Several studies have been performed on non-human primates but none of them have investigated the genomic outcome of prion infection.

In this study, we performed the first large-scale transcriptome gene expression analysis on BSE-infected cynomolgus macaques (*Macaca fascicularis*), which are an excellent model for studying human acquired prion disease. Indeed, cynomolgus macaques are evolutionary very close to humans, have a high degree of amino acid homology in PrP sequence. In addition, like the human sequence, macaque PrP possesses the same polymorphism at codon 129. Furthermore, BSE can be transmitted either intracranially or orally to these animals leading to a disease that is

very similar to the human disorder, as regards preclinical incubation time, clinical symptoms and pathophysiology.

Aim of the work: The initial objective of the present work was to identify the main genes that are differentially expressed in the frontal cortex of intracranially infected monkeys compared to non-infected ones. This approach could shed some light on the biological processes underlying the pathogenesis of human prion diseases, which may therefore become potential targets for both diagnostic and therapeutic strategies.

Following the encouraging results obtained in monkeys, we decided to further confirm the dysregulation pattern highlighted in macaques in human prion disorders. At this step of the study, the final aim was to investigate the specificity of the identified gene signature for CJD in comparison to both healthy subjects and to other neurodegenerative diseases. This further analysis aimed at highlighting not only prion disease specific molecular mechanisms, but also potential common neurodegeneration processes.

Methods: Total RNA from the *gyrus frontalis superior* of 12 animals – 6 intracranially BSE-challenged (A1-A6), 1 orally BSE-infected (B6) and 5 non-infected age- and sex-matched control macaques (CovA, CovB, CovC, CovD1, CovD2) – was isolated homogenizing the material with micro pestles in TRIzol (Invitrogen). DNase I digestion was then performed and RNA was checked for quantity and purity on a NanoDrop 2000 spectrophotometer (Thermo Scientific™) and integrity on a 2100 Bioanalyzer (Agilent Technologies). Samples were labeled using the GeneChip 3'IVT Express Kit (Affymetrix) and hybridized to a GeneChip Rhesus Macaque Genome Array (Affymetrix). The bioinformatics analysis identified 300 probe sets that were up- or down- regulated about twofold (≥|1.95|). Because among them no candidate

appeared using FDR 0.05, we chose as criteria an unadjusted *p*-value of ≤0.005 together with a fold change ≥|2.0|. We then used the Ingenuity Pathways Analysis (IPA) to annotate genes according to their functional relationships and determine potential regulatory networks and pathways. In order to confirm the array results using an independent and more sensitive technique, we performed RT-qPCR for a subset of differentially expressed genes, with *GAPDH* and *ACTB* as reference genes. –RT controls were included in the plates for each primer pair and sample. The relative expression ratio was calculated using the $2^{-\Delta\Delta CT}$ method. Statistical significance was calculated with the unpaired student t-test ($p<0.05$). Regarding human samples, we collected about 120 samples from frontal cortex of frozen postmortem brain tissue, including: prion-infected patients (vCJD, sCJD, iCJD), neurodegeneration affected patients (AD, PD, CBD, tauopathies) and controls (healthy subjects). RNA was extracted using TRIzol with PureLink® RNA Mini Kit (Life Technologies) and on-column DNase I digestion. Quantity and integrity were checked as above, and only samples with a RIN around 4.5 or higher were included in the study. Reverse transcription was then carried out using Superscript III and RT-qPCR was performed for the previously selected gene transcripts, with *ACTB* and *RPL19* as reference genes. In addition, for all macaque and human samples, erythrocyte markers expression analysis was performed in order to exclude any relevant blood contamination. Results: The microarray-based transcriptome analysis of brains from BSE-infected macaques revealed 300 transcripts with expression changes greater than twofold. Among these, the bioinformatics analysis identified 86 genes with known functions, most of which are involved in cellular development, cell death and survival, lipid metabolism and transport and acute phase response signaling. RT-qPCR was performed on selected gene transcripts in order to validate the differential expression in infected animals versus controls. The results obtained

with the microarray technology were confirmed and a five-gene signature was identified. In brief, *HBB* (hemoglobin, beta chain) and *HBA2* (hemoglobin, alpha chain 2) were down-regulated in intracranially infected macaques, whereas *TTR* (transthyretin), *APOC1* (apolipoprotein C1) and *SERPINA3* (serpin peptidase inhibitor 3) were up-regulated. Interestingly, we found a completely different expression pattern for B6, the only orally-infected sample available, in comparison to the intracranially infected animals, for three genes (*USP16, NR4A2, HBB*), suggesting that the route of infection might play a substantial role in determining the gene expression regulation. Given that the autopsy procedure could have led to the presence of some blood in the brain material, we analyzed all the samples also for expression of two specific erythrocyte markers, *ALAS2* (5'-aminolevulinate synthase 2) and *RHAG* (Rh-associated glycoprotein), in order to assess the reliability of the results related to the regulation of both chains of hemoglobin and exclude any major influence of potential blood contamination. RT-qPCR analysis for both markers revealed negligible blood contamination ($C_T \geq 35$) within some samples.

Given the encouraging results found in macaques, we decided to investigate if this BSE-infection gene signature was reliable also in discriminating CJD patients from healthy ones. In humans, the disease that corresponds to BSE infection in macaques would be vCJD, which arose in human population in late 90s after consumption of BSE contaminated bovine meat. However, given the limited numbers of definitive diagnosed vCJD patients (slightly more than 200 worldwide, two of which are in Italy) and considered their reduced accessibility, we decided to extend our analysis also to sCJD patients. This would also allow us to shed some light on the possible differences in gene regulation mechanisms between acquired and sporadic human prion disorders. In addition, to better investigate the influence of different etiologies,

we also included some patients with iatrogenic CJD (iCJD), an acquired prion disease -as vCJD- but with a different origin, in this case patients that followed treatment with growth hormone derived from prion contaminated cadavers. Regarding control samples, we had to face the very limited availability of brain samples from healthy subjects, either age-matched with vCJD (around 30 years) or with sCJD (around 65 years). Therefore, we decided to introduce in our study some samples from patients with non-CJD neurodegenerative disorders as an additional "control" group; this would also enable the identification of possible prion-specific gene expression alterations. In general, the gene expression trend observed in macaques was confirmed in humans, with similar FC values, for four out of five genes: *HBA1/2* is down-regulated in both sCJD cases and also in patients affected by other non-CJD neurodegenerative diseases, while *APOC1*, *TTR* and *SERPINA3* are up-regulated in CJD patients, but not in patients affected by other neurodegenerative diseases, as they show levels of expression not different from that of the healthy controls (FC < |2|).

Conclusions: In our work we used both microarray and RT-qPCR technologies that allowed us to identify a gene signature able to distinguish BSE-infected macaques from control animals. The identified genes are involved in oxygen transport and iron homeostasis (*HBB, HBA2*), cholesterol metabolism and lipid transport (*APOC1, SERPINA3)* as well as acute phase response (*SERPINA3, TTR*). Therefore, these results suggest that, in order to identify potential biomarkers and drug targets for prion diseases and other neurodegenerative disorders, a combination of various pathways has to be targeted, including oxygen homeostasis, cholesterol metabolism and inflammation response. Importantly, the dysregulation of four of these genes (*HBA2, APOC1, TTR, SERPINA3)* has been validated with similar FC values also in

CJD affected human samples, confirming the reliability of our previous analysis on BSE-infected monkeys and providing important hints on some prion-specific alterations in CJD disease. These results could be extremely helpful in understanding the mechanism underlying the progression of the disease, allowing for the identification of some key players which, if not being the cause of the onset, could however be some of the target genes affected by the disease. In addition, some of our findings support the hypothesis of a potential shared mechanism underlying the onset and the development of all neurodegenerative disorders. This is in agreement with recent data supporting the idea of a unifying role of prions in these diseases in general and maybe a prion-like behavior for most neurodegenerative disorder.

INTRODUCTION

In the last decades, the striking advancements of our knowledge in biomedicine have led to a significant improvement of health conditions. This fact has ultimately led to the lengthening of life expectancy: by 2050, almost 400 million people all over the world will be ≥ 80 years old. As a consequence, the prevalence of neurodegenerative disorders has rapidly increased. The fact of this augment is likely to represent a major social and economic issue in the near future, not only for high-income countries but also in low- and middle-income ones [1].

Even though great efforts have been dedicated to research for many years, we are still far from understanding the precise molecular mechanisms that lead to neurodegeneration in pathologies such as Alzheimer's, Parkinson's, Huntington's or

Creutzfeldt-Jakob's disease. In addition, for all these disorders no therapy is still available [2].

In general, these disorders share a common mechanism of aberrant folding of distinct proteins that, upon misfolding, become more prone to aggregation, and, in turn, may become highly neurotoxic. This mechanism is nowadays referred to as "prion paradigm". The latter can be explained in a canonical model for the seeded aggregation of misfolded proteins: (i) recruitment of monomers by aggregates of misfolded proteins that impose their aberrant structure on the native polypeptides; (ii) growth and fragmentation of oligomers; (iii) spreading of the pathology [2]. Since the 1930s, when a spongiform encephalopathy of a sheep was shown to exhibit atypical infectivity; such as very long incubation period, absence of inflammation, no demonstrable microbial or viral agent, several other species, including humans, have been found to be affected by a similar pathology. Only half a century later, Prusiner and colleagues were able to show that the infectious agent of these transmissible spongiform encephalopathies (TSEs) consists solely of an abnormally folded protein, hereafter called "prion" – an acronym to indicate a proteinaceous infectious particle. The physiological cellular prion-related protein (PrP^{C}) is a membrane-bound protein predominantly expressed in the nervous tissue, where it probably plays a role in neuronal development and function [3]. When in its misshapen state, the molecules aggregate with one another and impose its anomalous structure on benign PrP molecules. Prions thus act as corruptive templates (seeds) that initiate a chain-reaction of PrP misfolding and aggregation. As prions grow, fragment and spread, they cause neuronal loss perturbing the function of the nervous system and ultimately cause the death of the affected individual [4].

Prion protein structure

The human *PRNP* gene is located on the short arm of chromosome 20 and, in all mammals, contains three exons. The open reading frame (ORF) lies entirely within exon 3 and transcribes an mRNA of 2.1–2.5 kb in length, with approximately 50 copies/cell in neurons [5]. PrP^C is the related encoded glycoprotein that resides in lipid rafts and is attached to the outer leaflet of the plasma membrane via a C-terminal glycosylphosphatidyl inositol (GPI) anchor. Following the cleavage of the N-terminal signal peptide, PrP^C is exported to the cell surface. Then, after ~5 h at the cell surface (its average half-life) it is internalized through a caveolae-dependent mechanism and is degraded in the endolysosome compartment [6]. Human PrP^C is a 253 amino acid protein, which has a molecular weight of 35-36 kDa [7]. Its highly conserved structure is composed of a flexible unfolded N-terminal domain and an α-helical enriched globular domain; in the N-terminus of the protein there is a cleavable signal peptide and a glycine-rich octapeptides region – made up of four octarepeats - that binds copper and other divalent cations. In addition, a non-octarepeat copper binding site can be found immediately after this region. The C-terminal moiety is composed of a cleaved signal peptide, 3 α-helices and a short 2-stranded antiparallel β-sheet, and also contains a disulfide bridge linking α2-α3 helices and 2 N-linked glycosylation sites (Figure 1) [8]. PrP^C is present in un-, mono- or di-glycosylated forms, which correspond to the variable N-glycan attachment to two highly conserved residues, asparagine 181 and 197 in the human protein. While the ratios of the various glycosylated forms of PrP^C remain reasonably constant in uninfected individuals, the ratios of the glycosylated bands of PrP^{Sc} are highly variable in brains infected with different TSE agents. Moreover, it has been recently shown that the glycosylation status of PrP^C affects the inter-species transmissibility of some prion diseases [9].

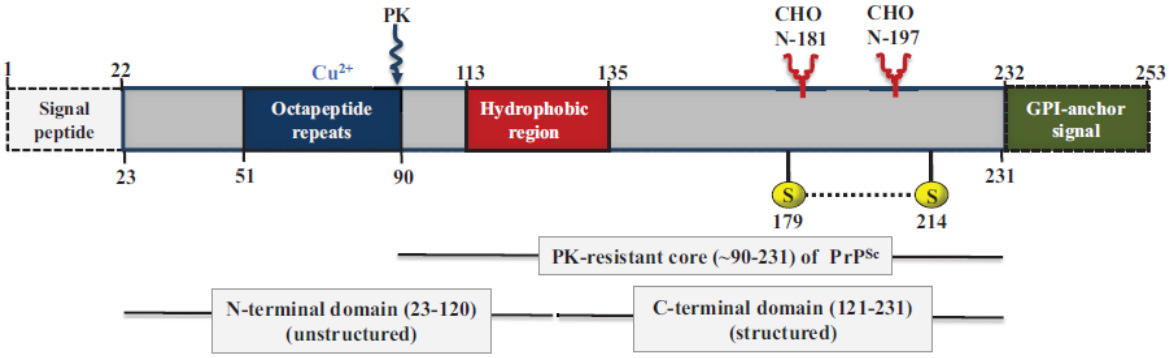

Figure 1. Schematic representation of human PrP.
The unprocessed PrP is 253 amino acid residues in length and includes a signal peptide (1–22), four OR, a hydrophobic region (113–135), one disulfide bond between cysteine residues (179–214), two *N*-linked glycosylation sites (at residues 181 and 197), and a GPI-anchor attached to the *C*-terminus of PrP replacing the GPI-anchor signal (residues 232 to 254). A palindromic region, AGAAAAGA (113–120), lies in the hydrophobic region (113–135) and is thought to be important in the conversion of PrP^{C} to PrP^{Sc}. OR: Octapeptide repeat; GPI: glycophosphatidylinositol; PK: proteinase K; CHO: carbohydrates (from Acevedo-Morantes 2014)

As regards non-human primates, the *Macaca* genus is closely related to humans, thanks to a common ancestor ≈25 million years ago. Nevertheless, some studies have shown that in general macaques harbor much higher genetic diversity than humans [10]; however, Mauritian macaques used in this study have been known to show extremely low genetic diversity, due to their recent colonization [11]. It is known that amino acid substitutions in PrP gene sequence can alter susceptibility to TSE agents [12]. The macaque *PRNP* shares a 96% identity with the human sequence, with 32 residues differing within the CDS region (Figure 2). Similarly, also the two proteins show a 96% identity, with 9 residues (97, 100, 108, 138, 143, 155, 166, 168 and 220) that differ between macaque and human primary sequence.

Species	Gene ID	Peptide ID	Peptide length	% identity (Protein)	% coverage	Genomic location
Human (*Homo sapiens*)	ENSG00000171867	ENSP00000368752	253 aa	96 %	100 %	20:4686236-4701590
Macaque (*Macaca mulatta*)	ENSMMUG00000019949	ENSMMUP00000026231	253 aa	96 %	100 %	10:38018549-38034091

```
CLUSTAL W(1.81) multiple sequence alignment


ENSP00000368752/1-253    MANLGCWMLVLFVATWSDLGLCKKRPKPGGWNTGGSRYPGQGSPGGNRYPPQGGGGWGQP
ENSMMUP00000026231/1-253 MANLGCWMLVLFVATWSDLGLCKKRPKPGGWNTGGSRYPGQGSPGGNRYPPQGGGGWGQP
                         ************************************************************


ENSP00000368752/1-253    HGGGWGQPHGGGWGQPHGGGWGQPHGGGWGQGGGTHSQWNKPSKPKTNMKHMAGAAAAGA
ENSMMUP00000026231/1-253 HGGGWGQPHGGGWGQPHGGGWGQPHGGGWGQGGGTHNQWHKPSKPKTSMKHMAGAAAAGA
                         ***********************************.**:*******.************


ENSP00000368752/1-253    VVGGLGGYMLGSAMSRPIIHFGSDYEDRYYRENMHRYPNQVYYRPMDEYSNQNNFVHDCV
ENSMMUP00000026231/1-253 VVGGLGGYMLGSAMSRPLIHFGNDYEDRYYRENMYRYPNQVYYRPVDQYSNQNNFVHDCV
                         ****************:****.***********:**********:*:************


ENSP00000368752/1-253    NITIKQHTVTTTTKGENFTETDVKMMERVVEQMCITQYERESQAYYQRGSSMVLFSSPPV
ENSMMUP00000026231/1-253 NITIKQHTVTTTTKGENFTETDVKMMERVVEQMCITQYEKESQAYYQRGSSMVLFSSPPV
                         ************************************:*******************


ENSP00000368752/1-253    ILLISFLIFLIVG
ENSMMUP00000026231/1-253 ILLISFLIFLIVG
                         *************
```

Figure 2. Sequence identity between human and macaque PrP sequences.
Numbering is based on the human sequence. Dots indicate residues different from human residues. Alignment of the sequences was obtained from Ensembl database. Macaca mulatta and Macaca fascicularis protein sequences are identical.

Notably, both species display serine homozygosity at codon 170, whose polymorphism has been recently linked with transmission of infectivity in red-backed vole (RBV). Indeed, amplification of human vCJD PrP^{Sc} in PMCA occurred only with RBV 170S/S and not in RBV 170N/N or 170S/N [13, 14]. Considering all these notions, we can assume that the macaques involved in this study represent an accurate model for a human species barrier.

Prion protein expression and function

Prion protein is highly conserved in mammals, where it is almost ubiquitously expressed, suggesting some relevant physiological roles particularly in the central nervous system and in the immune system. Indeed, together with neurons, lymphocytes and antigen presenting cells (such as dendritic cells and monocytes) show the highest levels of PrP^{C} expression [15]. However, the biological functions of PrP^{C} still remain elusive. Numerous experiments using mice and murine cell lines in

which the expression of PrP is abolished (*Prnp*$^{0/0}$) suggest that PrP^{C} is involved in several physiological functions such as myelin maintenance, metal homeostasis, apoptosis prevention and also hematopoiesis and erythroid differentiation [16]. In particular, in different cell culture models PrP^{C} showed to promote neurite outgrowth and to prevent neuronal cell death, particularly through inhibition of the mitochondrial proapoptotic pathway [17-19]. PrP^{C} is also involved in early synaptic transmission, in regulation of circadian activity and in memory formation [15]. In addition, *Prnp*$^{0/0}$ are resistant to prion infection and that neuron-restricted PrP^{C} expression is sufficient to allow and sustain scrapie infection in transgenic mice [20]. Even if some evidences suggest an implication of PrP^{C} in the activation of T lymphocytes and phagocytosis, the precise role of PrP^{C} in both innate and adaptive immune system still remains unclear [15].

PrP^{Sc} formation

The stochastic, genetically- or infectivity- linked misfolding of the essentially α-helical PrP^{C} entails a 40% β-sheet enrichment of the aberrant PrP^{Sc} isoform, whose different biophysical characteristics favor attraction and conformational conversion of other PrP^{C} molecules. This process leads to the formation of soluble oligomers of increasing length (Figure 3). In this chain reaction of elongation, PrP^{Sc} functions as a template that imposes its aberrant structure on native PrP^{C} molecules, resulting in drastic modifications of PrP^{C} biochemical properties [2]. Indeed, PrP^{Sc} is insoluble in non-denaturant detergents, it is only partially hydrolyzed by proteases to form a fragment designated PrP 27-30, denoted after its electrophoretic mobility in reducing and denaturing SDS-PAGE, and it accumulates in the brain with a pattern distinct from the distribution of PrP^{C} [21]. It has been speculated that the PrP^{C} conversion to PrP^{Sc} may occur in caveolae-like domains [7]. Oligomers and larger aggregates can

fragment, amplifying in this way the seeding capacity, and may ultimately deposit outside neurons as insoluble amyloid fibrils, characterized by ordered β-sheet repeats perpendicularly oriented to the fiber axis [2]. In particular, the oligomeric states of pathogenic mammalian prions are thought to be the toxic forms, and assembly into larger polymers, such as amyloid fibrils, seems to be a mechanism for minimizing toxicity [22].

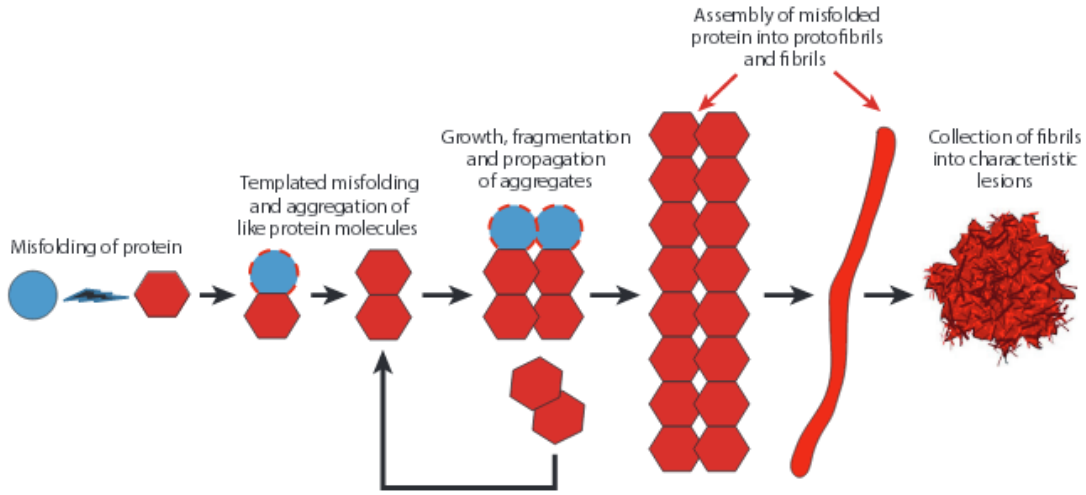

Figure 3. The prion paradigm of template-assisted, seeded protein aggregation.
A schematic diagram shows the hypothetical series of events leading from the misfolding and self-aggregation of protein molecules to the formation of characteristic lesions. The assemblies that act as seeds for the templated misfolding of other molecules can vary in size from small oligomers to large polymers. These seeds initiate and sustain the disease process and may be the agents by which the aggregates proliferate and spread within the nervous system. In addition, small, oligomeric assemblies have been identified as cytotoxic agents in several instances. The lesions that result from the seeding cascade can occur as intracellular inclusions (such as neurofibrillary tangles or Lewy bodies) or extracellular masses (such as amyloid plaques). (from Walker 2015)

Prion diseases

Pathologically, prion diseases are marked by spongiform change (vacuolation) in the brain, neuronal loss, astrocytosis, and the accumulation of PrP^{Sc} [3]. TSEs are mostly idiopathic in origin and typically late-onset, while the genetic forms (about 10%) have a slightly earlier age at onset and a slower course. Iatrogenic cases are due to contaminated neurosurgical instruments, brains derivatives such as pituitary

hormones, corneal transplantation, dura mater graft. In addition, more recently, consumption of prion-tainted beef products and transfusion of prion-infected blood has occurred [2].

Prion diseases are infectious provided that the amino acid sequences between PrP^{Sc} in the inoculum and PrP^{C} expressed in the recipient are identical; therefore, PrP^{Sc} from one species fail to or inefficiently transmit the disease to an organism expressing heterologous PrP^{C}, a feature known as transmission barrier [23]. Furthermore, differences in incubation time can occur also when the invading PrP^{Sc} and the host PrP^{C} have identical sequences. This phenomenon is caused by the existence of prion strains that have the ability to generate distinct incubation times and neuropathological lesions in homologous hosts. Given that structural information for PrP^{Sc} is not available at high resolution, this theory is currently based on distinct biochemical and biophysical properties of different strains. One tempting hypothesis would be that the transmission barrier is determined as well by distinct conformations of PrP^{Sc} in different species [24].

Animal TSEs

Animal prion diseases include scrapie in sheep and goats, the aforementioned bovine spongiform encephalopathy (BSE) in cattle, chronic wasting disease (CWD) in cervids, transmissible mink encephalopathy in ranch-raised mink, feline spongiform encephalopathy (FSE) in cats and exotic ungulate spongiform encephalopathy (EUE) of captive wild ruminants. In contrast to humans, animal TSEs are generally acquired (Table 1).

Also, as already mentioned above, it is known that there are transmission barriers that operate at the molecular level, whose efficacy depends on compatibility between the PrP^{Sc} from the infecting species and the PrP^{C} from the host. Similarities in the

species-specific primary *PRNP* sequences may account for part of this effect, but prion strains and host *PRNP* polymorphic genotype may affect susceptibility in ways not yet fully understood [25].

Animals affected by TSEs increase the risk of transmission to humans, as in the case of BSE that captured worldwide attention in the 1990s because of food-borne transmission to humans, causing a fatal variant form of Creutzfeldt-Jakob disease (CJD). The frequency of classical BSE cases has declined dramatically following the implementation of appropriate measures to control animal feed. However, atypical forms of BSE have recently been described in Europe, Japan and North America, posing major concerns for public health [26-28]. These atypical forms are bovine amyloidotic spongiform encephalopathy (L-type BSE) and H-type BSE, both with a pathology and epidemiology distinct from classical BSE, thus representing distinct prion strains [25]. Some studies suggest that L-type BSE, but not H-type, is able to infect cynomolgus macaques [29, 30] and humanized transgenic mice, indicating that a zoonotic risk may exist [31].

Concerning cervids, in North America both the native and farmed deer and elk populations are currently suffering the rapid spread of CWD; whether it has the potential to be infectious to humans is uncertain and represents a relevant concern [32]. Indeed, while CWD transmission failed to occur in humanized mice overexpressing human PrP bearing the129M polymorphism [33-35], squirrel monkeys, but not cynomolgus macaques, are susceptible to CWD infection [36, 37]. Furthermore, brain homogenate from CWD infected cervids, used as a seed in PMCA reaction, was able to convert normal human PrP^{C}, indicating that there is not an absolute barrier between human PrP and cervids PrP^{Sc} [25].

Regarding sheep, both classical and atypical scrapie are considered to represent a negligible risk to the human population as they appear not to be infectious to humans [32].

Animal transmissible spongiform encephalopathies	*Probable aetiology*
Scrapie (in sheep and goats)	Acquired
Transmissible mink encephalopathy (TME, in mink)	Acquired
Chronic wasting disease (CWD, in deer and elk)	Acquired
Bovine spongiform encephalopathy (C-type BSE)	Acquired
Feline spongiform encephalopathy (FSE, in cats)	Acquired
H-type and L-type BSE	Idiopathic
Atypical scrapie (for example, Nor98 in sheep)	Idiopathic

Table 1. Animal transmissible spongiform encephalopathies (from Head 2012)

Human TSEs

Human prion diseases include of Creutzfeldt-Jakob disease (CJD), Gerstmann-Sträussler-Scheinker syndrome (GSS), kuru, fatal familial insomnia (FFI), PrP cerebral amyloid angiopathy (PrP-CAA) and variably protease-sensitive prionopathy (VPSPr). CJD is by far the most common prion disorder in humans, with a worldwide incidence of 1-2 cases per million of population per annum; among these, the vast majority of cases are idiopathic and then termed sporadic CJD. With lower incidence are familial or genetic (fCJD or gCJD) cases and are found in association with a growing list of mutations in the ORF of the PrP gene, *PRNP*. The remaining are acquired (iCJD) through contaminated surgical instruments or cadaveric derivatives (growth hormone, dura mater and corneal transplantation) or, as mentioned above, following the consumption of infected bovine meat (vCJD) [38]. Besides CJD, there are other even rarer prion diseases, either inherited such as FFI and GSS, sporadic such as fatal insomnia or acquired due to mortuary feast rituals such as kuru (Table

2). Regardless of the origin, it seems as though *PRNP* gene has an influence on prion susceptibility [39]. Indeed, codon 129 is the site of a common methionine (M)/valine (V) polymorphism: in the Caucasian population around 51% of individuals are heterozygous (M/V), 37% M homozygous (M/M) and 12% are V homozygous (V/V) [38]. Interestingly, the phenotype of the prion diseases, whether sporadic, familial or acquired, often differs depending on the 129 genotype of the affected subject. Furthermore, more than 70% of sporadic and 100% of variant CJD are M homozygous, providing evidences of a genetic predisposition for human prion diseases [40]. Another well-known non-pathogenic polymorphism in the *PRNP* gene is glutamic acid (E) or lysine (K) at codon 219, which is mainly found in Asian and Pacific population where 219E/K heterozygosity seems to confer resistance against sCJD but not entirely against the acquired or genetic form of prion disease [41].

Human prion disease	*Probable aetiology*
Sporadic CJD (sCJD) and its subtypes	Idiopathic
Sporadic fatal insomnia (sFI)	Idiopathic
Variably protease sensitive prionopathy (VPSPr)	Idiopathic
Kuru	Acquired (sCJD)
Iatrogenic CJD (iCJD)	Acquired (sCJD)
Variant CJD (vCJD)	Acquired (BSE)
Familial or genetic CJD (fCJD or gCJD)	Genetic (*PRNP* mutations)
Gerstmann–Straussler–Scheinker disease (GSS)	Genetic (*PRNP* mutations)
Fatal familial insomnia (FFI)	Genetic (*PRNP* mutations)
Prion protein cerebral amyloid angiopathy (PrP-CAA)	Genetic (*PRNP* mutations)

Table 2. Human prion diseases
The probable source of infectivity in the acquired forms shown in parenthesis. (from Head 2012)

Genetic prion diseases

In particular, regarding familial prion diseases, there are a number of polymorphisms and more than 40 different pathogenic mutations in the human *PRNP* gene that are

linked to familial CJD, FFI or GSS; they include 35 point mutations and expansions or deletions within an unstable region of *PRNP* rich in proline, glycine and glutamine (octapeptide repeat region) (Figure 4). Interestingly, one to four additional octarepeats cause late-onset fCJD with a mean age of 62 years, while 5 to eight additional octarepeats cause early-onset fCJD or GSS with a mean age of 32 [22]. Curiously, one particular mutation, Asp178Asn, is related with fCJD – if valine is present at codon 129 – or FFI -if methionine is instead encoded at codon 129. In general, codon 129 determines earlier onset and a shorter course of genetic prion diseases for M/M homozygous individuals [39, 42].

Generally, these diseases manifest with cognitive difficulties, ataxia and myoclonus and show different neuropathological features according to different causative mutations. While fCJD is characterized by spongiform degeneration with diffuse astrogliosis throughout the brain cortex and deep nuclei, GSS shows multiple PrP-positive amyloid plaques and FFI presents a relative lack of spongiform degeneration together with neuronal dropout and gliosis in the thalamus and brain stem [43, 44]. The age at onset ranges from the third to the ninth decade of life, while the course ranges from a few months to several years with death occurring often from infection (pneumonia or urosepsis).

With regards to fCJD, progressive confusion and memory impairment are the first symptoms, and the typical age of manifestation is from 30 to 50 years. Clinical symptoms of GSS usually develop between 40 to 60 years of age, with cerebellar dysfunction (unsteady gait, mild dysarthria) together with spasticity and bradykinesia, and a slow progression from a few to seven years. A typical sign of FFI is insomnia, with disruptions in autonomic functions followed by ataxia. The age of onset for FFI spans from 40 to 50 years. Disease duration is generally 12 months in individuals homozygous for the disease causing mutation and becomes significantly longer in

heterozygous individuals (around 21 months. This suggests a gene dosage effect [32, 43].

Interestingly, mutations that generate a premature stop codon in the *PRNP* gene are known to cause a particular prion disease characterized by neurofibrillary tangles and PrP-positive amyloid fibril deposits in arteries and arterioles walls, a condition known as cerebral amyloid angiopathy (CAA). As for GSS, the truncated C-termini resulting from these mutations determine the loss of the GPI anchor, required to attach the protein to the outer leaflet of the plasma membrane; this indicates that the GPI moiety might interfere with the ability of PrP to form amyloid fibrils and that its absence could trigger the cerebrovascular amyloid deposition of these readily formed fibrils [45, 46].

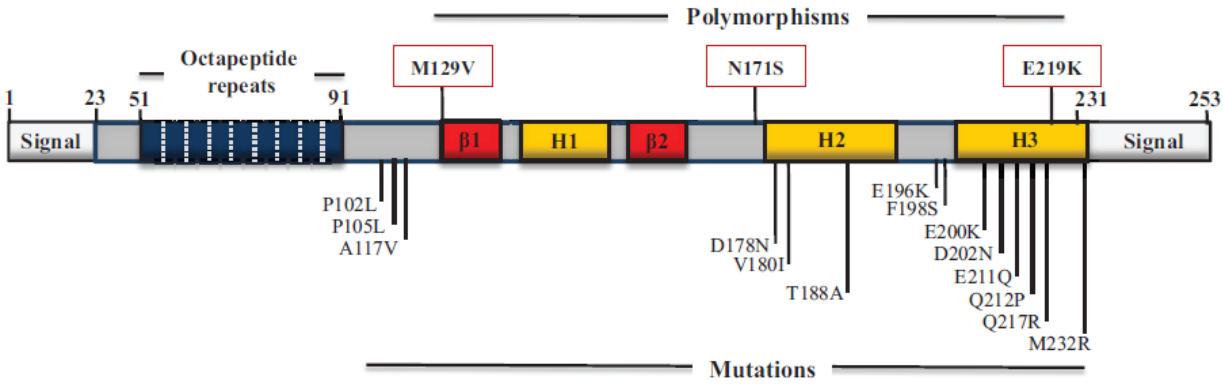

Figure 4. Schematic representation of human PrP mutations and polymorphisms.
The *N*-terminal octapeptide repeat motif is comprised of eight residues: P(H/Q)GGG(-/G)WGQ. Normal PrP contains five copies of this motif; a single OR deletion is considered a non-pathogenic polymorphism. However, insertional mutations consisting of one to nine additional OR are pathogenic. Polymorphisms and pathogenic mutations of the *PRNP* gene are represented above and below the schematic, respectively. Letters preceding the numbers indicate the normal amino acid residue for the position and letters following the numbers designate the new residue. **(**from Acevedo-Morantes 2014)

Sporadic prion diseases

Sporadic Creutzfeldt-Jakob disease (sCJD)

One other major disease modifier, together with the polymorphism at codon 129, is the type of PrP^{Sc} present in the affected individual: indeed, type 1 PrP^{Sc} is mainly associated with the MM genotype (60-70% of all sCJD cases) while type 2 PrP^{Sc} is more often present with MV or VV genotype [39]. These two types of prions differ by the molecular weight of the unglycosylated band, which migrates at 21kDa in type 1 and at 19kDa in type 2, on Western blot [47]. Phenotypic heterogeneity indeed is one of the most intriguing features of prions, influencing the progression rate of the disease, the pattern of PK-resistant fragments of PrP^{Sc}, the neuropathological characteristics of brain lesions and transmissibility properties in mice. For instance, it has been recently shown that human MM1 sCJD prion replication rate *in vitro* is markedly higher than that of MM2 sCJD: this diversity is probably the consequence of specific structural features of each PrP^{Sc} type that control the intrinsic growth rate of the aggregates [48]. The issue is further complicated by the fact that around 25% of sCJD cases present both type 1 and type 2 PrP^{Sc}, with their ratio varying among different brain regions, suggesting regional or cellular tropism of PrP^{Sc} [47].

Based on the polymorphism at codon 129 and the type of PrP^{Sc} present, sCJD has been historically divided into six phenotypically different subtypes:

Subtype 1: MM1 and MV1 – this is the most common subtype of sCJD, with a large prevalence of MM homozygosity. Symptoms, mainly cognitive impairment, arise around a mean of 65 years of age, with a mean clinical duration of 4 months. Histopathologically, this subtype presents with diffuse fine spongiform degeneration particularly severe in the cortex, astrogliosis and neuronal loss. PrP immunostaining is synaptic-like.

Subtype 2: VV2 – this is the next common subtype, accounting for 16% of all sCJD cases, and is also known as “cerebellar” or “ataxic” variant. Indeed, the main difference with the subtype 1 relies on the fact that ataxia is the most recurrent symptom at diagnosis. One other distinctive characteristic is the presence of focal PrP plaque-like aggregates, especially in the cerebellum.

Subtype 3: MV2 – this subtype comprises around 9% of all sCJD cases. Its main characteristics are a longer clinical duration (average of 17 months) and the presence of kuru plaques in the cerebellum. Ataxia and cognitive impairment are almost equally the earliest signs of disease at the onset.

Subtype 4: MM2 – this is a quite rare subtype (2-8% of all cases) with a clinical duration similar to that of MV2 subtype including cognitive impairment as the first most common symptom. The hallmark here is the spongiform degeneration with large vacuoles, referred as “coarse spongiosis”, diffused in the cortex and thalamus together with astrogliosis.

Subtype 5: VV1 – it represents about 1% of all sCJD cases, with an early onset of, on average, 39 years and a clinical duration of about 15 months. The main symptom is a fronto-temporal dementia, with severe fine spongiform degeneration and a faint synaptic-like PrP immunostaining pattern.

Subtype 6**: sporadic fatal insomnia (sFI)** – this subtype, also referred as “thalamic” variant, accounts for about 2% of the sporadic prion diseases and it’s phenotypically identical to FFI. sFI is linked to the 129MM genotype and PrP^{Sc} type 2, but it differs from MM2 subtypes as it has a significantly longer clinical duration (average of 24 months) and the eventual presence of insomnia at diagnosis. The main histopathological feature is severe astrogliosis and neuronal loss in the thalamus without spongiosis. The PrP^{Sc} type 2 of sFI shows however a different glycoform ratio compared to that of FFI. Indeed, while in the genetic form of the disease there is a

marked under-representation of the unglycosylated form, in sFI the ratio of the three glycoforms is similar to that of the other sCJD subtypes. As mentioned above, about one fourth of all the sCJD cases present both type 1 and type 2 PrP^{Sc}, either in the same anatomical region or not, with predominance of type 1 in MM cases and predominance of type 2 in VV cases, which also dictates the related phenotype [39].

Variably Protease-Sensitive Prionopathy (VPSPr)

In 2008, a new human sporadic disease involving PrP was reported in the USA, with some other cases later identified also in the UK, Netherlands and Spain. This disease has a distinctive neuropathology characterized by the presence of microplaques, but it is defined by the observation that PrP^{Sc} in the brain is less resistant to protease digestion than the PrP^{Sc} in other human prion diseases and by the presence of N- and C-terminally cleaved ≈ 8kDa PK-resistant PrP [49]. The mean age of onset is around 67 years with an average duration of disease of about 30 months. However, in the presence of 129VV genotype there is a slight prevalence for an earlier onset and shorter disease duration. As for sCJD, this prion disease also displays heterogeneity, indeed according to the genotype at codon 129 VPSPr can be classified into three subtypes. In 129VV cases, which represent around 65% of total VPSPr cases, the first clinical symptoms are psychiatric signs such as mood and behaviour changes, speech deficit and cognitive impairment, while 129MV cases (≈23%) and 129MM subjects (≈12%) often present with parkinsonism followed by ataxia/myoclonus and progressive cognitive impairment. The common hallmark among all 129 genotypes is the presence of moderate spongiform degeneration with vacuoles in the major cerebral regions, together with occasional cerebellar microplaques in 129VV e 129MV cases; these genotypes generally have more severe lesions. Also, all three genotypes are characterized by a ladder-like

electrophoretic profile of PK-resistant fragments, consisting of 5 major bands migrating approximately at 26kDa, 23kDa, 20kDa, 17kDa and 7kDa, the latter being highly PK resistant in all subtypes. 129MM cases display relatively high PK resistance, the genotype 129MV display intermediate PK resistance while cases with the 129VV genotype show low or are even lacking band profile [50]. To date, no published studies on VPSPr transmissibility are available; however preliminary data indicate that transmission, if it occurs at all, is not efficient, specifically in comparison to CJD [49].

Acquired prion diseases

Variant Creutzfeldt-Jakob disease (vCJD)

In 1996, the National CJD Surveillance Unit reported a new form of human prion disease in the UK, now known as variant CJD (vCJD). This form of the disease has a clinical and pathological phenotype that is distinct from sporadic CJD. Interestingly, all confirmed cases of vCJD to date are MM homozygous at codon 129, a very strong association, but it is not yet clear whether the polymorphism is the major determinant of susceptibility or only of incubation time [32, 51]. Indeed, in 2008 in the UK a new case of vCJD has been diagnosed in a patient who was MV heterozygous at codon 129. However no autopsy was performed to confirm the diagnosis [52].

Experimental transmission studies of BSE and vCJD to inbred and transgenic mice found that the transmissible agent was the same, confirming the epidemiological evidence that vCJD is acquired from another species [40, 53]. The main distinguishing features of vCJD as opposed to sCJD are the clinical presentation, a younger age at clinical onset (mean around 28 years) and the speed at which the disease progresses to death (average of 13 months) [32]. Given that the most likely

route of infection from contaminated BSE-affected bovine meat is the oral one, it was predictable that both PrP^{Sc} and infectivity are detectable within lymphoid tissues. Indeed, unlike sCJD and iCJD, in vCJD the infectious agent can be detected in tonsils, lymph nodes, spleen and appendix even in the preclinical phase of the disease [53]. More importantly, this evidence suggests that lymphocytes may carry infectivity in blood during the incubation period of vCJD, which poses a major health issue considering that the estimated prevalence of asymptomatic individuals in the UK as determined by epidemiological studies and from the retrospective screening of appendix and tonsil tissues is around 1 per 2000-10000 [40, 54-56]. Furthermore, one recent model predicts more than 300 further cases in the next 150 years, most of which are predicted to be the result of blood-derived infection [57].

Regarding clinical features, the most common sign is dementia together with ataxia, involuntary movements and psychiatric features [58]. Currently, 226 vCJD cases have been reported worldwide, 175 had been UK residents during the high-risk period 1980-1996. To date, cases were registered in several other countries in addition to the UK, including France, Ireland, Italy, USA, Canada, Saudi Arabia, Japan, Netherlands, Portugal, Spain and Taiwan (data as of 29-04-2015 from National Creutzfeldt-Jakob Disease Research & Surveillance Unit). Successful prion disease transmission is thought to be dependent on the strain of the prion agent and its genetic compatibility with the host. Experimental transmission studies in mice have shown that the strain of agent causing vCJD has identical properties to that of BSE, which differs from the scrapie or sCJD strains [59].

Interestingly, although the UK population at different ages has been exposed to BSE in the food chain, the majority of vCJD cases are younger than 40-years-old [51]. This suggests a higher rate of dietary exposure, increased susceptibility to infection or a reduced incubation period in this age group [60]. Another possible explanation is

that as part of the development of the human immune system, there is a greater volume of gut-associated lymphoid tissues when younger, with a consequent higher volume of available tissue to absorb the infected material and therefore a more efficient infection [51].

Kuru

Kuru is an epidemic disease that in the 1950s had a dramatic impact on a restricted geographic area of the Papua New Guinea highlands, leading to more than 1800 deaths and therefore providing evidence for direct human-to-human prion transmission [61]. Indeed, the current hypothesis is that a sporadic case of CJD was propagated by mortuary feast practice of deceased tribe members, leading to an epidemic that affected predominantly women and children, the main participants of these mortuary feasts. In 1959 cannibalism was banned and since then no new cases have been reported.

As with other prion disorders, codon 129 homozygosity has been associated with an earlier onset and a shorter clinical duration. In general, the mean incubation period for kuru has been estimated to be around 12 years, however in some cases it may exceed five decades [62]. Some years ago a polymorphism was identified in codon 127 (G127V) whose heterozygosity seemed to provide strong resistance to kuru. Given the highly restricted geographic distribution of the protective V127-associated haplotype, it is believed that this genetic resistance developed as a consequence of the selective pressure imposed by kuru in the 20th century [61]. Very recently, the heterozygosity at codon 127 polymorphism confers complete protection against kuru and sCJD, but not vCJD in transgenic mice. Also, given the observation that V127 was seen exclusively on a M129 *PRNP* allele, its interaction with the common M129V PrP polymorphism was investigated. Notably, homozygosity for V127

polymorphism completely prevented the infection of 18 different human prion disease isolates –comprised of kuru, vCJD, iCJD and sCJD-, regardless of the 129 codon genotype of the inoculum. Therefore, this polymorphism seems to act in a different manner than that in codon 129. Indeed, while 129 polymorphism is partially protective against sCJD only in the heterozygous state, probably through inhibition of protein-protein interactions during the process of prion propagation, V127 seems to act as a dominant-negative inhibitor of prion conversion and propagation [63].

Iatrogenic Creutzfeldt-Jakob disease (iCJD)

iCJD is caused by the accidental transmission of prions from person to person during medical or surgical procedures. Several routes of transmission have been implicated such as a corneal transplant from a donor with sCJD [64], or human dura mater grafts from a contaminated commercial source that have resulted in over 200 iatrogenic infections worldwide [32, 65]. A similar number of cases arose from the use of growth hormone and gonadotropin derived from pituitary glands of CJD affected cadavers. One other minor route of transmission is represented by the re-use of neurosurgical instruments and intracerebral electrodes used on CJD affected patients. Regarding vCJD, but not sCJD, transmission via blood transfusion or infected blood-derived products in human patients has been reported in four clinical cases and one asymptomatic case, all in the UK [32, 55]. Interestingly, while the four symptomatic cases showed typical MM homozygosity at codon 129 and presented with the same clinical and pathological characteristic of BSE-derived vCJD, the neurologically asymptomatic patient had the 129MV genotype and presented with only splenic and lymph node infection [51].

Differentiating iCJD from sCJD cases is important for the identification and prevention of human-to-human prion transmission. Despite no significant differences

identified in gel profiles, stability and PrP^{Sc} infectivity between the two CJD forms, protein misfolding cyclic amplification (PMCA) conversion efficiency is greater for iCJD in comparison to sCJD [66]. Additionally, iCJD (as is the case for vCJD) often lacks the C-terminal 12-13kDa fragment present in sCJD cases, suggesting that acquired and spontaneous prion diseases may have distinct prion formation pathways [66].

Prion-like diseases

Clinical outcome of prion disorders, such as a high percentage of sporadic cases and late onset of the inherited forms, are also shared by many other neurodegenerative diseases, such as Alzheimer's diseases, Parkinson's diseases and amyotrophic lateral sclerosis (ALS) (Table 3). This suggests that certain molecular events may occur with aging that lead disease-specific proteins to become pathogenic. More than two decades ago, Prusiner suggested that this event involves the stochastic refolding of the etiologic protein into a misfolded infectious state known as "prion" that, when it exceeds a certain threshold, impairs the degradation pathways, thereby enabling the prion to self-propagate [67, 68]. This issue has been recently addressed by a number of groups that proposed different definitions for these disorders in relation to the particular behavior of their disease causing agent [69]. Fernandez-Borges and colleagues proposed the term "prion-like diseases", highlighting the similarities with prion protein self-perpetuating aggregation and spreading characteristics [70]. Aguzzi and Rajendran coined the term "prionoids" given that, unlikely prions, none of the other misfolded proteins presents high infectivity under natural conditions [71]. The lack of global scientific consensus on a unique definition is considerably dependent on the meaning of "infectivity". Very recently, Castilla proposed to consider "infection" as a process by which and exogenous or

spontaneously generated self-propagating agent interacts with the host – with or without causing damage and/or disease - as a consequence of its intrinsic capacity to replicate itself through diverse mechanisms [69].

Regardless the definitions used, there is much evidence that points out to the observation that many neurodegenerative diseases should effectively be considered prion-like disorders, notwithstanding the involvement of misfolded proteins being *bona fide* prions. For example, many of the mutant proteins causing heritable neurodegenerative diseases are found in insoluble aggregates known as amyloid deposits, such as amyloid-β plaques and neurofibrillary tangles (NTs) in AD, and Lewy bodies in PD. Moreover, both seeding and cell-to-cell transmission has been shown for AD, PD, ALS and AA amyloidosis [69]. As regards the latter, evidence exists for transmission of serum amyloid A (SAA) protein in a prion-like manner. SAA, an acute phase apolipoprotein reactant, can undergo N-terminal cleavage leading to the formation of amyloid protein A (AA) that is then deposited extracellularly and systemically as amyloid in vital organs. In humans, this process appears as a complication of chronic inflammatory diseases -such as rheumatoid arthritis- in which the plasma SAA levels are consistently high [72]. This stimulus is supposed to trigger an autonucleation-dependent process in which AA protein interacts with AA-derived fibril seeds, possibly leading to the formation of SAA oligomeric conformers. Regarding mice, it has been shown in secondary reactive amyloidosis that small quantities of misfolded AA aggregates can be orally transmitted between individuals and cause disease [73]. In addition, bovine AA-fibrils demonstrated to be able to induce AA- amyloidosis in mice, but with a reduced efficiency if compared to murine AA-fibril, a phenomenon reminiscent of the species barrier observed for prions [72].

Also, Huntington's disease (HD), an autosomal-dominant neurodegenerative disorder caused by an increased number of CAG repeats in the huntingtin gene, is characterized by the accumulation of abnormal aggregates largely composed of N-terminal fragments of the mutant huntingtin protein (mHTT) [74]. Furthermore, seeded aggregation occurs in mammalian cells. Indeed, internalized fibrillar polyglutamine peptide aggregates were able to selectively recruit soluble cytoplasmic sequence-homologous proteins [75]. In addition, transneuronal propagation of mHTT occurs in neural networks, both in cell models and in mice [74].

However, despite that sequence-specific nucleated protein aggregation constitutes the molecular basis of prion formation, one key feature of all prions is that they do not need to polymerize into fibrils, but can undergo self-propagation as oligomers, which are increasingly thought to represent the toxic species [68, 76].

Neurodegenerative diseases	Causative prion proteins	Percent inherited
Creutzfeldt-Jakob disease	PrP^{Sc}	10–20
Gerstmann-Sträussler-Scheinker		90
Fatal insomnia		90
Bovine spongiform encephalopathy		0
Scrapie		0
Chronic wasting disease		0
Alzheimer's disease	Aβ → tau	10–20
Parkinson's disease	α-synuclein	10–20
Frontotemporal dementia (FTD) Posttraumatic FTD, called chronic traumatic encephalopathy	tau, TDP43, FUS, C9orf72 (progranulin)	10–20
Amyotrophic lateral sclerosis	SOD1, TDP43, FUS, C9orf72	10–20
Huntington's disease	huntingtin	100

Table 3. Neurodegenerative diseases caused by prions or prion-like proteins (from Prusiner 2013)

Alzheimer's Disease (AD)

AD, the most common human neurodegenerative disease, is clinically defined by a progressive decline in memory and cognitive functions and neuropathologycally by atrophy and the accumulation of extracellular amyloid plaques made of aggregated amyloid-β (Aβ) peptide as well as intracellular neurofibrillary tangles composed of aggregated and hyperphosphorylated tau protein in the brain [77]. The Aβ peptide is generated by the subsequent cleavage of the amyloid precursor protein (APP) by β- and γ-secretase enzymes. The amyloid cascade hypothesis suggests that the accumulation and subsequent deposition of Aβ in the brain are the initiating pathological events in AD that lead to the downstream aggregation of tau [78]. In order to assess transmissibility of the disease, some years ago AD brain homogenate was intracerebrally inoculated into marmosets, leading to the development of Aβ amyloid plaques after ≈4 years and thus showing that the disease may be transmissible [79]. Similar results have been obtained using APP transgenic mice and rats (Table 4) [80-82]. Ultimately, using Aβ synthetic peptides, it has been shown that the disease agent consists solely of Aβ prions [83]. Like prions, Aβ seeds range in size from small, soluble, protease-sensitive aggregates to large, insoluble, protease-resistant fibrils. Moreover, the recent finding of the existence of "strain-like" Aβ morphotypes which retain their properties after repeated passaging between animals might at least partly explain the heterogeneous morphology, pathogenicity and progression of Aβ lesions and associated pathologies in AD [84]**.** Additionally, it further supports the concept of prion-like templated misfolding of Aβ [4].

Parkinson Disease (PD)

PD is the second-most common neurodegenerative disease whose symptoms include progressive bradykinesia and additionally one among rigidity, resting tremor

or gait disturbance [85]. PD is characterized by the widespread degeneration of subcortical structures of the brains, particularly dopamine neurons in the *substantia nigra pars compacta*, coupled with the accumulation of α-synuclein within Lewy bodies (LBs) in neurons [77]. The cause of cell death in PD is still not known, but proteolytic stress with the accumulation of misfolded proteins has been implicated [86]. α-synuclein, a 140-amino acid protein that is highly enriched in presynaptic nerve terminals, usually seems to be in an unstructured form when in aqueous buffers or in a α-helical-rich form when bound to membranes. However, α-synuclein can also adopt a β-sheet-rich conformation that easily polymerizes into fibrils when present in high concentration or in a mutant form and that is able to seed aggregation of the soluble protein [68, 87]. Furthermore, α-synuclein is a key player also in the pathogenesis of a group of other neurodegenerative diseases defined as synucleinopathies, comprised of dementia with Lewy bodies (DLB) and multiple system atrophy (MSA) [88]. It is likely that β-sheet-enriched α-synuclein can transmit through a cell-to-cell mechanism from neurons of patients with PD into transplanted fetal mesencephalic dopaminergic neurons inducing the formation of *de novo* Lewy bodies in the grafted cells [89]. Moreover, it has been shown that intracranial inoculation of brain extracts from DLB affected patients into wild-type mice is sufficient to cause the appearance of LBs/neurite-like α-synuclein *in vivo* [90]. Further evidence for α-synuclein “prions” come from studies with recombinant α-synuclein fibrils able to induce self-propagation as well as aggregation in transgenic mice [91] and in cell culture models [88] (Table 4). Moreover, in both wild-type mice and macaques, intranigral or intrastriatal inoculations of PD-derived LB extracts resulted in progressive nigrostriatal neurodegeneration together with intracellular and presynaptic accumulation of pathological α-synuclein in different brain areas, processes reminiscent of PD neuropathology [92]. Similar results were observed

after inoculation of TgM83(+/-) mice heterozygous for a mutant A53T alpha-synuclein transgene with brain homogenate from MSA affected patients [93]. Recently, the existence of distinct α-synuclein strains that differentially promote tau inclusion in neurons has been reported. Strains are a feature typical of prions, and this may explain the tremendous heterogeneity of synucleinopathies [94].

Amyotrophic lateral sclerosis (ALS)

ALS is a motor neuron degenerative disease affecting two out of 100,000 individuals worldwide, with death occurring within 3 years after diagnosis in over than 80% of cases [95]. The etiology of sporadic ALS is still unknown, however at least two proteins associated with this disease have to date demonstrated multiple aspects of prion-like activity: SOD1 and TDP-43 [96]. After the identification of SOD1 mutations in familial cases (less than 10% of the total) [97], some years later misfolded SOD1-containing inclusions were identified in both familial and some sporadic cases [98]. Moreover, it has been shown that the vast majority of sporadic ALS cases present TDP-43 cytosolic inclusion [99]. There is increasing evidence that all types of ALS are associated with misfolded and aggregated SOD1 [100, 101], which also seems to have the ability to impose its misfolded conformation to the native protein [102, 103] in a sequence/structure-dependent way, reminiscent of the species barrier phenomenon observed in classical prion diseases [103]. Similarly, hyperphosphorylated and aggregated TDP-43 is found mislocalized in cytoplasmic inclusions both in frontotemporal dementia (FTD) and ALS [104]. In addition, TDP-43 displays a C-terminal prion-like domain prone to misfolding which is essential for aggregation and toxicity [105] and also self-propagation and seeded aggregation properties have been observed (Table 4) [106, 107].

Tauopathies

Tau is a cytoplasmic protein that normally stabilizes microtubules, but it becomes hyperphosphorylated and prone to aggregation during the course of a variety of neurodegenerative diseases such as Pick's disease, progressive supranuclear palsy (PSP), argyrophilic grain disease (AGD) and corticobasal degeneration (CBD), collectively called tauopathies [68, 108]. In human adult brain, six tau isoforms ranging from 352 to 441 amino acids are produced through the alternative mRNA splicing from *MAPT* gene, but only the three forms containing four repeats are present in PSP, CBD and AGD [77].

Hyperphosphorylated tau is a component of the neurofibrillary tangles present in several neurodegenerative diseases, including AD. Also, tau mutations cause familial forms of FTD, indicating that tau protein dysfunction is sufficient to cause neurodegeneration and dementia. Evidence for mutant tau transmissibility also exists; indeed, the injection of brain homogenate from mutant P301S tau-expressing mice into transgenic wild-type expressing animals induced the formation of tau aggregates one year after inoculation (Table 4) [108]. More recently, intracerebral injections of brain extracts from various human tauopathies (AGD, PSP, CBD) have been shown to cause filament formation and neurodegeration in mutant tau-overexpressing mice, similar to what happens in the human diseases. Importantly, the induced formation of tau aggregates could be propagated between mouse brains [109]. As in the case of prions, tau seeds are of many sizes with small, soluble assemblies being the effective seeds [110]. Assembled tau can behave like prion; in the human AD brain, neurofibrillary lesions appear to spread along neural pathways from one brain region to another, following the opposite direction to Aβ plaques. Even though tau deposition is probably necessary, but not sufficient for AD

development, it is still unclear whether tau inclusions and Aβ plaques formation is independent from each other [77].

		Seeded aggregation in different model systems		
Protein	**Type of seed**	**Non-neuronal cells**	**Neuronal cells**	**Mice**
Aβ	Synthetic fibrils	Not tested	Not tested	Yes
	Mouse brain lysates	Not tested	Not tested	Yes
	Human brain lysates	Not tested	Not tested	Yes
Tau	Synthetic fibrils	Yes	Yes	Yes
	Mouse brain lysates	Not tested	Not tested	Yes
	Human brain lysates	Not tested	Not tested	Yes
α-Syn	Synthetic fibrils	Yes	Yes	Yes
	Mouse brain lysates	Not tested	Not tested	Yes
	Human brain lysates	Not tested	Not tested	Yes
TDP-43	Synthetic fibrils	Yes	Not tested	Not tested
	Human brain lysates	Not tested	Yes	Not tested
SOD1	Synthetic fibrils	Not tested	Yes	Not tested
PolyQ	Synthetic fibrils	Yes	Not tested	Not tested

Table 4. Summary of studies showing the transmissibility of non-prion protein aggregates. (modified from Guo 2014)

Non-human primate models

Several animal models have been employed to investigate neurodegenerative diseases, from invertebrates such as *Caenorhabditis elegans* or *Drosophila melanogaster* to numerous mouse strains and transgenics and several primate species as marmosets or macaques [111]. The transmissibility of human prion diseases to non-human primates was first shown in 1966 when kuru was successfully transmitted to chimpanzees and, a couple of years later, the same results were obtained for CJD [112, 113]. Later on, prion diseases were efficiently transmitted also to marmosets, macaques, gibbons and other primate species. In the 80's, oral transmission to primates was reported for kuru, CJD (both sporadic and

iatrogenic) and scrapie: the latter, however, to date has never been reported to be transmitted to humans [114]. Evidence also exists for the transmissibility of both GSS and FFI to primates. In general, all these studies indicated that efficiency of transmission depends on the primate species (host), the origin of the inoculated material (donor) as well as the inoculation route. These studies also indicated that incubation times varied greatly among different animals even within the same species [115]. After the BSE epidemic and the following characterization of vCJD, a second round of experiments involving primates was initiated, with the main objective to assess the zoonotic potential and risk of transmissibility of BSE and vCJD [116]. However, due to ethical considerations, the use of non-human primates was drastically reduced and therefore the number of animals used in these studies, mainly cynomolgus and rhesus macaques, is usually small [117]. Importantly, rhesus and cynomolgus macaques are evolutionary very close to humans, have a high degree of amino acid sequence identity in the PrP sequence and bear also the polymorphism at codon 129 [118]. In 1996 BSE was successfully transmitted by intracerebral inoculation, leading to a pathology which resembled vCJD: “florid” plaques in brain tissue, identical vCJD PrP^{Sc} type, and the same clinical presentation [119]. Years later, secondary transmission of macaque adapted BSE, both via intravenous or intracerebral inoculation, lead to a shortening in incubation time. In particular, as shown in figure 5, both routes of inoculation led to similar immunopathological lesions such as severe vacuolation and astrocytosis in the thalamus, together with a patchy distribution of vacuolation in the cortex with presence of dense plaques harboring, in some cases, a florid morphology. Importantly, the pattern of PrP deposition and plaque morphology were identical to those observed at first passage of BSE in adult inoculated animals, reminiscent of human vCJD immunopathology [53].

In 2004 oral transmission of BSE was accomplished, showing however a considerably longer incubation time [120]. The recent discovery of atypical forms of BSE, L-BSE/BASE and H-BSE, gave rise to questions about their transmissibility to humans. This has been shown for BASE both via intracerebral and oral inoculation, to macaques and lemurs, respectively [30, 121]. Showing that the BSE agent behaves similarly in humans and macaques, all these studies indicate that non-human primates are an excellent model for studying human prion diseases, since they reproduce all the main characteristics in terms of incubation time, clinical symptoms and neuropathological signs.

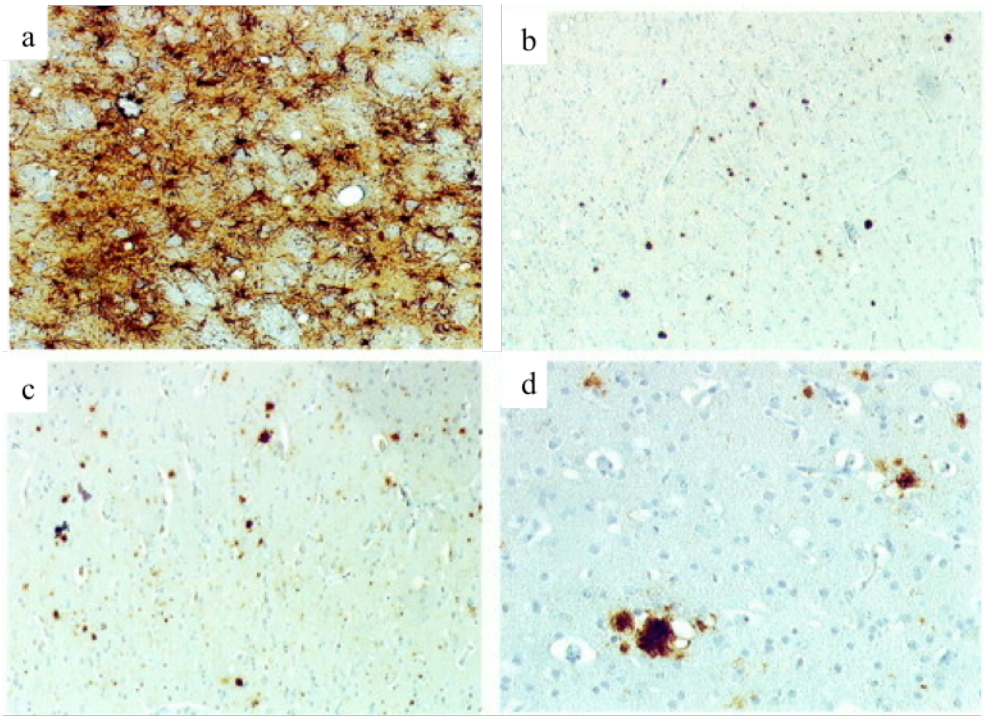

Figure 5. Immunopathology of BSE in cynomolgus macaques.
All panels show the pattern of PrP deposition with the 3F4 antibody, except *a,* which depicts glial fibrillary acidic protein immunohistochemistry. (*a*) Thalamus in BSE, ×10. (*b*) Cerebral cortex in BSE (i.v.), ×2.5. (*c*) Cerebral cortex in BSE (i.c.), ×2.5. (*d*) Immature florid plaque with a dense core of PrP surrounded by few vacuoles in the cerebral cortex (BSE, i.c.), ×20. (modified from Lasmezas 2001)

Diagnosis

Concerning sporadic CJD, the diagnosis is complicated by the fact that the clinical presentation is highly variable, often with a subacute onset. Most diagnostic criteria

are generally based on the recognition of progressive dementia together with two of the following symptoms: myoclonus, visual/cerebellar dysfunction, pyramidal/extrapyramidal signs, akinetic mutism. These criteria have been developed primarily for epidemiological purposes and therefore are not particularly sensitive early in the disease course as many of the symptoms are common also among the other neurodegenerative diseases. Brain MRI is currently the most accurate diagnostic criterion for early detection of sCJD, through the identification of characteristic hyperintensity patterns. Cerebrospinal fluid (CSF) instead is typically normal in sCJD, with only a mild and low specific increase in neuron-specific enolase 14-3-3 and total tau protein [47, 122]. Also, EEG generally shows relatively specific sharp waves in about two-thirds of sCJD patients [123].

Even for genetic prion disease, the diagnosis poses some issues. Indeed, a single *PRNP* mutation can be associated with different phenotypes and up to 60% of the genetic cases do not have a positive family history, either due to previous AD or PD misdiagnosis or to incomplete penetrance [124]. Recently, CSF RT-QuIC showed modest sensitivity but high specificity for sCJD and, more interestingly, RT-QuIC using nasal brushings from 15 sCJD and 2 fCJD patients was able to detect PrP^{Sc} in all of the samples [125-127].

Acquired prion diseases, mainly iCJD and vCJD, are less common in comparison to sporadic cases but, due to their higher potential for human-to-human transmission, their diagnosis is of particular relevance. Concerning iCJD, the main indication would come from the report of the use of cadaveric-derived hormones or tissues from afterwards diagnosed CJD patients. Variant CJD is typically distinguished from sCJD by its younger age of onset and prominent early psychiatric symptoms that often precede neurologic symptoms. While EEG rarely shows anomalies, brain MRI usually shows the characteristic “pulvinar sign”, a highly specific hyperintense signal

in the posterior thalamus [128]. Recently, both a novel stainless steel powder-based blood test and a PMCA-based urine test were able to detect vCJD with high specificity [129, 130]. Nevertheless, it is unclear whether these tests can be used for preclinical diagnosis of asymptomatic CJD patients. Nonetheless, for all CJD cases, current criteria for definite diagnosis require brain biopsy or autopsy for evidence of positive PrP^{Sc} tissue immunoreactivity.

Therapy

Despite all active efforts, there are no currently available drugs to change disease progression of prion disorders. Symptomatic treatment is the only available option, including antipsychotics such quetiapine, clonazepam to treat myoclonus and selective serotonin re-uptake inhibitors (SSRIs) to treat depression [131].

Clinical trials have been done with flupirtine and pentosan polysulfate, but both have failed to show consistent benefits. Two recently published randomized, double blind placebo-controlled trials with quinacrine and doxycycline were, as well, unable to demonstrate significant improvements [132, 133]. Despite this, doxycycline is currently being tested in presymptomatic patients from a family with FFI in order to assess whether the drug is able to delay the onset of the disease [47].

Currently, drug discovery for the identification of compounds for the treatment of prion diseases follows two main strategies. One is the so-called small molecule design, whose rationale relies in the ability of a given compound to interfere with PrP^{C} conversion into PrP^{Sc} thereby blocking self-amplification of misfolded proteins and, hopefully, halting the pathology spreading [134]. The other option is to investigate the molecular mechanism underlying the onset and the progression of prion disorders, identifying the specific altered pathways that may be therefore become potential targets for new drugs [135].

Functional genomic approach in prion disorder

For early ante-mortem diagnosis of prion diseases, neither specific biomarkers nor effective therapeutic targets have been identified. Increasing evidence suggests that other genes in addition to *PRNP* also contribute to the genetic susceptibility of acquired TSEs [26]. In this context, microarray-based gene expression analysis offer unique tools to approach neurodegenerative disorders. In particular, transcriptome profiling can be used to find altered transcripts in response to pathogens and select potential targets for novel therapeutic approaches [136]. In the prion biology field, several studies have been performed in order to identify differentially expressed genes (DEGs) in healthy and diseased systems, such as cell cultures and mouse models in addition to sheep and cattle [26].

These analyses identified molecular pathways that are altered upon prion infection, including cholesterol synthesis, apoptosis, lysosomal pathway, immune and inflammation response [136]. The commonalities among prion diseases and PD and AD disorders highlight either similar neurodegenerative molecular mechanisms or similar pathological secondary events. Comparative analyses of altered pathways in prion diseases, PD and AD could expose characteristic gene targets that could be used as potential diagnostic biomarkers for risk determination and also as general indicators of disease progression [26, 136].

AIM OF THE WORK

To date, a number of studies have been carried out to investigate the gene expression alterations occurring in prion-infected organisms (reviewed in [26, 135]), but most involved animal models such as mice [137-142], sheep [143-147] and cattle

[27, 28, 148-151]. Some studies have been performed on non-human primates [37, 152-155], but none have investigated the genomic outcome of prion infection.

In this study, I performed a whole transcriptome gene expression analysis on BSE-infected cynomolgus macaques (*Macaca fascicularis*), which are an excellent model for studying human acquired prion disease [154-158]. Indeed, BSE can be transmitted either intracranially or orally to these animals leading to a disease that is very close to the human one with regards to preclinical incubation time, clinical symptoms and pathophysiology [120, 156].

The initial objectives of the present work were to identify the main genes that are differentially expressed in the frontal cortex of intracranially infected monkeys compared to non-infected ones. This analysis would help to shed some light on the biological processes underlying the pathogenesis of human prion diseases that may therefore become potential targets for both diagnostic and therapeutic strategies.

Following the encouraging results obtained in monkeys, I decided to further confirm the dysregulation pattern in human prion disorders. For this second analysis I investigated the specificity of the identified gene signature for CJD in comparison to both healthy subjects and to other neurodegenerative diseases such as AD and PD. This approach could shed some light not only on prion disease molecular mechanisms, but also on neurodegeneration processes in general.

MATERIALS AND METHODS

Ethics statement

Ethical approval for the animal study was released by the Lower Saxony Ministry for consumer protection and food safety (509.42502/08/07.98). Animal experimentation was performed in accordance with section 8 of the German Animal Protection Law in

compliance with EC Directive 86/609. Ethical committee authorization for human samples is currently under approval.

Animals

Cynomolgus macaques (Macaca fascicularis) were obtained from the Centre de Recherche en Primatologie, Mauritius and maintained in social groups of six monkeys housed in a microbiological containment BSL3 facility. Six 1-year old female cynomolgus macaques (A1-A6), all MM homozygous at codon 129, were intracerebrally inoculated with 50 mg of bovine BSE-positive brain stem material derived from an EU-standard inoculum. The inoculum was a pool of homogenized bovine brain stems from 11 naturally infected, histopathologically and immunohistochemically confirmed cases of BSE. The BSE stock tested positive for PK-resistant prion protein by Western blotting. Inoculation was performed via slow injection of 250 µl of a 20% BSE brain homogenate (w/v) diluted in sucrose into the right hemisphere through the dura mater into the caudo-putamen region. The preclinical incubation time was on average 1,100 days. One additional cynomolgus macaque (B6) was orally challenged with the same material; inoculation was performed *per os*, as single dose. The preclinical incubation time of this animal was 1950 days. Brain material from age-and sex-matched non-infected cynomolgus macaques (CovA, CovB, CovC, CovDI, CovDII) was obtained from Covance Laboratory Münster GmbH and processed with the same protocol. It should be taken into account that the diet and housing conditions of the experimental and the control animals were not perfectly identical. These differences may have led to some inter-individual variations among the animal groups.

Patient samples

A total of 37 brains were collected. 16 of them were from sCJD affected patients, 11 were Type 1, 5 were Type 2. 6 brains were from vCJD patients (one from Italy and five from France), 5 were from iCJD ones (growth hormone treatment), 6 were from non-CJD neurodegenerative disease affected patients (NEG), 4 were from healthy subjects (CTRL). All vCJD patients were MM homozygous at codon 129, while iCJD cases were either MM homozygous (3) or MV heterozygous (2).

All the samples were kindly provided by Fondazione I.R.C.C.S Istituto Neurologico Carlo Besta, (via Celoria 11, Milan, Italy) with the exception of 5 vCJD and all iCJD samples that were provided by ICM-Hôpital Pitié-Salpêtrière (47, Boulevard Hôpital, 75013 Paris – France) and two control samples that were kindly provided by University of Verona, Department of Neurological and Movement Sciences, Policlinico G.B. Rossi (P.le L.A. Scuro 10, Verona, Italy).

Tissues and RNA extraction

Seven BSE-infected cynomolgus macaques at advanced stage of disease and five non-infected control animals were sacrificed, and for each animal one hemisphere of the brain was dorso-ventrally sliced and immediately frozen on dry-ice. The *gyrus frontalis superior* region was macroscopically identified on the frozen tissue and removed via a biopsy stamp**.** Tissues were manually homogenized with micro pestles (Kisker Biotech GmbH) and total RNA was isolated using TRIzol (Invitrogen). Following RNA isolation, DNase I digestion was performed using 1 unit of enzyme per µg RNA (Fermentas) for 30 min at 37°C and then heat inactivated for 5 min at 95°C followed by precipitation with Sodium Acetate / Ethanol. RNA was checked for quantity and purity on a Spectrophotometer 2000 (PEQLAB) and for integrity of the

18S and 28S ribosomal band by capillary electrophoresis using the 2100 Bioanalyzer (Agilent Technologies).

Regarding human samples, total RNA was isolated from about 100mg of frontal cortex from each of the following individuals: vCJD (n=6), iCJD (n=5), sCJD T1 (n=11), sCJD T2 (n=5) affected patients; CJD negative patients affected by other neurodegenerative diseases (NEG) (n=6) and controls (n=4). The brain material was manually homogenized with pestles and glass vessels using TRIzol (Invitrogen). Then, RNA was extracted with PureLink RNA Mini Kit (Life Technologies) and on-column DNA digestion was performed using PureLink DNase Set (Life Technologies). RNA was checked for quantity and purity on a NanoDrop 2000 spectrophotometer (Thermo Scientific) and integrity on a 2100 Bioanalyzer (Agilent Technologies).

Immunoblot analysis

PK-treated (50 µg/mL for 1 hour at 37°C) and untreated brain homogenates were separated on 12% Bis/Tris Acrylamide gels (NuPAGE, Invitrogen) and transferred to nitrocellulose membranes (Protran, Schleicher & Schüll, Germany). Detection of macaque PrP^{Sc} was performed using the monoclonal anti-PrP antibody 11C6 and a HRP-conjugated anti-mouse IgG-antibody (Sigma-Aldrich, Germany). Signal was visualized using a chemiluminescent substrate (Super Signal West Pico, Pierce) and high sensitivity films (Amersham). Densitometric analysis of PrP^{Sc} was performed using the Image J program 1.37v.

Microarray analysis using the GeneChip® Rhesus Macaque genome array

Microarray analyses using the GeneChip® Rhesus Macaque genome array samples were labeled using the GeneChip® 3'IVT Ex- press Kit (Affymetrix®). Reverse transcription of RNA was achieved using 500 ng of total RNA to synthesize first-strand cDNA. This cDNA was then converted into a double-stranded DNA template for transcription. In vitro transcription included a linear RNA amplification (aRNA) and the incorporation of a biotin-conjugated nucleotide. The aRNA was then purified to remove un-incorporated NTPs, salts, enzymes, and inorganic phosphate. The labeled aRNA of each animal was fragmented (50–100 bp) and hybridized to a GeneChip® Rhesus Macaque Genome Array (Cat N° 900656; Affymetrix®). The degree of fragmentation and the length distribution of the aRNA were checked by capillary electrophoresis using the Agilent 2100 Bioanalyzer (Agilent Technologies). The hybridization was performed for 16 h at 1 × g and 45°C in the GeneChip® Hybridization Oven 640 (Affymetrix®). Washing and staining of the arrays was performed on the Gene Chip® Fluidics Station 450 (Affymetrix®) according to the manufacturer's recommendations. The antibody signal amplification, washing and staining protocol were used to stain the arrays with streptavidin R-phycoerythrin (SAPE; Invitrogen). To amplify staining, SAPE solution was added twice with a biotinylated anti-streptavidin antibody (Vector Laboratories, Burlingame, CA, USA) staining step in-between. Arrays were scanned using the GeneChip® Scanner 3000 7G (Affymetrix®).

Microarray data analysis

Intensity data from the CEL files were imported to the Partek® software including a quality control based on internal controls. All chips passed the quality control and

were analyzed using the Limma package [159] of Bioconductor [160, 161] and the Partek® software. The microarray data discussed in this paper were generated conforming to the MIAME guidelines and are deposited in the NCBI's Gene Expression Omnibus (GEO) database [162]. They are accessible through GEO series accession number GSE52436 (see section: Availability of supporting data). The microarray data analysis consisted of the following steps: 1. quantile method normalization, 2. global clustering and PCA-analysis, 3. fitting the data to a linear model, 4. detection of differential gene expression and 5. over-representation analysis of differentially expressed genes. Quantile-normalization was applied to the log2- transformed intensity values as a method for between array normalization to ensure that the intensities had similar distributions across arrays. For cluster analysis, we used a hierarchical approach with the average linkage-method. Distances were measured as 1 - Pearson's Correlation Coefficient. The PCA was performed using the princomp-function in the Partek® software. To estimate the average group values for each gene and assess differential gene expression, a simple linear model was fitted to the data, and group-value averages and standard deviations for each gene were obtained. To find genes with significant expression changes between groups, empirical Bayes statistics were applied to the data by moderating the standard errors of the estimated values [159]. P-values were obtained from the moderated t-statistic and corrected for multiple testing with the Benjamini–Hochberg method [163]. The p-value adjustment guarantees a smaller number of false positive findings by controlling the false discovery rate (FDR). For each gene, the null hypothesis, that there is no differential expression between degradation levels, was rejected when its FDR was lower than 0.05. Because no candidates appeared using FDR 0.05, we made the selection using another p-value (unadjusted p-value ≤ 0.005) and a fold change ≥ |2|.

Reverse transcription and qPCR

Quantitative reverse transcription real-time PCR (RT-qPCR) was performed using gene-specific primer pairs. For macaque samples, cDNA synthesis was accomplished using 100ng RNA, 10ng random hexamer primer, 2 mM dNTPs, 0.5 U RNase inhibitor and 5 U reverse transcriptase (Bioline) in 1 x reaction buffer. For human samples, cDNA was obtained using 3µg RNA, 1µl 50µM oligo$(dT)_{20}$, 1µl 10mM dNTP mix, 40 U RNAse inhibitor and 200 U Superscript III Reverse Transcriptase (Life Technologies).

For each sample a negative control was performed by omission of the reverse transcriptase (-RT control). The cDNA was diluted 1:10 (macaques) or 1:15 (humans) prior to RT-qPCR. The reaction mix included 2x iQ ™ SYBR® Green Supermix (Bio-Rad Laboratories, Inc.) and 400 nM of the corresponding forward and reverse primer (Sigma). Technical triplicates were quantified on an iQ5 Multicolor Real-Time PCR Detection System (Bio-Rad Laboratories, Inc.). All primers used for RT-qPCR are listed in Table 5 and 6.

Gene	Chromosome	Primer and probe sequence		Amplicon length (bp)	Accession number
ACTB	3	F:	GTTGCGTTACACCCTTTCTTG	146	NM_001033084.1
		R:	CTGTCACCTTCACCGTTCC		
		P:	ACAAGATGAGATTGGCATGGC		
GAPDH	11	F:	CCTGCACCACCAACTGCTTA	74	NM_001195426.1
		R:	CATGAGTCCTTCCACGATACCA		
		P:	CTGGCCAAGGTCATCCATGA		
AKR1C1	9	F:	CCGCCATATTGATTCTGCTCAT	132	NM_001195574.1
		R:	TGGGAATTGCACCAAAGCTT		
NCAM1	14	F:	GAGCAAGAGGAAGATGACGAG	150	XM_001083697.2
		R:	GACTTTGAGGTGGATGGTCG		
NR4A2	12	F:	CCAGTGGAGGGTAAACTCATC	145	NM_001266910.2
		R:	AGGAGAAGGCAGAAATGTCG		
USP16	3	F:	GCAGAACTTGTCACAAACACC	146	NM_001260999.2
		R:	CTAAAGTAAGAGGGCCTGGAG		
SAP18	17	F:	GGAAATGTACCGTCCAGCGA	109	NM_001261034.1
		R:	TGCCCTTCTTTCTAGCTTCTGG		
IRF3	19	F:	TGGGTTGTGTTTAGCAGAGG	90	NM_001135797
		R:	GAAAAGTCCCCAACTCCTGAG		
SERPINA3	7	F:	GCTGGGCATTGAGGAAGTCT	123	NM_001195350.1
		R:	GTGCCCTCCTCAGACACATC		
		P:	TTCCTGGCCCCTGTGATCCC		
HBA2	20	F:	CGACAAGAGCAACGTCAAGG	126	NM_001044724.1
		R:	TCGAAGTGGGGGAAGTAGGT		
		P:	TGGCGAGTATGGTGCGGAGG		
HBB	14	F:	GTCCTCTCCTGATGCTGTTATG	102	NM_001164428.1
		R:	TTGAGGTTGTCCAGGTGATTC		
		P:	AAGTGCTTGGTGCCTTTAGTGATGG		
APOC1*	19	F:	TTCTGTCGATGGTCTTGGAAG	138	AK240617.1
		R:	CACTCTGTTTGATGCGGTTG		
		P:	TGGAGGACAAGGCTTGGGAAGTG		
TTR	18	F:	TCACTTGGCATCTCCCCATTC	114	NM_001261679
		R:	GGTGGAATAGGAGTAGGGGCT		
		P:	ATCGTTGGCTGTGAATACCACCTCTG		
ALAS2	X	F:	TCCCTTCATGCTGTCGGAAC	108	XM_002806252.1
		R:	GAGCTAGGCAGATCTGTTTTGAA		
RHAG	4	F:	AGGCAAGCTCAACATGGTTC	87	NM_001032815.1
		R:	GGGTGAATTGCCATATCCGC		

Table 5. Genes analyzed in macaques by RT-qPCR
Primers (F: forward and R: reverse) and probes (P: probe) used for gene amplification, amplicon length, and GenBank accession numbers of the macaque cDNA sequences used for primer design. All primers were designed according to the genome sequence of *Macaca mulatta*.
*Apolipoprotein C-I (*APOC1*) primers and probe were designed according to the genome sequence of *Macaca fascicularis* because the *Macaca mulatta* mRNA sequence was not annotated (TSA *Macaca mulatta* Mamu_450725, accession number: JV045807.1). Homology between the two sequences was 99%.

Gene	Chromosome	Primer sequence		Amplicon length (bp)	Accession number
ACTB	7	F:	AGAGCTACGAGCTGCCTGAC	184	NM_001101.3
		R:	AGCACTGTGTTGGCGTACAG		
RPL19	17	F:	CTAGTGTCCTCCGCTGTGG	169	NM_000981.3
		R:	AAGGTGTTTTTCCGGCATC		
HBB	11	F:	AGGAGAAGTCTGCCGTTACTG	190	NM_000518.4
		R:	CCGAGCACTTTCTTGCCATGA		
SERPINA3	14	F:	TGCCAGCGCACTCTTCATC	167	NM_001085.4
		R:	TGTCGTTCAGGTTATAGTCCCTC		
HBA1/	16	F:	GCTCTGCCCAGGTTAAGGG	160	NM_000558.4
HBA2		R:	CAGTGGCTTAGGAGCTTGAAG		NM_000517.4
APOC1	19	F:	GTCACCCTTCAGGTCCTCAT	145	NM_001645.3
		R:	AACACACTGGAGGACAAGGC		
TTR	18	F:	AGCCGTGGTGGAATAGGAG	131	NM_000371.3
		R:	CTTACTGGAAGGCACTTGGC		
PRNP	20	F:	CTTCTTGCAGAGGCCCAG	113	NM_000311.3
		R:	CGAGCTTCTCCTCTCCTCAC		
ALAS2	X	F:	TGTCCGTCTGGTGTAGTAATGA	150	NM_001037968.3
		R:	GCTCAAGCTCCACATGAAACT		
RHAG	6	F:	AGGCAAGCTCAACATGGTTC	87	NM_000324.2
		R:	GGGTGAATTGCCATATCCGC		

Table 6. Genes analyzed in humans by RT-qPCR
Primers (F: forward and R: reverse) used for gene amplification, amplicon length, and GenBank accession numbers of the human cDNA sequences used for primer design.

The cycling conditions included an initial denaturation of 3 min at 95°C then 45 cycles at 95°C for 15 sec and 58°C for 1 min. Differential gene expression of candidates was normalized to *GAPDH* and *ACTB* (macaques) or *ACTB* and *RPL19* (humans) expression. –RT controls were included in the plates for each primer pair and sample. The relative expression ratio was calculated using the $2^{-\Delta\Delta C_T}$ method [164]. Statistical significance was calculated with the unpaired student t-test (p<0.05). Fold change values smaller than 1 were converted using the equation -1/fold change, for ease of representation. Melting curve analysis and gel electrophoresis of amplification products was performed for each primer pair to verify that artificial

products or primer dimers were not responsible for the obtained signals. Some results on macaque samples were further confirmed using TaqMan® MGB probes and iQ™ Multiplex Powermix (Bio-Rad Laboratories, Inc.). The primer sequences, the reaction setup and the cycling conditions were the same described above. The FAM-probes used are listed in Table 5.

Immunohistochemistry on human brain slices

Immunohistochemistry analysis was performed on alcolin-fixed paraffin-embedded 7µm-thick frontal cortex brain slices. In order to eliminate paraffin, glass slides were kept at 56° C for 20 min and then immersed in xylene for 20 min. After this, slides were re-hydrated using decreasing ethanol concentrations (from 100% to 70%) for 5 min each and lastly put in water for 10 min. Antigen retrieval was achieved with pH6 citrate buffer (100° C for 20 min). Endogenous peroxidase blocking was accomplished by treating slides with 6% H_2O_2 for 20min. Goat serum (1:20 in PBS-Tween) was incubated for 20 min at RT, and then primary antibodies were incubated overnight. After washing the slides with PBS-tween (3 times, 2 min each) secondary anti-rabbit HRP-polymer Ab EnVision™ (Dako) was incubated for 1h at RT. After washing, DAB was added to each slide and, after development, it was blocked in water. Counterstaining with hematoxylin was also performed in some cases. Antibodies and dilutions used were: Anti-TTR (1:200), Anti-APOC1 (1:100), Anti-SERPINA3 (1:1000), Anti-HBB (1:100), from Sigma, Anti-HBA2 (1:50) from Thermo Scientific.

Availability of supporting data

The microarray data set supporting the results illustrated here is available in the Gene Expression Omnibus (GEO) repository

[http://www.ncbi.nlm.nih.gov/geo/query/acc.cgi?token=wnmjowqqhrcpzod&acc=GSE52436]. The DEGs were analyzed for their functions, pathways and networks using Ingenuity Pathways Analysis (IPA) [http://www.ingenuity.com/products/ipa/try-ipa-for-free].

RESULTS

PrP^{Sc} content in brain tissue of macaques

PrP^{Sc} presence in brain homogenate of 6 BSE-infected macaques was assessed by Western Blot (Figure 6).

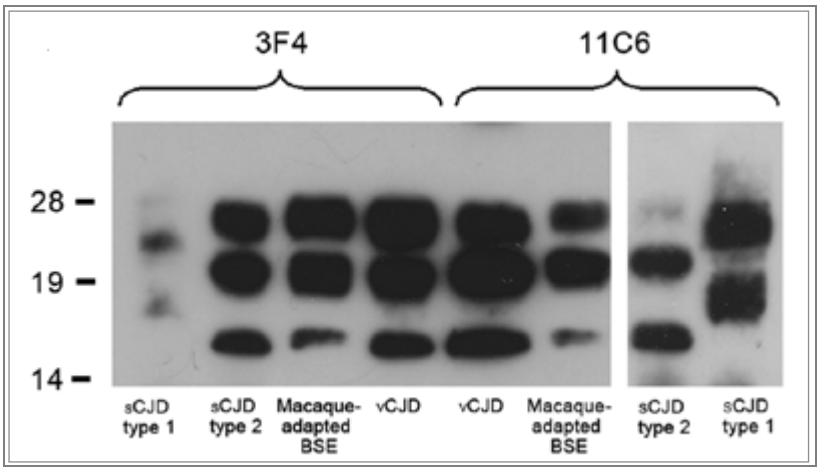

Figure 6. PrP^{Sc} profile of macaque-adapted BSE in comparison to human CJD.
Brain homogenates from human sCJD type 1, sCJD type 2, vCJD, and BSE-infected macaques were subjected to PK treatment, separated on 12% sodium dodecyl sulfate–polyacrylamide gel electrophoresis, and blotted onto nitrocellulose membranes. PrP^{Sc} for human and macaque brain was detected with the widely used monoclonal antibody 3F4 or with 11C6. (from Montag 2013)

Densitometric analysis of the monoglycosylated band revealed that the relative amount of PrP^{Sc} strongly differed between individual macaques. We hypothesized that this variation was dependent either on the preclinical incubation time or rather it corresponded to the gradual accumulation of PrP^{Sc} during the clinical phase of disease as reported for sCJD [165, 166]. As anticipated, we found a significant

correlation between PrP^{Sc} content and the duration of the symptomatic phase (Figure 7).

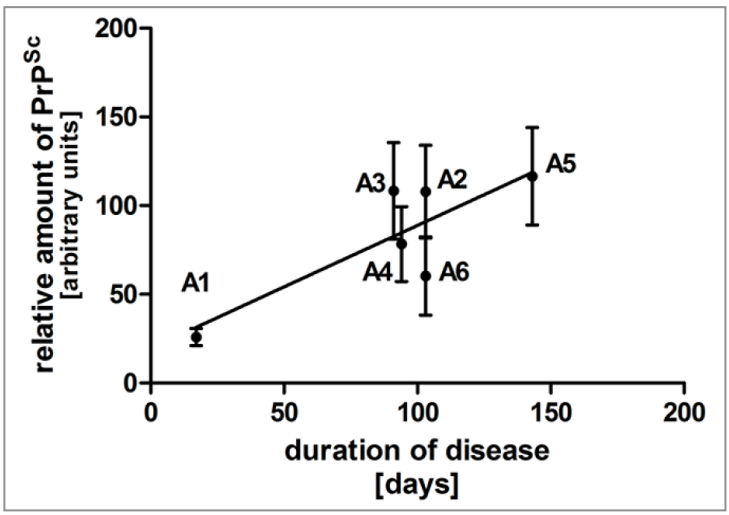

Figure 7. Correlation between PrP^{Sc} content and duration of clinical phase.
WB analysis from PK-treated homogenates of brain samples derived from BSE-infected macaques was performed. The monoglycosylated bands of PrP^{Sc} were analyzed by densitometry. Relative amounts of PrP^{Sc} from brain homogenates were averaged and correlated to the disease duration.

This correlation analysis included only the 6 intracranially inoculated macaques. Given that these animals were housed within the same social group, environmental factors, which could influence the disease course and duration, were identical. These factors can slightly differ for the orally inoculated animal, which was therefore omitted from this analysis. All infected animals were sacrificed at an advanced stage of prion disease; the details of their clinical course have been previously described [155]. Briefly, animal A1 showed the shortest duration of disease (17 days) and a short pre-clinical incubation time (931 days) together with the lowest PrP^{Sc} content, while animal A5 showed the longest survival period (143 days), compared to an average clinical phase of about 90 days, together with the highest PrP^{Sc} content and the second longest pre-clinical phase (1340 days). In general, animals A1, A3, A4 and A6 were considered as early onset, while A2 and A5 were late onset, the difference

between the two groups being statistically significant. Early symptoms included coordination impairment and ataxia, followed by dysmetria and dementia [155]. As regards B6, the only orally inoculated animal, limited data are available. However, from another study involving animals orally infected with the very same inoculum as the one used in the present study, it is known that the main neurological symptoms (gait ataxia, disturbed social behavior or loss of social status ranking, panic-stricken responses provoked by optical stimuli, reduced escape reactions in the presence of humans, abnormal shrieking, decreased competitiveness, restlessness) are present in BSE-infected monkeys regardless of the route of infection, and the same for spongiosis and PrP^{Sc} deposits [158]. Of note, no florid plaques were observed; neither in IC nor in orally inoculated animal brains, in contrast with what has been shown in a similar study involving IV and IC infected monkeys [53, 119]. It should be considered however that in Yutzy *et al.* the IC inoculum was a low-dose one (5mg) while in our case (and in Lasmezas *et. al* one too) it was ten times higher. Nevertheless, some evidence (orally infected animals showed absence of the "stage 1" characterized by disturbed body growth, no neurological signs, CSF-negative for 14-3-3 proteins) exist that the clinical course may be influenced by the inoculation route [158].

Microarray analysis of brain gene expression in cynomolgus macaques

To investigate differential mRNA expression in BSE-infected macaques (*Macaca fascicularis*) we used brain samples from 6 animals that were intracranially challenged [155]. One macaque that was orally infected with 50 mg BSE-homogenate was also included in our study. For comparison purposes, we used 5 brain samples derived from non-infected age- and sex-matched control macaques.

RNA was isolated from the *gyrus frontalis superior* of all animals and checked for quality by nano-scale electrophoresis, which resulted in an overall RNA Integrity Number (RIN) of about 6. This value suggest that the RNA was at least partially degraded; one possible explanation for the limited RNA integrity in the samples may reside in the procedure used to remove the *gyrus frontalis superior* region from the frozen tissue slice. Indeed, the biopsy stamp was attached to a cordless screwdriver that was used to drill a borehole in the frozen tissue block of +/- 1 cm height. This technique was preferred in order to ensure that the tissue did not thaw; however, the local heat induced by the rotating biopsy stamp may have led to substantial degradation of the RNA. Nevertheless, human brain material showing a comparable RIN value was successfully used for similar studies [167]. All samples were analyzed using the GeneChip® Rhesus Macaque Genome Array (Affymetrix®) that contains more than 50,000 rhesus probe sets to enable gene expression studies of *Macaca mulatta* transcriptome interrogating more than 47,000 transcripts. The genomes of *M. mulatta* and *M. fascicularis* display a small genetic divergence of around 0.4% [168] [169], which confidently allows the detection of homologue transcripts with a high specificity.

Raw data were quality checked and analyzed using Affymetrix® proprietary analysis tools, a hierarchical clustering performed and a heat map generated. Then the signals were aligned to the annotation library and a spreadsheet containing gene symbols, *p*-values and expression fold changes was created. Microarray data were submitted to Gene Expression Omnibus (GEO). The bioinformatics analysis identified 300 probe sets that were up- or down-regulated about twofold (≥| 1.95|). Since among them no candidate appeared using FDR 0.05, we chose as criteria an unadjusted *p*-value of ≤0.005 together with a fold change ≥| 2.0|. Additional table 1

lists the resulting 86 probe sets that were then used to generate the heat map shown in Figure 8.

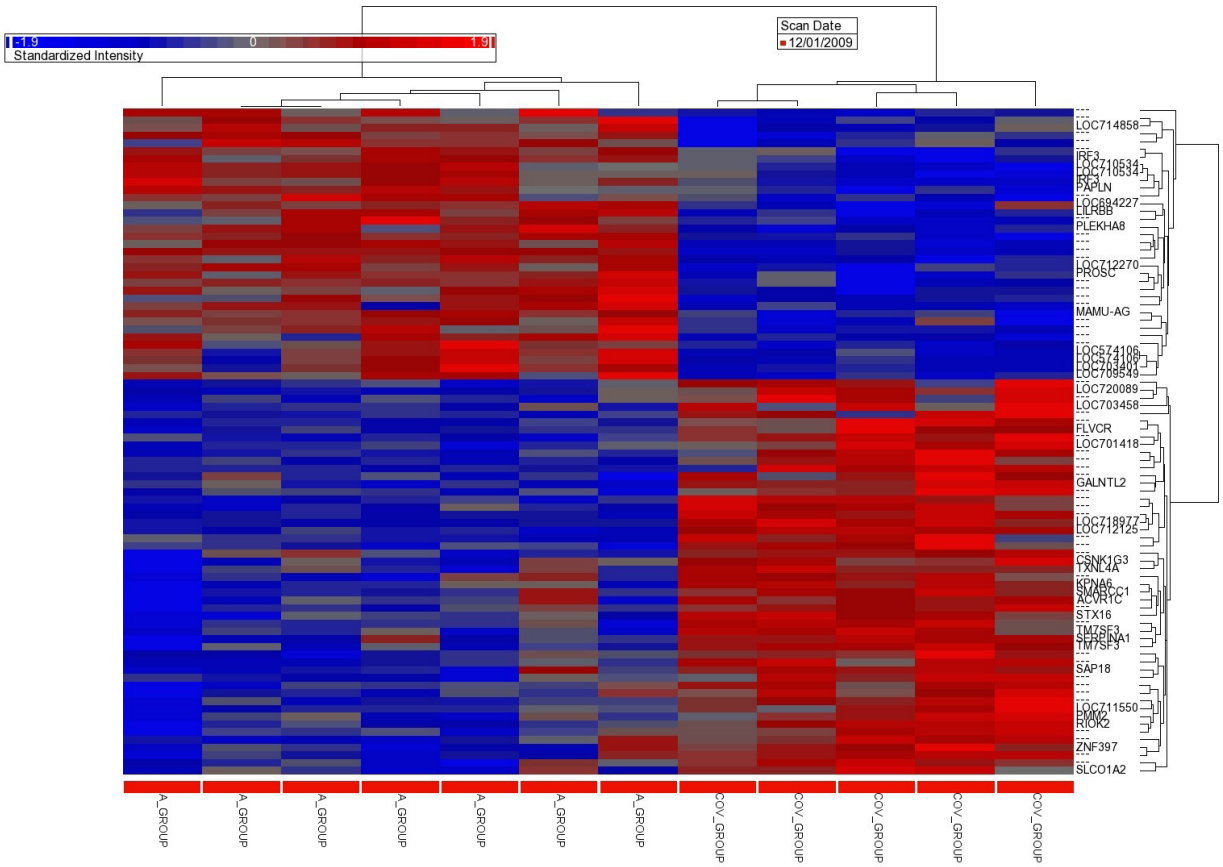

Figure 8. Condition trees of the clustering analysis
The cluster analysis was performed using a hierarchical approach with the average linkage-method (R and Partek® Software, Partek® Inc.): 86 probe sets showed a differential expression with FC ≥ 2. The color represents the level of expression (red: up-regulation, blue: down-regulation) and the sample information is listed across the bottom. The names of the known genes are indicated. More details on all genes are reported in Additional file

Functional classification of differentially expressed genes (DEGs) in macaques

We used the Ingenuity Pathways Analysis (IPA®, see section: Availability of supporting data) to annotate genes according to their functional relationships and to determine potential regulatory networks and pathways. Among the 300 differentially expressed (about twofold, ≥| 1.95|) probe sets identified, 105 were associated to mapped IDs. Of them, 53 were identified as network eligible genes, while 86 were identified as function eligible genes. We would like to clarify that the designation of

functional classes in this study cannot be considered definitive or exclusive, given that the annotation of gene function is incomplete and that the same multifunctional gene products can be involved in several different cellular pathways.

As a first step we identified key biological functions and/or diseases that contain a disproportionately high number of genes from the DEGs list compared to the total gene population from the microarray. The analysis was initiated by identifying the top categories (p<0.01) of DEGs within three main classes (Table 7). In the "Diseases and Disorders" class the top scoring categories were cancer and developmental disorder, while within the "Molecular and Cellular functions" class most genes were involved in cellular development and cell death/survival. The two main categories for the "Physiological System Development and Function" class were tissue morphology together with nervous system development and function.

Top Bio Functions

Diseases and Disorders

Name	p-value	# Molecules
Cancer	1.13E-05 - 9.19E-03	58
Developmental Disorder	2.10E-05 - 9.19E-03	24
Hematological Disease	2.10E-05 - 6.83E-03	7
Organismal Injury and Abnormalities	6.76E-05 - 9.19E-03	22
Reproductive System Disease	7.30E-05 - 9.19E-03	22

Molecular and Cellular Functions

Name	p-value	# Molecules
Cellular Development	4.22E-06 - 9.19E-03	35
Cellular Assembly and Organization	3.30E-05 - 9.19E-03	13
DNA Replication, Recombination, and Repair	3.30E-05 - 1.57E-03	10
Cell Death and Survival	5.67E-05 - 9.19E-03	35
Lipid Metabolism	1.17E-04 - 9.19E-03	19

Physiological System Development and Function

Name	p-value	# Molecules
Tissue Morphology	9.70E-08 - 9.19E-03	30
Skeletal and Muscular System Development and Function	4.22E-06 - 9.19E-03	17
Nervous System Development and Function	1.04E-05 - 9.19E-03	26
Organ Morphology	2.10E-05 - 9.19E-03	17
Hematological System Development and Function	5.31E-05 - 9.19E-03	22

Table 7. Top three classes of key biological functions and/or diseases.

Subsequently, genes were clustered in relation to the main pathways they belong to: the top three canonical pathways (*p*-value < 0.005) in our DEGs list were LXR/RXR activation, which is associated with lipid metabolism and transport, acute phase response signaling and the neutral pathway of bile acid biosynthesis, which is also involved in lipid metabolism and is a major route of cholesterol catabolism (Figure 9).

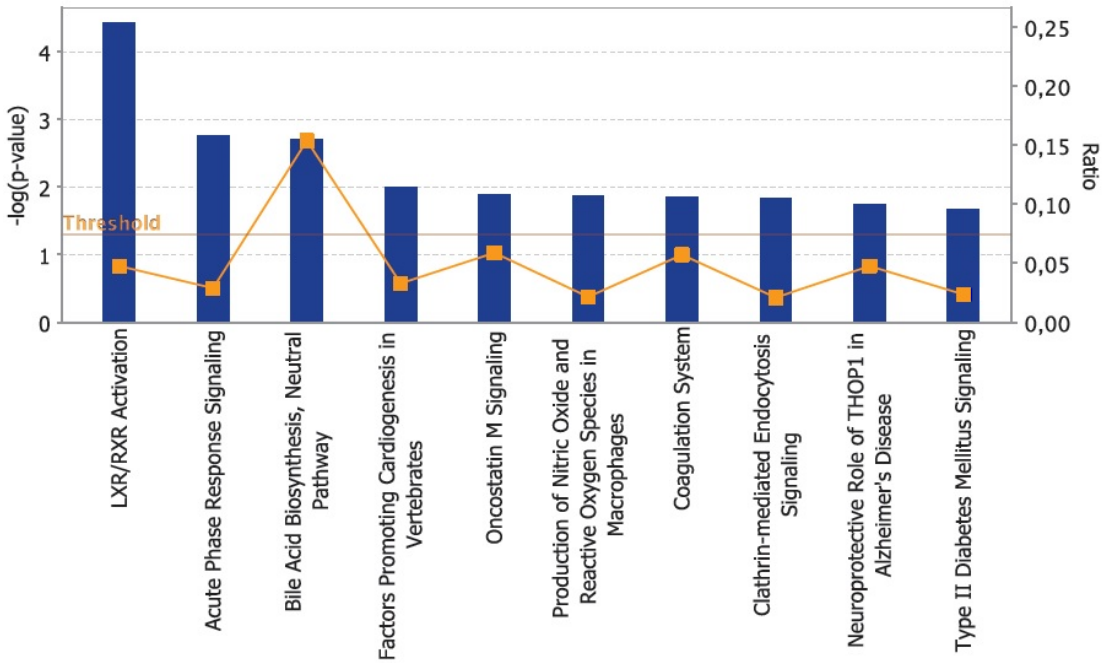

Figure 9. Top 10 significant canonical pathways over-represented in the DEGs list

Identification of biologically relevant networks in macaques

To further investigate the global expression response to BSE infection and to define interactions among the identified specific pathways containing the regulated genes, potential networks of interacting DEGs were identified using IPA®. All potential networks with score >9 (a score ≥3 was considered significant, *p*<0.001) are listed in

Table 8, with information on network genes, score, focus molecules and top functions associated with the focus genes in each network.

ID	Molecules in Network	Score	Focus Molecules	Top Functions
1	ACVR1C, AKR1D1, Alp, AMPK, Ap1, APOC1, Calcineurin protein(s), CARTPT, caspase, CD3, CHI3L1, Creb, cytochrome C, DACH1, DLK1, ERK, ERK1/2, F13A1, Focal adhesion kinase, GNRH1, HBA1/HBA2, HBB, HDL, hemoglobin, HEY2, HINT1, HIPK2, Ikk (family), IL1, IRF3, Jnk, KDELR2, LDL, LGALS1, Mapk, MEF2C, Mek, MET, MT2A, N4BP1, NADPH oxidase, NGFR, NR4A2, OTX2, P38 MAPK, p85 (pik3r), Pdgf (complex), PDGF BB, PI3K (complex), PI3K (family), PIK3R3, Pkc(s), PLC gamma, PON3, Pro-inflammatory Cytokine, Ras, SERPINA1, SERPINA3, Shc, SHOC2, SLCO1A2, Sos, STK4, TCF, TCR, TNFSF10, TTR, TWIST1, Vegf, WSB1	71	35	Tissue Morphology, Cell Death and Survival, Developmental Disorder
2	ABR, ACTL6B, ARMC6, ASB6, C10orf137, C6orf211, CAMKV, CHMP2A, CLIC4, CLPP, CSNK1G3, CTBP2, DCLRE1A, DDX19B, DGKE, ECT2, FHL3, FLVCR1, GALNTL5, GLOD4, HEATR6, HSP90AA1, HSPA12A, ITFG1, KLF3, KPNA6, MCTS1, MEIG1, METTL7B, MRPL44, MXD3, MYBPC1, NCLN, NIPBL, NOL4, OSBPL10, PCBP3, PLEKHA8, PMM2, POLR2J, PPAP2C, PRCP, PROSC, RAI2, SAP18, SCAND1, SEPT6, SGTB, SMARCC1, SMC3, SPATA22, SPSB3, SRPK3, SSU72, STAG1, TATDN1, TESPA1, TM7SF3, TNK1, TNNI3K, TP53BP1, TRAPPC2L, TRIP12, TUFM, TXNL4A, UBC, ZNF131, ZNF235, ZNF397, ZNF420	54	28	Developmental Disorder, Hereditary Disorder, Hematological Disease
3	26s Proteasome, ADCY, AKR1C1/AKR1C2, Akt, APP, ARL4C, Arntl-Clock, AVP, AVPR1B, CACNA1B, CAMKV, CARTPT, CBLN2, CEACAM6, CLDN10, CLOCK, COX4I2, CTF1, DNAJC12, endocannabinoid, estrogen receptor, FAM46A, FSH, GABRE, GNA15, GPR158, GPX1, GPX2, GSK3A, Histone h3, HMGCR, HNF4A, HSPA12A, Insulin, JPH3, KCNC3, KCNS1, LINGO1, LPAR1, LXN, MGAT2, miR-125b-5p (and other miRNAs w/seed CCCUGAG), Mmp, MST1, NFkB (complex), Npff, OPN1LW, PDX1, PIK3R5, Pka, PKM, PLC, Proinsulin, RAB39A, RAI2, RIOK2, RUFY3, SERPINA3, SMAD5, SMC4, SOX7, SYT17, TCF19, Tnfrsf22/Tnfrsf23, TOR2A, tretinoin, trypsin, TXNL4B, ZBTB44, ZFHX3	36	21	Cellular Development, Neurological Disease, Skeletal and Muscular System Development and Function

Table 8. List of 3 Ingenuity networks generated by mapping the focus genes that were differentially expressed between non-infected and BSE-infected samples. Names in lowercase are genes/molecules that are not from the DEGs list but are associated with some of them within pathways identified by Ingenuity Pathway Knowledge Base (IPKB).

The highest ranked network identified by IPA® (Figure 10) was associated with tissue morphology (specifically the determination of cell quantity), developmental disorder and biological processes controlling cell death and survival (Table 8).

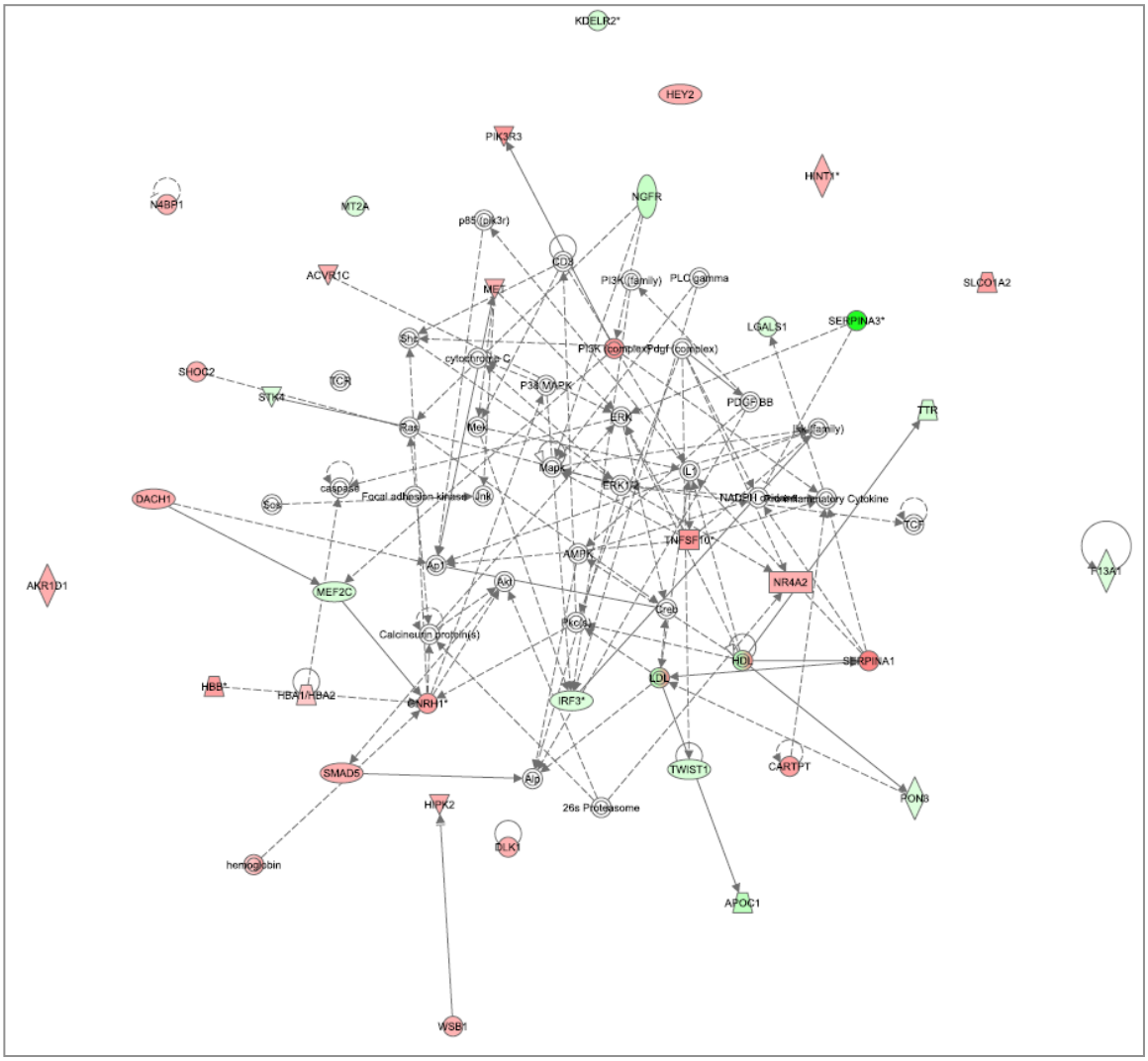

Figure 10. Identification of biologically relevant networks

Top ranking network generated by mapping the genes that were differentially expressed in infected animals *vs* controls. Pathway analysis based on the Ingenuity Pathway Knowledge Base (IPKB) is shown. Color shading corresponds to the type of dysregulation: red for up-regulated and green for down-regulated genes according to the microarray fold change calculation method. White open nodes are not from the list of 300 DEGs, but are transcription factors that are associated with the regulation of some of these genes identified by IPKB. The shape of the node indicates the major function of the protein. A line denotes binding of the products of the two genes, while a line with an arrow denotes 'acts on'. A dotted line denotes an indirect interaction.

This network contained genes that are known to be involved in several neurological diseases and nervous system functions, as shown in Figure 11.

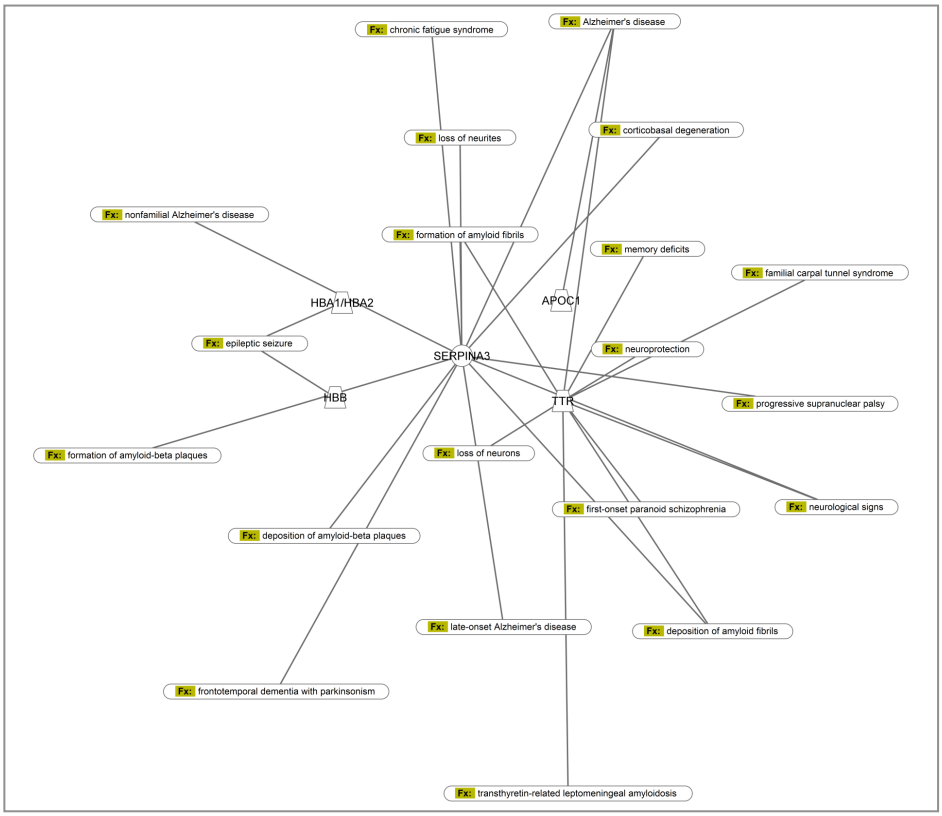

Figure 11. Schematic representation of nervous system-related functions for selected DEGs according to IPKB

Validation of differentially expressed genes in macaques by RT-qPCR

To further confirm the array results using an independent and more sensitive technique, we performed RT-qPCR analyses for a subset of differentially expressed genes. This group (Additional table 2) was selected in the subsequent steps. First, among the 86 probe sets identified in the microarray analysis (Additional table 1) we selected the top 36 with fold change ≥| 2.5| and $p \leq 0.005$. Then, we noticed that many were not annotated or did not have a known function and therefore we extended the selection to additional 29 probe sets having fold change ≥| 2.5| but $0.005 \leq p \leq 0.05$; however, even with these lower stringent criteria we still had few

eligible genes and so in the end we decided to consider for our analysis some additional probe sets with a consistent fold change of ≥| 2.5| but p>0.05 (24 candidates). At this point, having identified only 13 feasible candidate transcripts, we further added seven probe sets (corresponding to 5 additional transcripts) selected among those with a slightly lower fold change (FC>2 for at least 1 probe) but possessing an interesting function as indicated by the IPA® analysis or according to the literature. Finally, *HBA2* was added to the list because of its tight relationship with one of the previously selected genes of the hemoglobin complex (*HBB*), as revealed by the top ranking network from the IPA® analysis (Figure 10). Summarizing, we designed RT-qPCR assays for 19 genes (Table 9), most of which were already known to be involved in neurodegenerative disorders or nervous system regulation, even though very few had been implicated in prion diseases.

Gene	Accession number	Known relation with PrP/nervous system	References
AKR1C1	NM_001195574.1	putative role in myelin formation	[170]
HBB	NM_001164428.1	putative role in intraneuronal oxygen homeostasis, reduced in Alzheimer's and Parkinson's disease	[171]
NCAM1	XM_001083697.2	PrP/N-CAM complexes found in prion infected N2a cells	[172]
NR4A2	NM_001266910.2	Mutations related to dopaminergic dysfunction, including Parkinson schizophrenia and depression	[173]
USP16	NM_001260999.2	depletion of USP16 prevented ATMi from restoring transcription after DSB induction	[174]
CALB1	XM_001085269.2	plays a protective role in neurodegenerative disorders (depleted in HD)	[175]
DACH1	XM_001082371.2	required for normal brain development	[176]
LXN	NM_001266988.1	marker for the regional specification of the neocortex	[177]
PIK3R3	NM_001266826.1	involved in β-amyloid plaque formation and regulatory pathways in the AD brain	[178, 179]
SAP18	NM_001261034.1	possibly related to AD	[180]
SERPINA3	NM_001195350.1	increased in schizophrenia, SNPs affecting onset and duration of AD	[181, 182]
TNFSF10	NM_001266034.1	implicated in pathogenesis of MS (causing demyelination)	[183]
HBA2	NM_001044724.1	putative role in intraneuronal oxygen homeostasis, reduced in Alzheimer's and Parkinson's disease	[171]
GNRH1	NM_001195436.1	key regulator of the reproductive neuroendocrine system in vertebrates	[184]
IRF3	NM_001135797	putative protective role against prion infection	[185]
APOC1*	AK240617.1	binds to ApoE, risk factor for Alzheimer's disease	[186]
TM7SF3	XM_001099269.2	-	-
MYBPC1	XM_001091952.1	-	-
TTR	NM_001261679	amyloid neuropathies, interaction with Aβ	[187]

Table 9. Candidate genes for validation
List of 19 identified genes selected on the basis of FC value and known relevance for neurodegeneration. Because of very low signal (*LXN, PIK3R3, TNFSF10, GNRH1*) or lack of reliable sequence data *(CALB1, DACH1, TM7SF3, MYBPC1)*, only 11 genes (in bold) were successfully analyzed. **Macaca fascicularis* transcript.

Among these, we were able to successfully analyze only 11 genes (reported in bold Table 9) together with 2 housekeeping genes (*ACTB* and *GAPDH*), since all the other RT-qPCR assays either showed too low expression (C_T >35) or amplification of trace amounts of gDNA. In addition, because several gene names have changed

since the first annotation was done, updated names from the latest Affymetrix® annotated library are provided in Additional table 2, together with the old ones.

In order to achieve optimal RT-qPCR conditions we performed titration of template and primers as well as optimization of cycling conditions using human cDNA from SH-SY5Y neuroblastoma cells, in order to save the scarce macaque cDNA available for definitive assays. To assess the specificity of the chosen primer pairs prior to performing the final quantitative assays, some experiments were performed using macaque cDNA obtained from a different brain region of control animals, in order to check the correct amplicon length. Two housekeeping genes, *GAPDH* and *ACTB* [188], were selected as reference genes to normalize RT-qPCR data. Both genes were monitored across infected and control macaques in order to evaluate their expression stability, yielding very similar results (Figure 12).

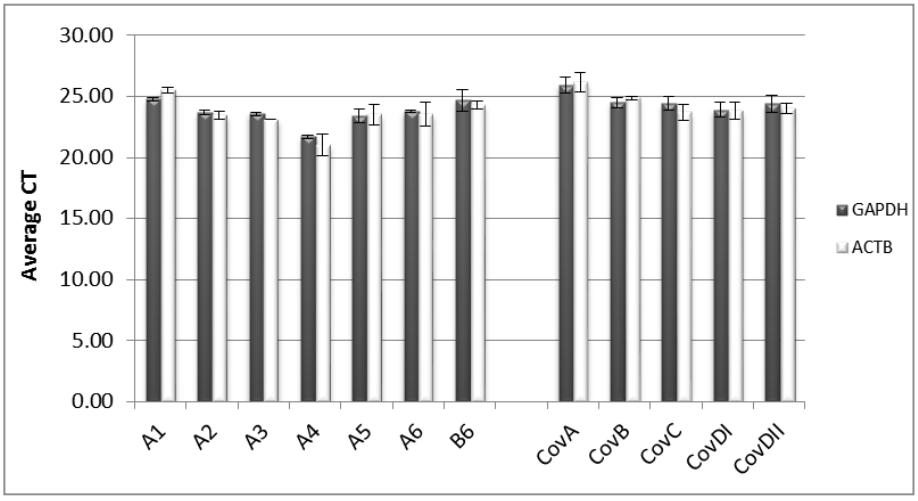

Figure 12. Evaluation of reference gene expression stability across non-infected and BSE-infected samples. For each sample, average values of absolute C_{Ts} (+/−SD) of triplicate wells for *GAPDH* (grey) and *ACTB* (white) are shown.

After these preliminary optimizations, we performed the quantitative analysis and in general we observed a large intra-assay variability for most genes across different samples, both for infected (Figure 13) and for control animals (Figure 14).

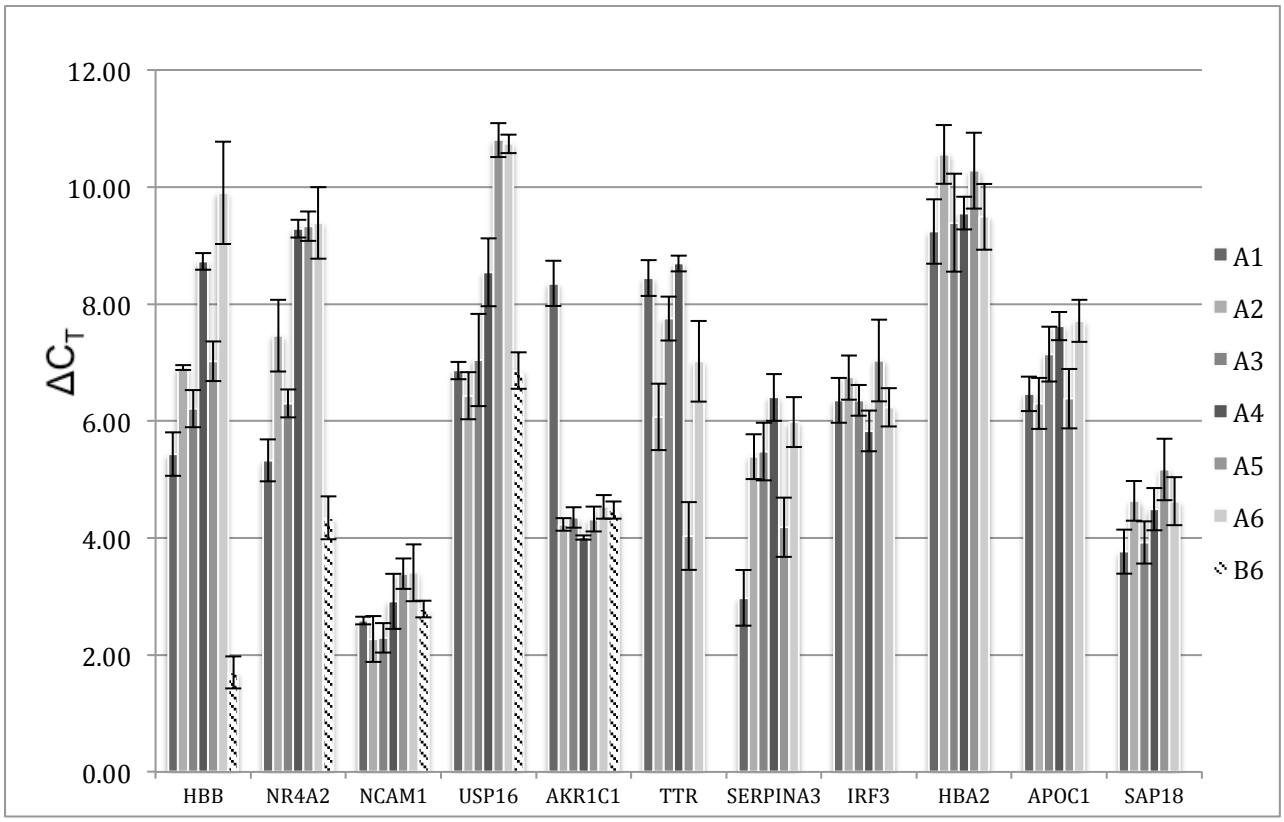

Figure 13. Variability of ΔC_T values among BSE-infected macaques.

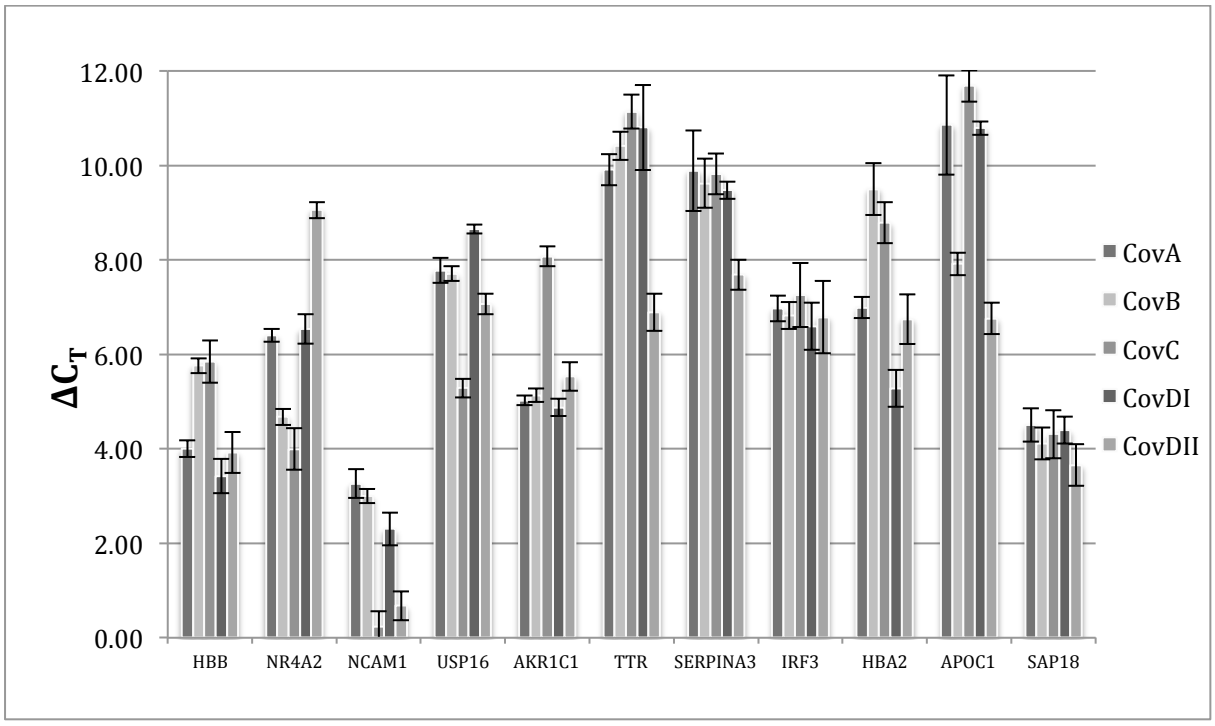

Figure 14. Variability of ΔC_T values among non-infected macaques

Interestingly, we found a completely different expression pattern for B6, the only orally-infected sample available, in comparison to the intracranially infected animals,

for three genes (*USP16, NR4A2, HBB*), suggesting that the route of infection might play a substantial role in determining the gene expression regulation (Figure 15).

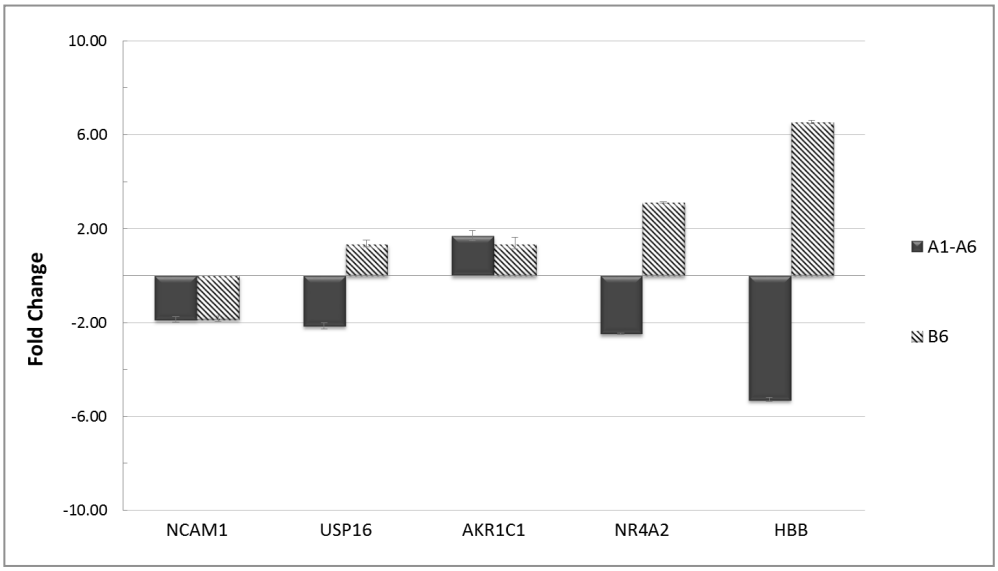

Figure 15. Comparison between the intracranially infected samples (A1-A6) and the orally infected one (B6)

In light of these results, we decided to carry out another microarray clustering analysis excluding this animal in order to assess its influence on the final results. As shown in Figure 16, the comparison of the two clustering analysis with (panel A) or without (panel B) the orally challenged animal (B6) does not show marked differences.

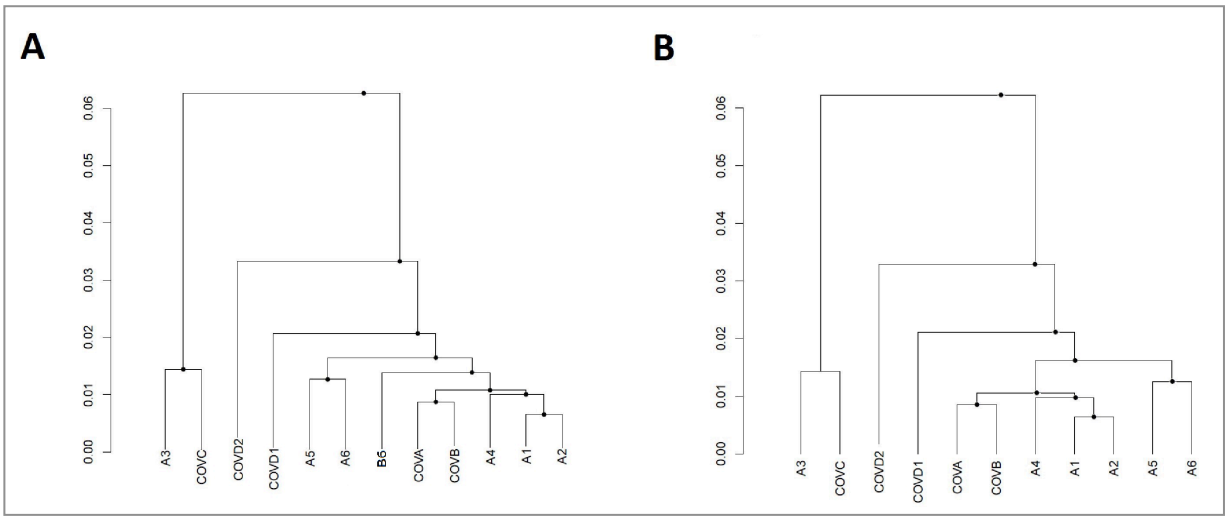

Figure 16. Cluster analysis
Cluster analysis was performed using a hierarchical approach with the average linkage-method for all animals (panel A) or excluding the orally infected one, B6 (panel B).

Using SYBR® Green-based RT-qPCR we were able to confirm the statistically significant up-regulation of *TTR* (FC= 7.11), *SERPINA3* (FC= 18.73) and *APOC1* (FC= 6.33) as well as the down-regulation of *HBB* (FC= 5) and *HBA2* (FC= -4.5), normalizing the data against *GAPDH*. Very similar results were obtained against *ACTB* (Figure 17).

Regarding all the other genes analyzed, the RT-qPCR results confirmed the regulation pattern observed in the microarrays, but without statistical significance (*p*-value> 0.05).

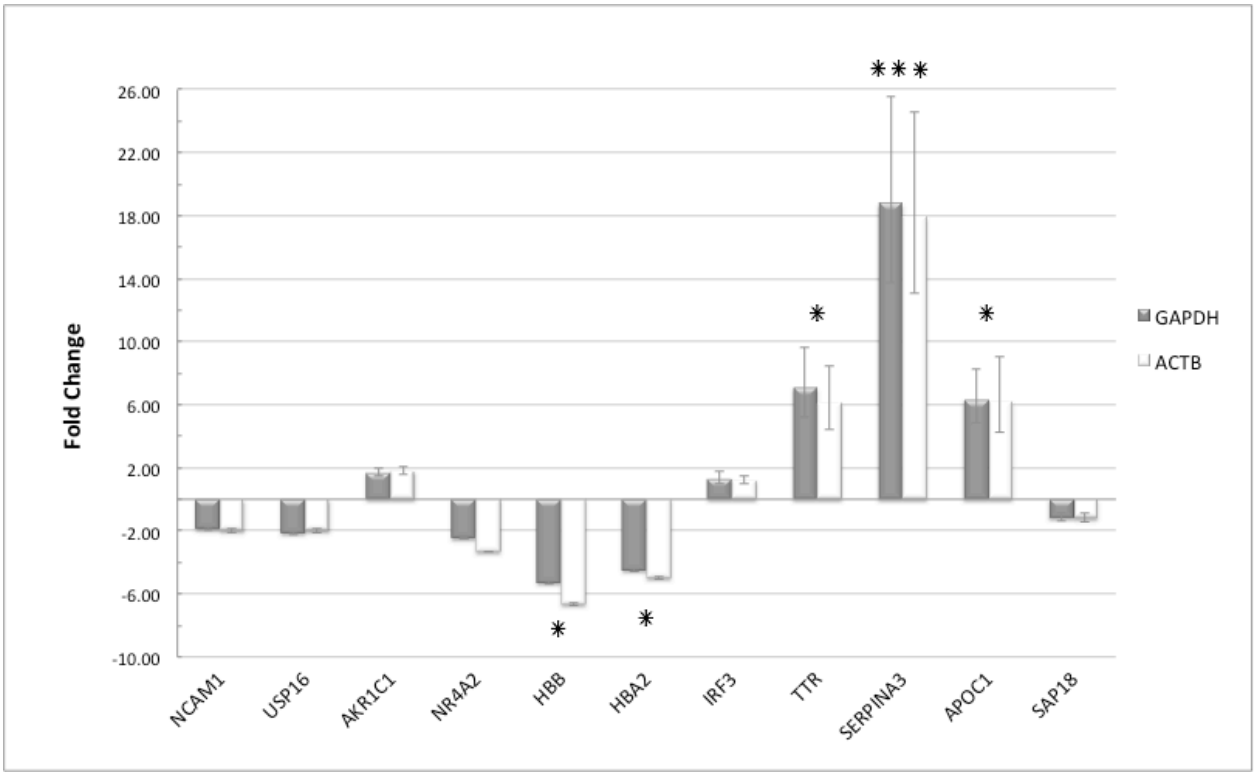

Figure 17. SYBR Green-based RT-qPCR validation of microarray results
Relative expression levels of 11 genes normalized against *GAPDH* o *ACTB* in BSE-infected cynomolgus macaques.

In order to further confirm the SYBR® Green-based results we performed additional RT-qPCR analyses using FAM-labeled TaqMan® probes, therefore providing higher sensitivity and specificity for those genes that showed a significant fold change. Using this approach we confirmed the regulation of *SERPINA3*, *APOC1*, *HBB* and

HBA2, but not of *TTR*, which showed a comparable fold change but lost statistical significance (Figure 18).

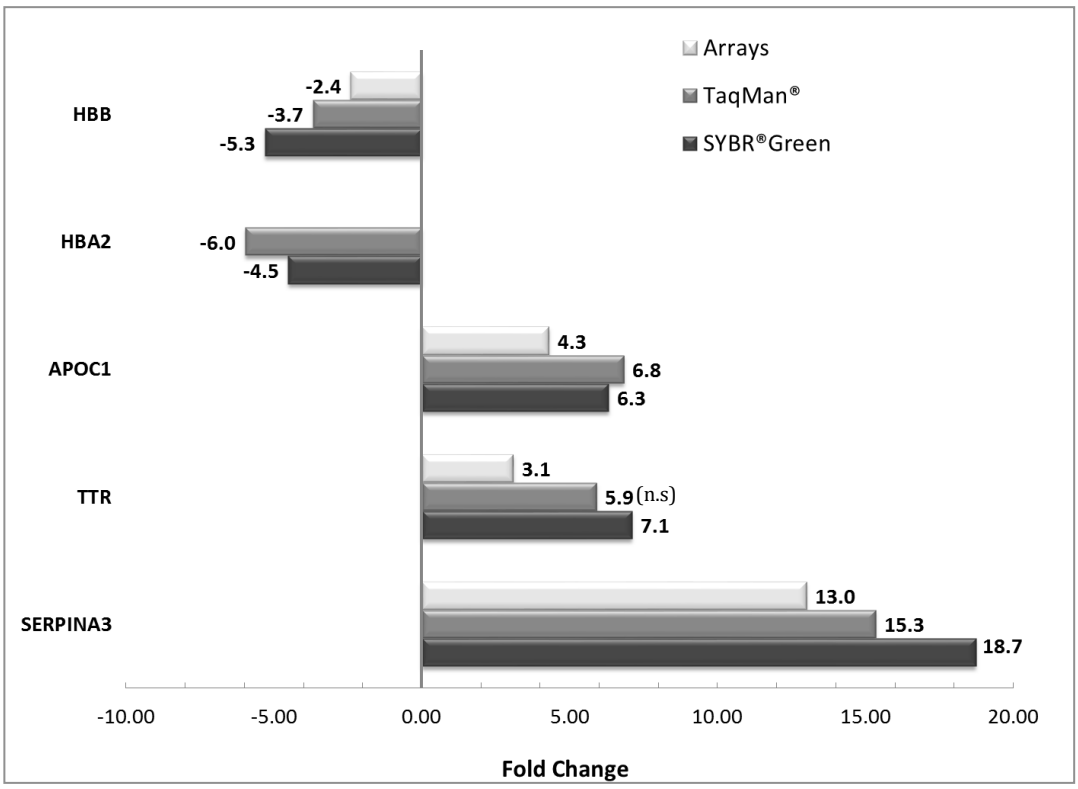

Figure 18. Comparison between microarray, SYBR Green-based and TaqMan probe-based results for the five selected genes.
Expression levels for each transcript are normalized against *GAPDH*. All three technologies yielded similar results.

This may depend on the higher variability among triplicates, due to C_T values higher than 35 obtained with the TaqMan® probe chemistry compared to SYBR® Green detection system (Figure 19).

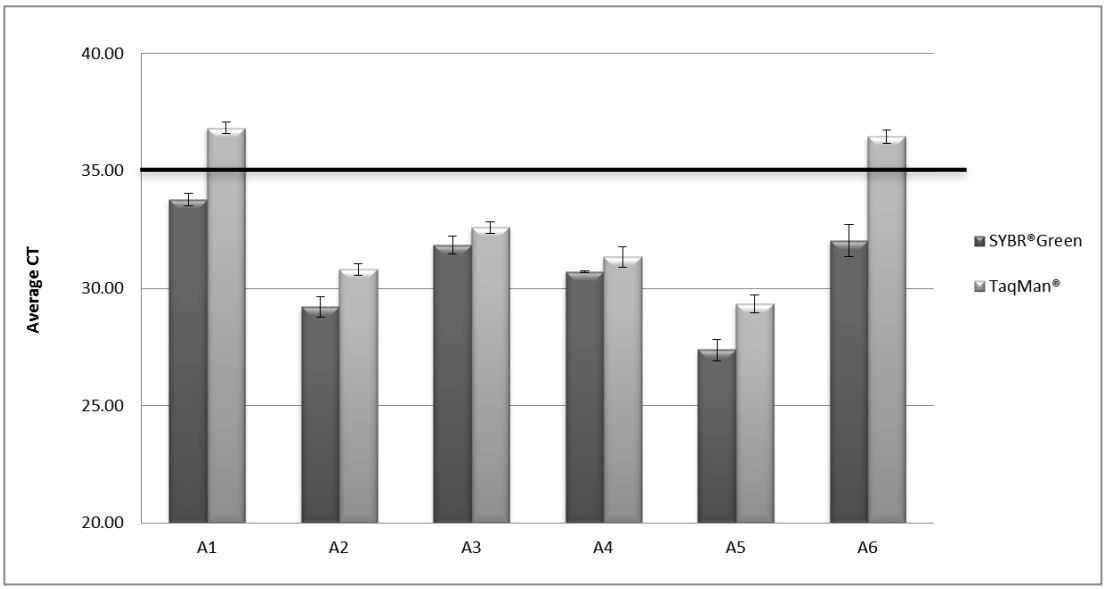

Figure 19. Comparison between SYBR-Green and TaqMan-based C_T values for TTR

In summary, we were able to confirm the results of the array platform obtaining consistent fold change values for all genes analyzed, even though we validated with statistical significance using the specific TaqMan® detection system only four of them: *HBB, HBA2, APOC1, SERPINA3* (see Table 10 for details on *p*-values and FC).

Gene symbol	Microarray fold change			RT-qPCR fold change			
				SYBR®		TaqMan®	
	Min	Max	**Mean**	FC	P value	FC	P value
AKR1C1	2.3	2.9	2.5	1.7	0.433	2.4	0.235
HBB	-2.2	-2.6	-2.4	-5.3	0.020	-3.7	0.021
NCAM1	-1.1	2.5	-0.3	-1.9	0.160	-	-
NR4A2	1.1	-2.1	-1.6	-2.5	0.248	-	-
USP16	-1.2	-5.5	-2.6	-2.0	0.308		
SAP18	-1.2	-2.6	-1.7	-1.2	0.393	-	-
SERPINA3	10.0	16.0	13.0	18.7	0.0001	15.3	0.0005
HBA2	-	-	-	-4.5	0.041	-6.0	0.019
IRF3	2.0	2.1	2.0	1.3	0.123	-	-
APOC1	4.3	-	4.3	6.3	0.047	6.8*	0.028*
TTR	3.1	-	3.1	7.1	0.025	5.9	0.076

Table 10. RT-qPCR confirmation of microarray results
Differential expression of selected genes analyzed by microarray and RT-qPCR. For microarray analysis, the lowest (Min), the highest (Max) and the average (Mean) fold change values of all the respective probes are shown. For RT-qPCR analysis, fold change (FC) and statistical significance (p-value) for both SYBR Green and TaqMan results are shown. In bold, genes validated with statistical significance. *HBA2* did not have a related probe set on the microarray. *normalization performed only against *ACTB*.

In addition, given that the autopsy procedure for these animals could have led to the presence of some blood in the brain material, and considering that some recent studies have highlighted the existence of active transcription within human red blood cells [189], we decided to analyze our samples also for the expression of two erythrocyte markers, *ALAS2* and *RHAG*, in order to ensure that the RT-qPCR signals of both hemoglobin-related genes (*HBB* and *HBA2*) reflected the actual brain gene expression dysregulation and not a blood contamination. In particular, *ALAS2* (5'-aminolevulinate synthase 2) gene product specifies an erythroid-specific

mitochondrially located enzyme, which catalyzes the first step in the heme biosynthetic pathway. *RHAG* (Rh-associated glycoprotein) instead, codes for an erythrocyte-specific protein which is thought to be part of a membrane channel that transports ammonium and carbon dioxide across the blood cell membrane and also it is thought to interact with Rh blood group antigens. The microarray data for these genes suggested a negligible but identical presence of blood in control and infected samples, RT-qPCR analysis revealed a small blood contamination ($C_T \geq 34$ for *ALAS2*, $C_T \geq 36$ for *RHAG*) within two samples, one control (CovDI) and one infected sample (A4) (Figures 20 and 21).

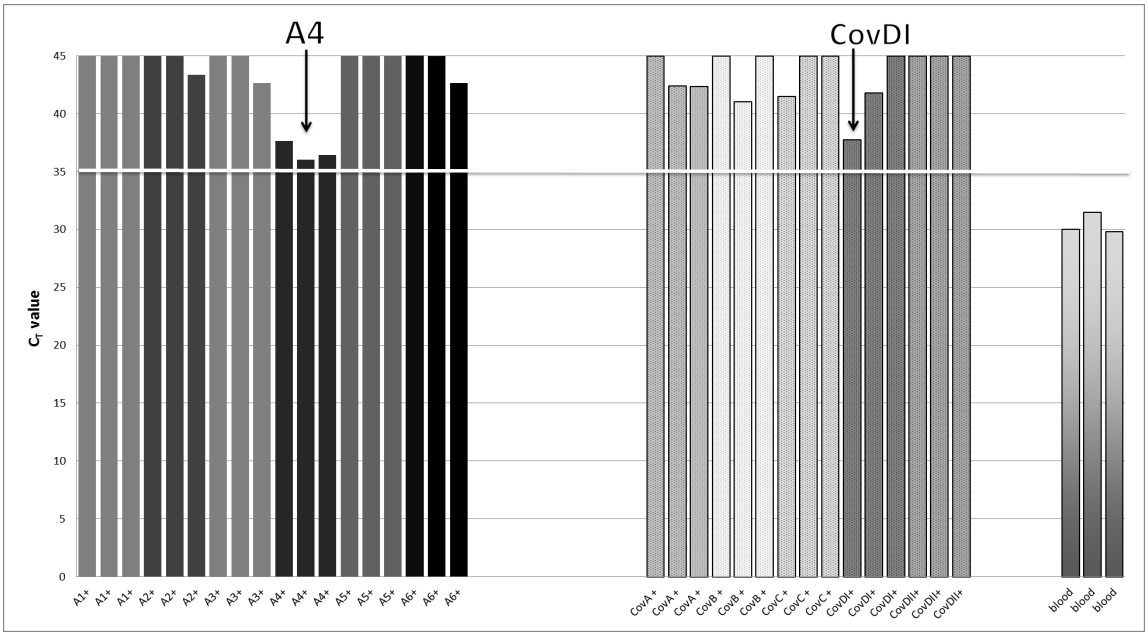

Figure 20. Blood erythrocyte markers expression across BSE-infected and non-infected macaque samples
Absolute C_T values for Rh-associated glycoprotein gene (*RHAG*)

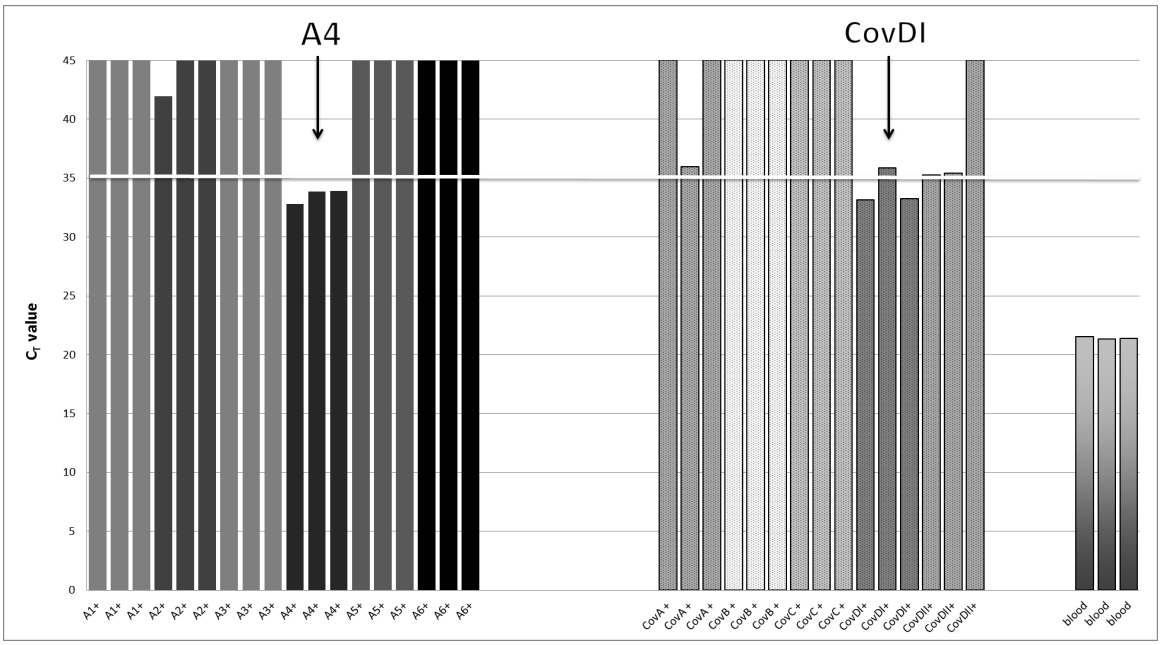

Figure 21. Blood erythrocyte markers expression across BSE-infected and non-infected macaque samples
Absolute C_T values for 5'-aminolevulinate synthase 2 (*ALAS2*)

In light of these results, we performed an additional gene expression analysis for *HBB* and *HBA2* excluding these two samples. As expected, we obtained slightly different results (FC~0.3 for *HBB* and FC~0.2 for *HBA2* using TaqMan® probes), but a relevant down-regulation still persisted with statistical significance. Given some recent reports about neuroinflammation involvement in sCJD patients [190], we wondered if immune system genes dysregulation occurred in BSE-infected macaques. However, analysis of the microarray data did not reveal relevant deregulation of cytokines that might be involved in neuroinflammation and/or immune response. Indeed for GFAP, a known marker of microgliosis, only one probe gave an indication of up-regulation (FC= ~1.97). For IL6 and TNFα, all the probes showed FCs around 1 with and CD68, another microglial marker, the single probe available showed a border-line up-regulation (FC~ 1.65). These data suggest that inflammatory responses may not be particularly relevant in this primate model or in the specific area of the frontal cortex that was examined.

Furthermore, one of our first candidates (TNFSF10), which is a member of the TNF family that triggers the release of pro-inflammatory cytokines [191], was down-regulated (FC= -2.7 and -2.08) for only two out of four probes. It was then analyzed by RT-qPCR, but the assay was not robust due to primer design difficulties. Therefore, this target was not validated.

Also, we noticed that a couple of genes coding for subunits of mitochondrial complexes, namely MT-CYTB and MT-ND4, were significantly dysregulated in our microarray data (Additional table 1). However, the very high FC value (> 300) observed for one of the probes led us to assume that probably it could have been a spurious result. Furthermore, we considered that the array probe was designed on *Macaca mulatta* genome which does not have a strong similarity with the *Macaca fascicularis* one in this region. Indeed, it is known that mitochondrial DNA displays substantial sequence diversity even between subpopulations of the same species, mainly due to high mutation rate [192]. Therefore, given also the very limited amount of cDNA available, we decided not to further investigate mitochondrial transcripts in macaque samples. Analyses on human samples are currently ongoing.

Validation of the gene signature in humans by RT-qPCR

Given the encouraging results found in macaques, we wondered if BSE-infection gene signature was reliable also in discriminating CJD patients from healthy ones. One of the closest human diseases to that of BSE-infected macaques is vCJD. However, given the limited numbers of definitive diagnosed vCJD patients (slightly more than 200 worldwide, two from Italy) and considered their reduced accessibility, we decided to extend our analysis including also sCJD patients. This would also allow us to shed some light on the possible differences in gene regulation

mechanisms between acquired and sporadic human prion disorders. In addition, to better investigate the influence of different etiologies, we also included some patients with iatrogenic CJD (iCJD), an acquired prion disease -as vCJD- but with a different origin, in this case treatment with growth hormone derived from prion contaminated cadavers. Regarding control samples, there is a limited availability of brain samples from healthy subjects, either age-matched with vCJD (around 30 years) or with sCJD (around 65 years). This is because for young individuals, the relatively rare deaths usually occur as a consequence of accidents (mainly unintentional injuries) or known diseases -all cases that generally do not contemplate autopsies since the cause of death is already established- while for aged people, in general it is likely that they present some neuropathological sign. Therefore, we decided to introduce in our study some samples from patients with non-CJD neurodegenerative disorders as an additional “control” group. This would also enable the identification of possible prion-specific gene expression alterations. Two additional common issues with postmortem human brain samples that we had to deal with were the stability of endogenous reference genes and the RNA integrity [193]. A number of different variables have been supposed to negatively correlate to different extents with RNA integrity: for example, higher degradation is observed in samples subjected to prolonged thawing [194] or storage [195] as well as in samples of patients showing longer agony before death (probably due to brain acidosis) [196]. Clearly, in studies involving postmortem human tissue is not possible to control all the variables that might impair RNA quality. This inevitably leads to non-homogenous sample collections with high degree of biological variance. However, it is widely accepted that moderate degradation does not preclude reliable analyses of small amount of RNA. Indeed, it has been shown that gene expression profiles from partially degraded RNA samples with still visible ribosomal bands are highly similar to that of intact samples [195], especially if the

RT-qPCR amplified products are smaller than 250bp [197]. This is not particularly surprising considering that reference genes transcripts most likely degrade gradually and in parallel with target ones [193]. For all these reasons, a minimum RIN ≥ 3.95 was suggested as including threshold for human brain tissue [198]. In order to ensure a sufficient reliability of the samples, in our study we applied a slightly more stringent threshold; indeed, only RNA that showed RIN around 4.5 or higher were selected for further analysis. As regards housekeeping genes, there is a lack of consensus about the optimal reference genes in postmortem brain tissues. Indeed, while some issues have been reported about GAPDH involvement in human neurodegenerative processes [199], ACTB and the ribosomal protein family seem to show good stability across different RIN values [196] and brain samples [199]. Therefore, we decided to use *ACTB* and *RPL19* as reference genes to normalize RT-qPCR data, also given that in our preliminary optimizations *GAPDH* showed sensibly higher C_T values in comparison to the two other housekeeping genes analyzed.

As for macaque samples, the relative mRNA levels were calculated using the $2^{-\Delta\Delta C_T}$ method and two reference genes (*ACTB* and *RPL19*, CV < 0.5, M value < 1 for both), obtaining very similar results. Firstly, the two housekeeping genes were analyzed across diseased and control patients in order to assess their expression stability (Figure 22).

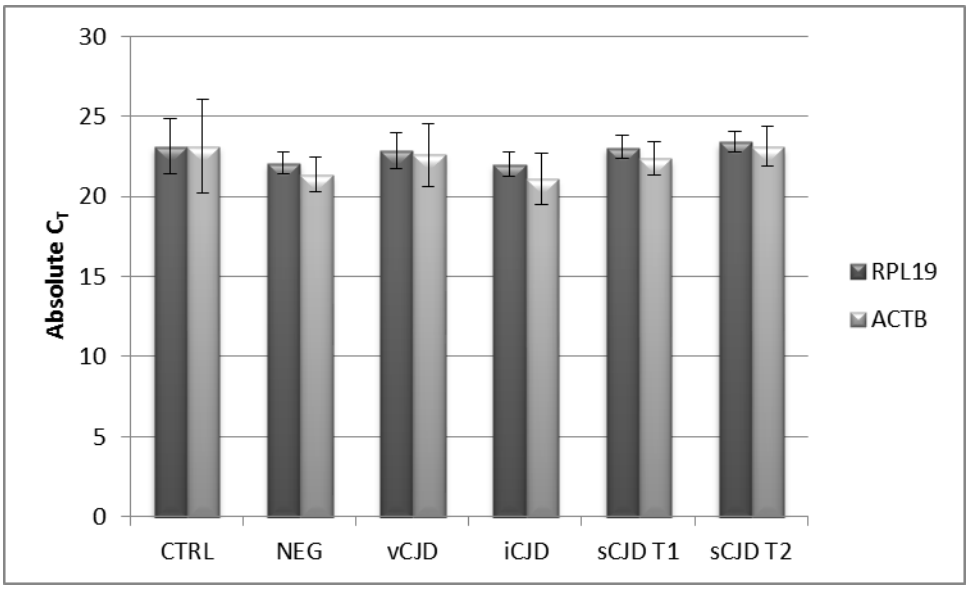

Figure 22. Comparison between *RPL19* and *ACTB* stability across control, CJD and non-CJD samples.
For each group, average values of absolute C_{Ts} among the samples for *RPL19* (dark grey) and *ACTB* (light grey) are shown. Each sample was analyzed in triplicates.

Fold change values smaller than 1 were converted using the equation -1/fold change, for ease of representation.

In general, the gene expression trend observed in macaques was statistically confirmed, with consistent FC values, for four out of five genes. *HBA1/2* (FC ~ -5.0) is down-regulated in both Type 1 (T1) and Type 2 (T2) sCJD patients, but not in vCJD and iCJD cases. As regards patients affected by other non-CJD neurodegenerative diseases (NEG), a trend of down-regulation (FC ~ -3) was observed as well, but without statistical significance. A similar trend was found also for *HBB*, which indeed showed a slight down-regulation in sCJD and NEG patients, even though without statistical significance (Figure 23, upper panel).

SERPINA3 is up-regulated in both sCJD T1 and T2 patients (FC ~6) as well as in vCJD (FC ~ 8.5) and iCJD (FC ~ 19) cases. *APOC1* shows an up-regulation in both sCJD T1 and T2 patients (FC ~7) and in iCJD cases (FC ~4.5), but not in vCJD patients. Both the two genes are not regulated in patients affected by other

neurodegenerative diseases (NEG), as they show levels of expression similar to that of the controls (FC < |2|) (Figure 23, lower panel).

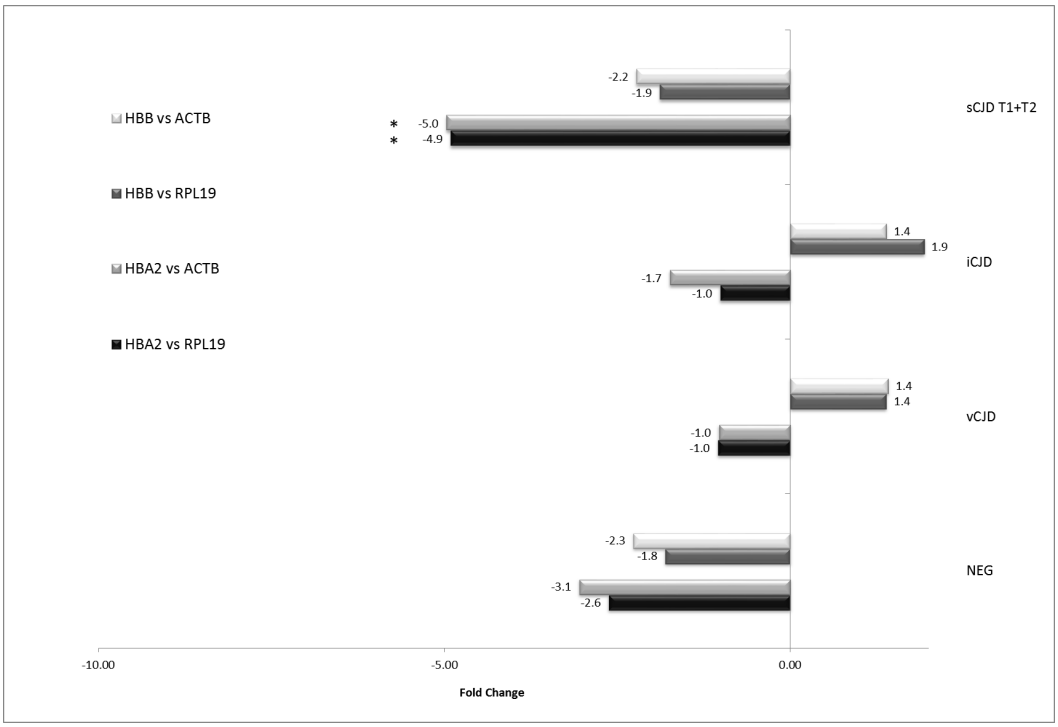

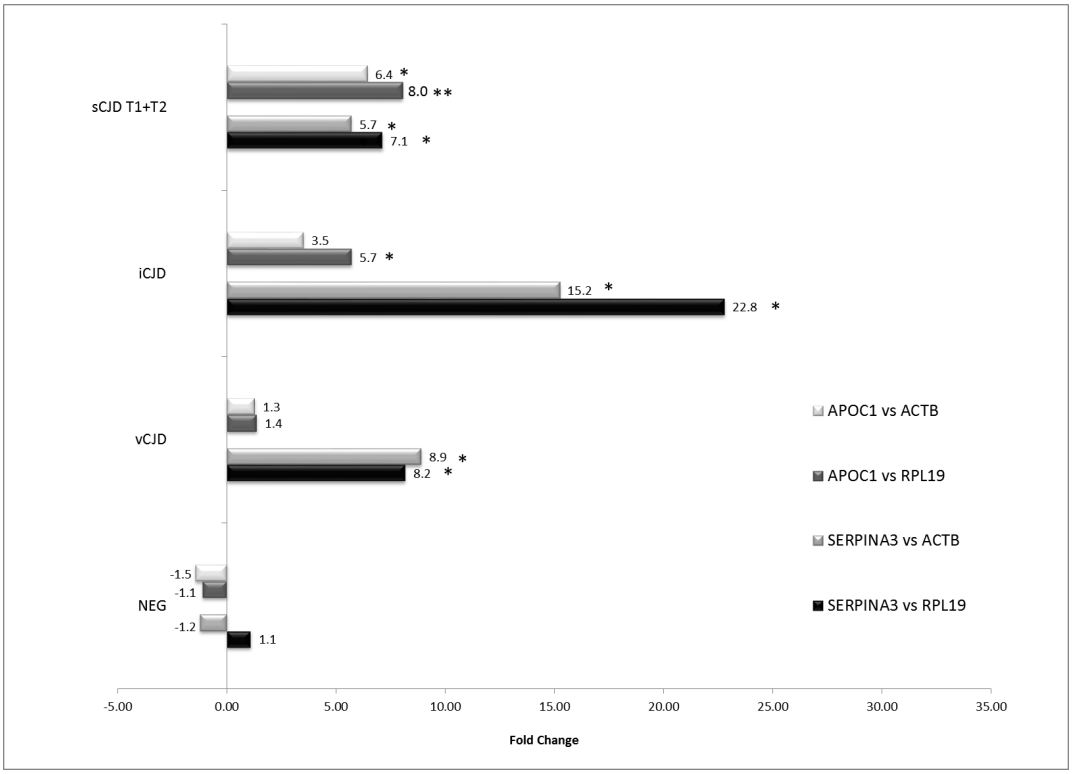

Figure 23. RT-qPCR validation of gene signature
Relative expression levels of *HBB, HBA1/2* (upper panel)*, APOC1, SERPINA3* (lower panel) normalized against *RPL19* or *ACTB* in sCJD, vCJD, iCJD and NEG patients. sCJD T1 and T2, showing similar results, were grouped for ease of representation.

Regarding *TTR*, an up-regulation which is consistent with the results obtained in BSE-infected macaques was found in both iCJD (FC~18) and sCJD cases (FC~2.5), but not in vCJD and NEG patients (Figure 24).

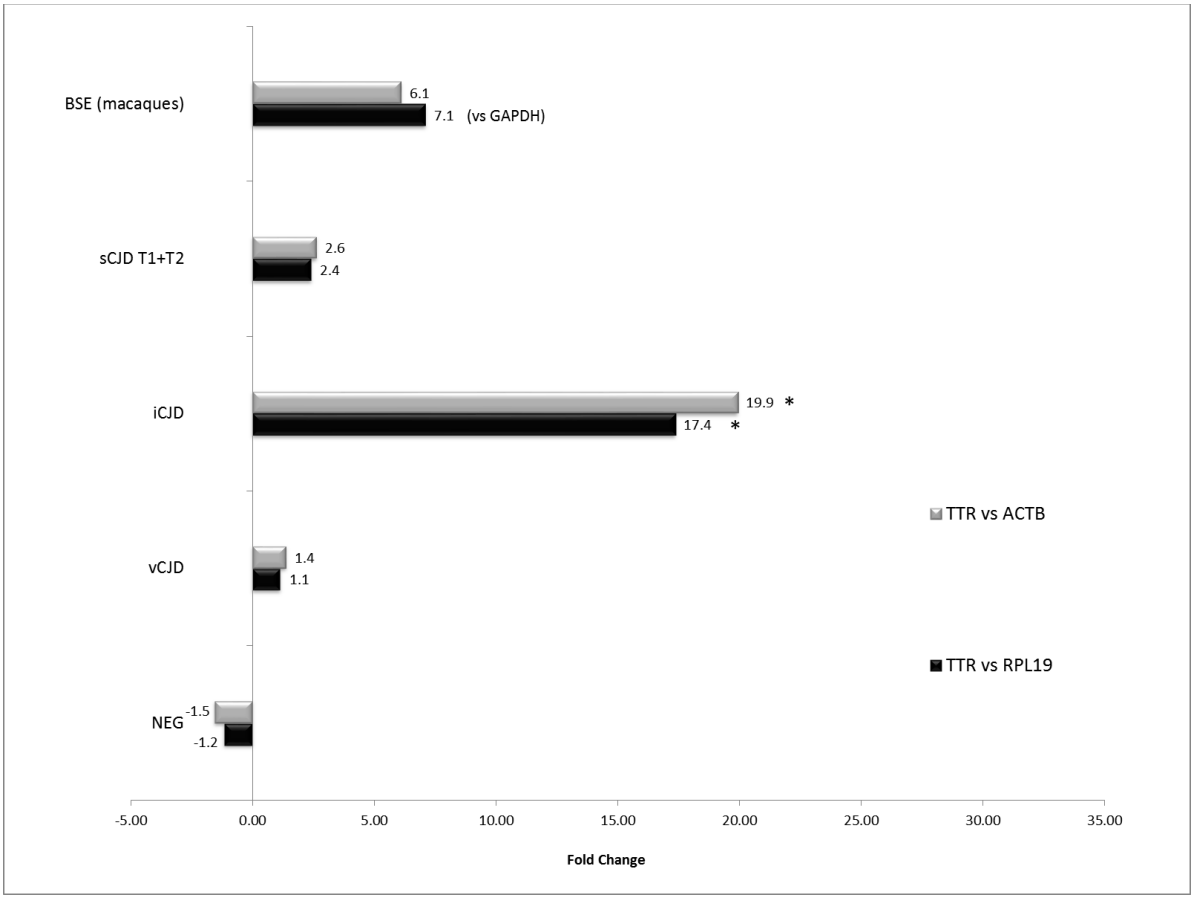

Figure 24. RT-qPCR analysis of *TTR* in human samples
Relative expression levels of *TTR* normalized against *RPL19* or *ACTB* in sCJD, vCJD, iCJD and NEG patients. sCJD T1 and T2, showing very similar results, were grouped for ease of representation.

For some genes, statistical significance was obtained only in a few cases (*), mainly due to the lack of appropriate sample size of control samples (N=4) and to the high variability of the samples within certain groups. Nevertheless, when comparing BSE-infected macaques with human vCJD, iCJD and sCJD patients, we observed consistent results between macaques and humans for all the genes, with the exception of *HBB* (Figure 25).

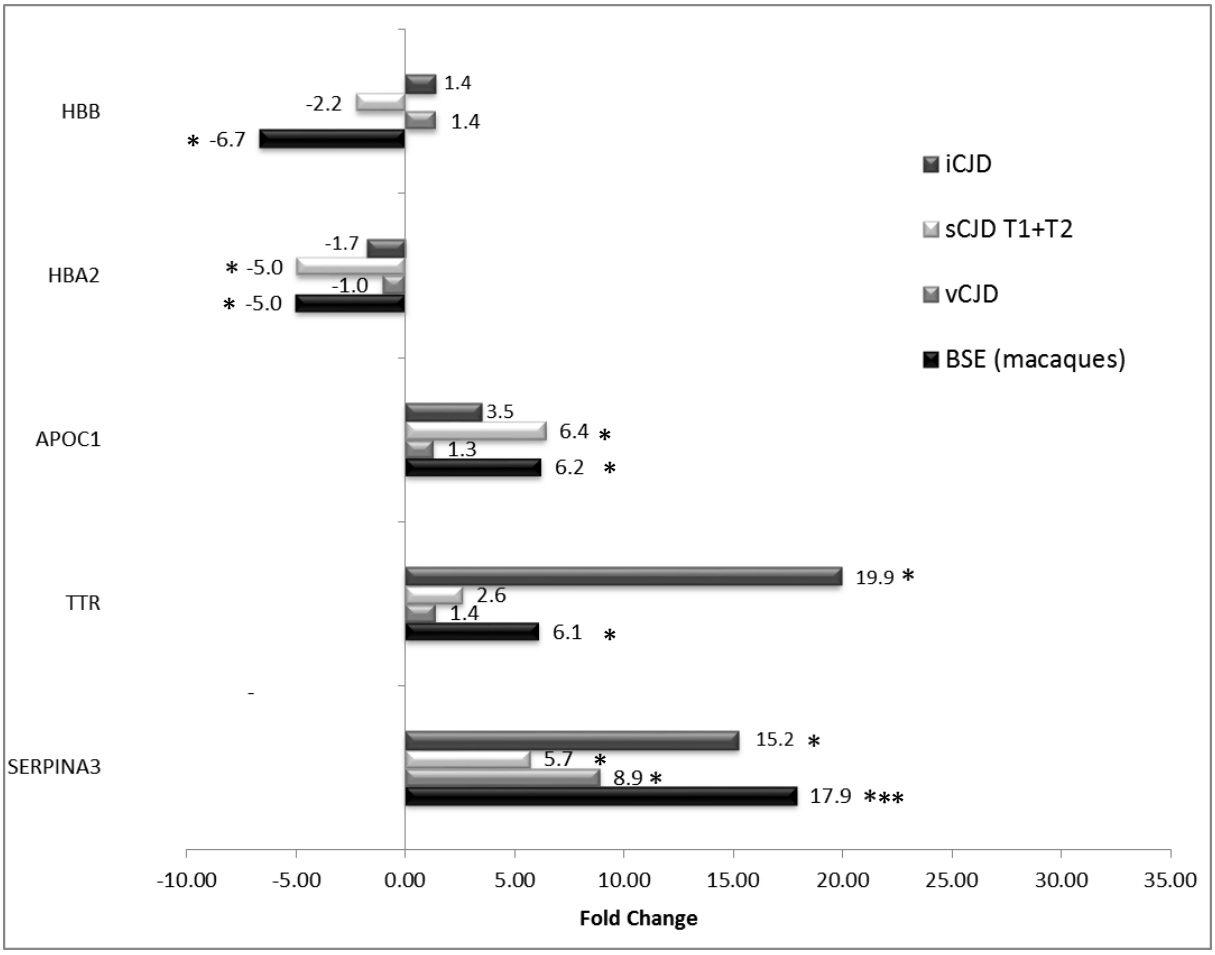

Figure 25. Comparison between BSE-infected macaques and CJD patients
Relative expression levels of *HBB, HBA1/2, APOC1, TTR* and *SERPINA3* normalized against *ACTB* in BSE-infected macaques, sCJD, vCJD, iCJD and NEG patients. sCJD T1 and T2, showing similar results, were grouped for ease of representation.

Therefore, we could confidently assume that our results on human patients may be reliable, despite the lack of statistical significance in some cases.

With regards to other neurodegenerative diseases (NEG), both *HBB* and *HBA* were found down-regulated similarly to BSE-infected macaques and CJD patients, while for *APOC1*, *SERPINA3* and *TTR* no significant dysregulation was observed. This last evidence prompted us to perform an additional analysis for these three genes, normalizing the data on NEG samples as a surrogate "control" group, in order to highlight a potential role of specific CJD markers in comparison to other

neurodegenerative diseases for these genes. In this case, the up-regulation of all genes in CJD samples was even stronger, in terms of FC values and/or statistical significance, suggesting that the dysregulation of these three genes might be specific to CJD (Figure 26).

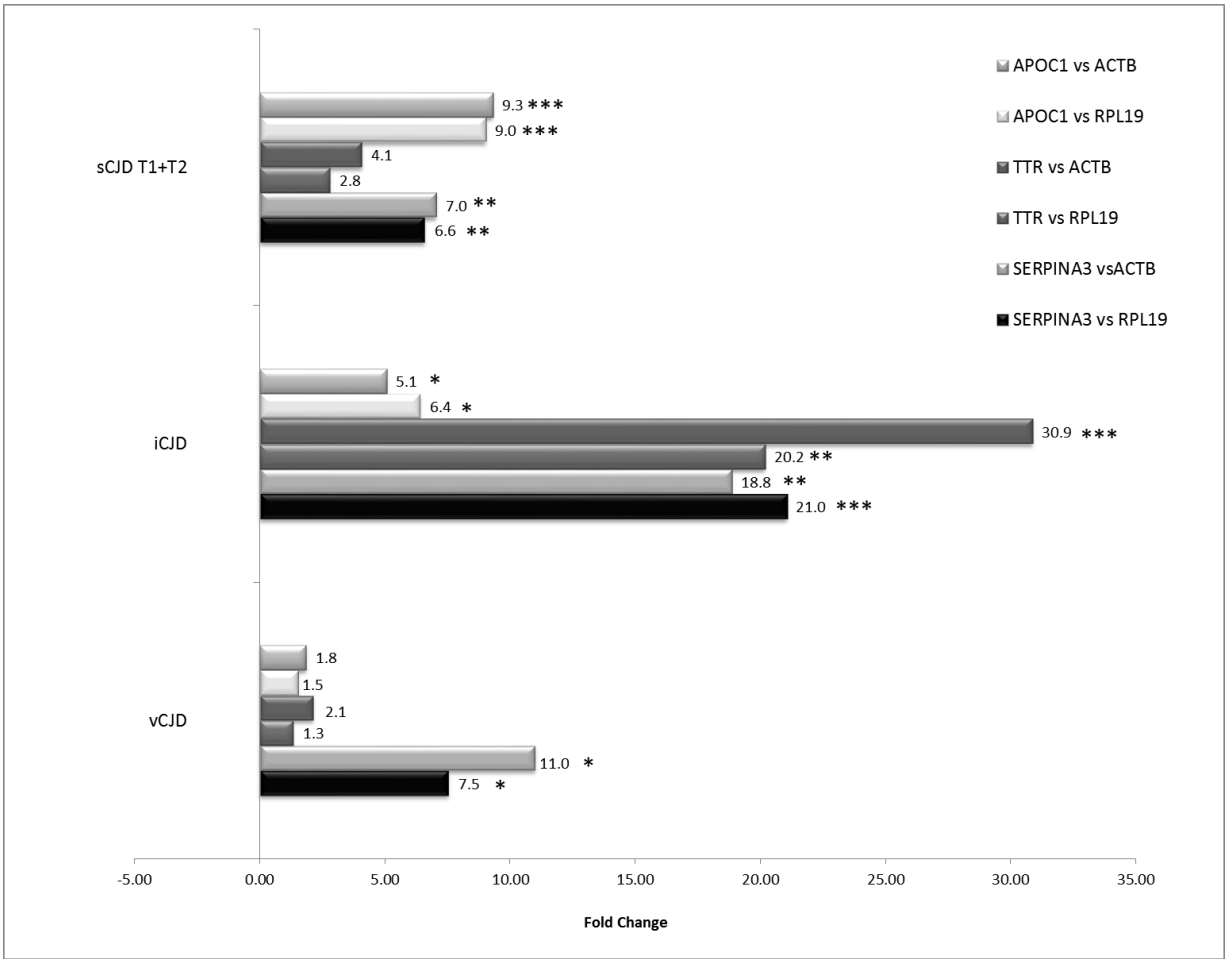

Figure 26. RT-qPCR results for *SERPINA3*, *APOC1* and *TTR* in sCJD, vCJD and iCJD patients in comparison with NEG group.
Relative expression of *SERPINA3*, *APOC1* and *TTR* normalized against *ACTB* or *RPL19* in sCJD, iCJD and vCJD patients. In this analysis, FC for sCJD, iCJD and vCJD group was calculated normalizing ΔC_T average of each group on the ΔC_T average of NEG group. sCJD T1 and T2, showing similar results, were grouped for ease of representation.

In addition to this, we analyzed all the samples for expression of two erythrocyte markers, *ALAS2* and *RHAG*, to exclude any major blood contamination that may be present as a consequence of the autopsy procedure. RT-qPCR analysis of *RHAG*

revealed a negligible blood contamination (C_T ≥ 35) within some samples, even though *ALAS2* C_{Ts} were slightly lower (≥30) (Figure 27). However, the difference in the expression levels of *ALAS2* between brain and blood samples (used as control) was ≥10 C_T, confirming the very limited influence of blood contamination in our analysis. In addition, blood traces were almost uniformly present in all the groups; therefore, we can conclude that our results were not significantly affected by blood presence.

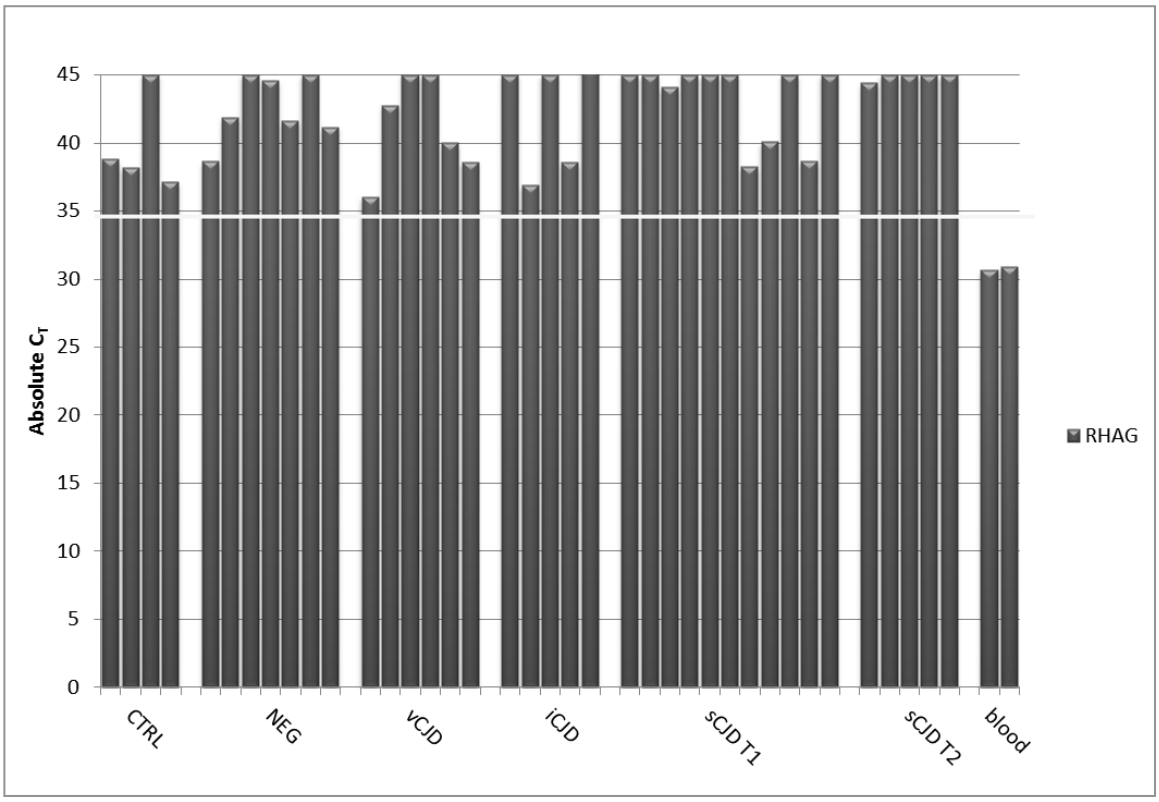

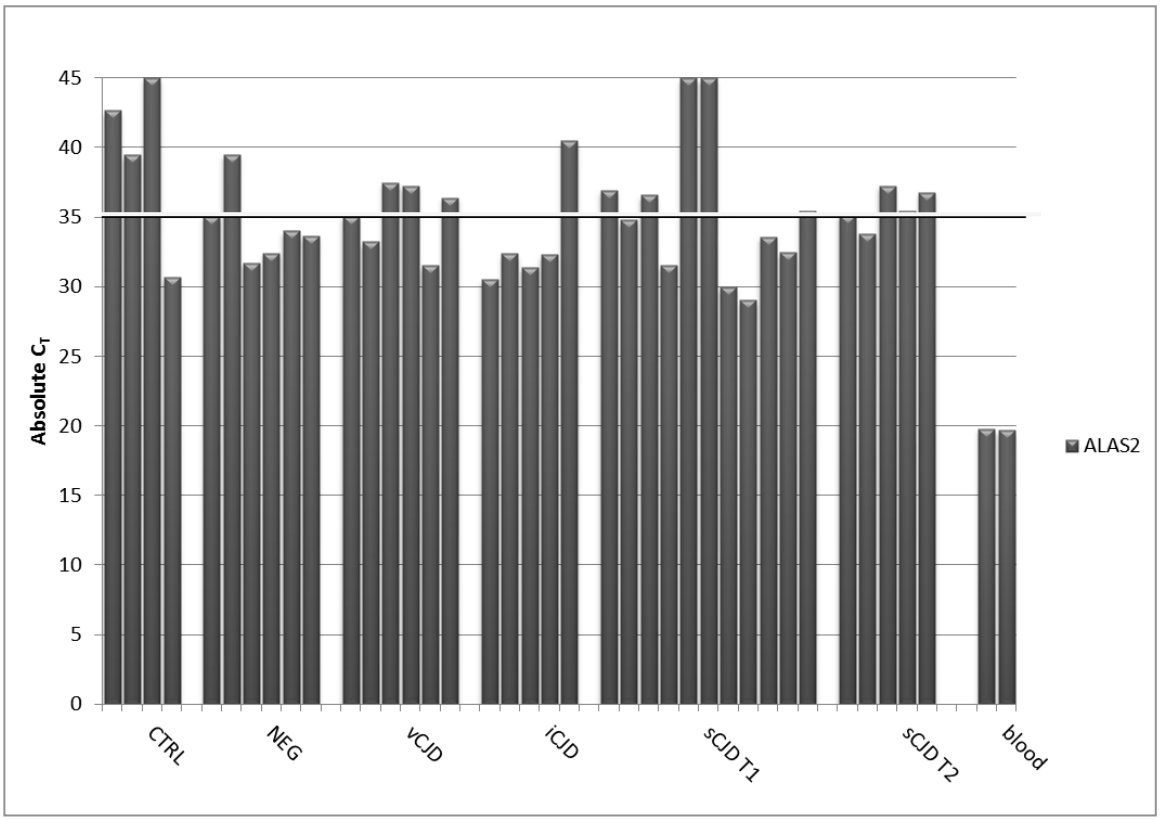

Figure 27. Blood erythrocyte markers expression across control, NEG and CJD patients
Absolute C_T values for *RHAG* (upper panel) and *ALAS2* (lower panel)

Lastly, we investigated the gene expression pattern of *PRNP*. No significant change of *PRNP* expression was observed in any of the groups analyzed. However, a different behavior clearly emerged between vCJD and iCJD: while iCJD samples showed a down-regulation of *PRNP*, vCJD samples showed an up-regulation. Indeed, the difference between the two groups was statistically significant, suggesting a role of the infection route in the modulation of PrP mRNA levels (Figure 28).

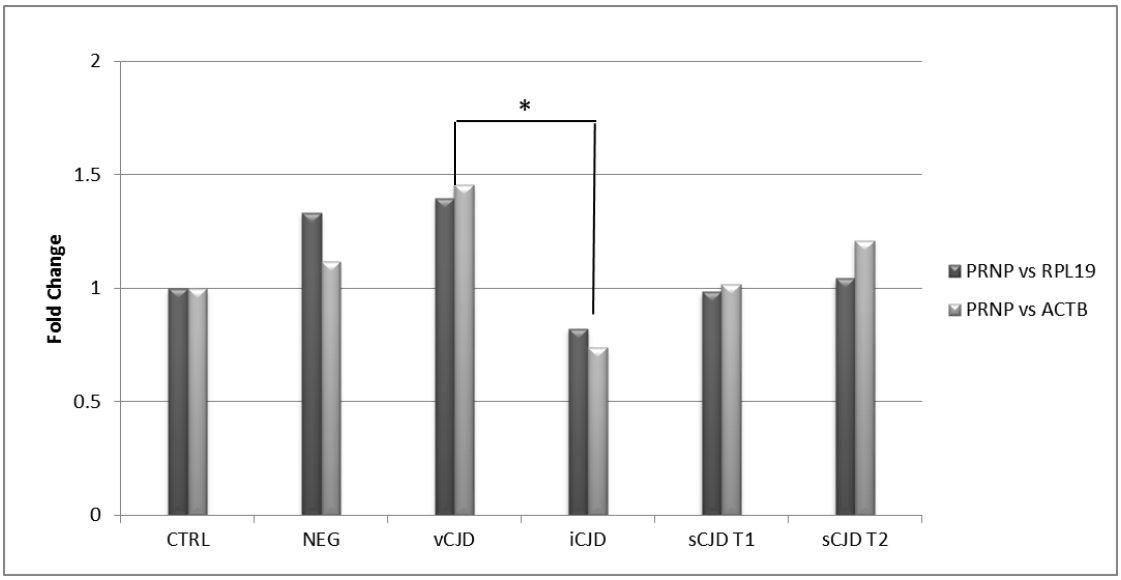

Figure 28. *PRNP* expression levels in CJD and NEG patients.

Immunohistochemistry

We are also conducting immunohistochemistry analyses on these brains to check the expression of the proteins encoded by the five genes. Preliminary analyses have been already performed for TTR, APOC1 and SERPINA3 on AD and sCJD brain slices in order to establish a suitable IHC protocol and check the specificity of the selected antibodies. So far, all the tested antibodies displayed a specific reactivity that mirrored the localization reported in literature for each of the related proteins (Figure 29). Further analyses on these and the remaining antibodies in other patient samples are ongoing, both in IHC and Western blot.

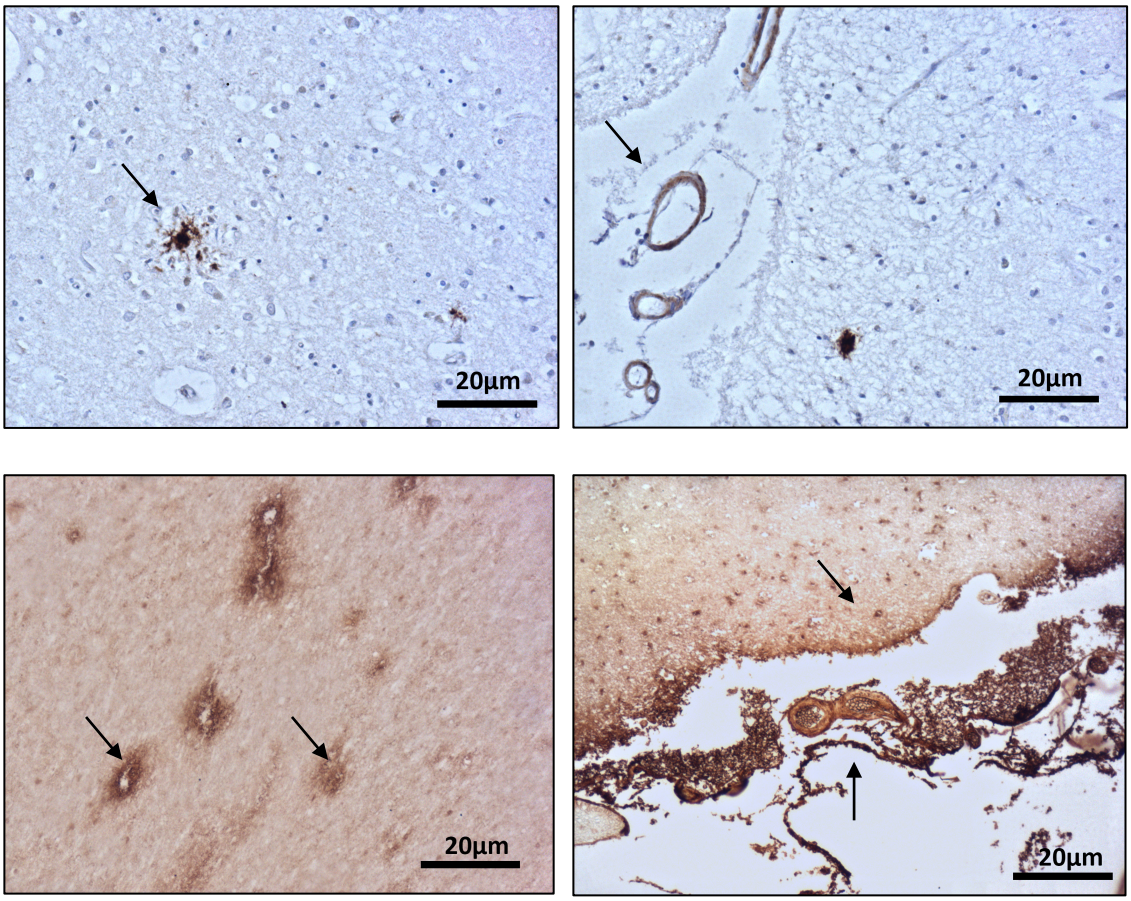

Figure 29. Immunohistochemistry analysis on human brain slices.
APOC1 antibody staining (upper boxes) in AD brain slice shows endothelial reactivity and co-localization with Aβ plaques. These slices were counterstained with hematoxylin. SERPINA3 antibody staining in sCJD brain slice (lower left box) shows endothelial/perivascular reactivity and extracellular/cytoplasmic localization. TTR antibody staining in sCJD brain slice shows endothelial reactivity and subpial mater localization. Magnification: 10X

DISCUSSION

To date, an in-depth knowledge of the molecular processes that lead to neurodegeneration onset and progression in TSEs is still missing. In this context, genomic approaches are unbiased and powerful tools to investigate the molecular basis of these complex diseases. In addition, since neither effective therapy nor specific diagnosis is available yet, genomics may also allow the identification of new potential biomarkers. Many investigators in past years have performed genomic analyses of brain tissues from different models of animal TSE; some of the studies involved the mRNA profiling of cattle BSE [27, 149-151] or ovine scrapie [143-147,

189], but obviously the vast majority employed rodent-adapted models of prion disease [137-142, 200, 201]. In a number of these prion-infected mouse models, genomic expression profiling showed increased oxidative and endoplasmic reticulum (ER) stress, activated ER and mitochondrial apoptosis pathways together with induction of cholesterol biosynthesis in the CNS of preclinical mice [201].

We present here the first large-scale transcriptome study of the superior frontal gyrus of BSE-infected macaques. This specific region was selected due to its histopathological and functional relevance in the majority of neurodegenerative disorders [179] and ultimately because it corresponds to Broadmann areas 10 and 11, known to be involved in strategic processes in memory recall, diverse executive functions (domain-general function in "cognitive branching") as well as in planning, reasoning, and decision making [202], all processes known to be affected by neurodegeneration.

As starting point, the microarray analysis revealed 300 transcripts that were differentially regulated in BSE-infected animals versus controls. Among these, 97 probe sets were selected as candidates for validation with RT-qPCR, a technique well known for its high sensitivity and wide dynamic range [203].

Due to the shortage of cDNA availability and to the technical difficulties in designing the RT-qPCR primers for some of the genes -the macaque genome has been recently sequenced, but it's far from being completely validated [10]- only 11 DEGs were actually analyzed by RT-qPCR.

In general, variations of the expression levels observed with RT-qPCR were slightly larger than those seen in the microarray analysis. This is an obvious consequence of the different detection ranges of the two techniques. Microarray platform tends to have a lower dynamic range in comparison to RT-qPCR, the latter is used to validate array results [203]. RT-qPCR results confirmed the regulation trend seen in the

microarray platform for all the analyzed genes, providing very similar FC values using either *GAPDH* or *ACTB* for normalization. For five of them (*HBB, HBA2, TTR, SERPINA3, APOC1*) we obtained statistical significance with one or both qPCR detection systems we used (SYBR Green® and TaqMan® probes). As highlighted from functional classification of the identified DEGs reported in the Results section, some genes were involved in the top three canonical pathways: APOC1 and TTR are part of the LXR/RXR activation pathway, which is associated with lipid metabolism and transport, and are also involved in the neutral pathway of bile acid biosynthesis, which is a major route of cholesterol catabolism. Indeed, the liver X receptors (LXRs) are central players in cholesterol homeostasis throughout the periphery, where they function as sterol sensor to induce expression of genes involved in the regulation of cholesterol and lipid metabolism: APOC1 is one of the several apolipoproteins involved in reverse cholesterol transport, and is also a transcriptional target for LXRs [204, 205]. Both subtypes of LXR, LXRα and LXRβ, are expressed and functional in the CNS, the second being present 2 to 5 fold higher than in the liver, demonstrating the importance of these receptors in CNS cholesterol metabolism [205]. Interestingly, these pathways have been previously related to prion infection, particularly at the preclinical stage, suggesting a potential involvement of these two genes in the onset of the disease [201, 206-208]. On the other hand TTR, as well as SERPINA3, are also involved in the acute phase response signaling pathway, a systemic reaction to inflammation that may arise also in response to the extracellular protein deposition. This has been associated with prion and in general neurodegenerative diseases in the literature [209-211]. All the other genes analyzed seemed to reside in the grey zone of both platforms and therefore their FC values could not be considered reliable. Nevertheless, it would be premature to conclude that no other DEGs are present in this BSE model, since the sample size we analyzed was modest for the

large animal-to-animal variability that characterized this study and therefore weak effects (FC <|2|) could have not been detected with statistical significance [212].

Analyzing the clinical and histological data available for the macaques, we observed that animal A1 showed the shortest preclinical incubation period, a very short duration of disease [155] and the lowest deposition of PrP^{Sc} in brain tissue (Figure 7). This may be explained considering that PrP deposits are more stable and hence less pathogenic/infective than smaller oligomers [68]. Thus, since this sample exhibits a low amount of deposited protein, a higher amount of free PrP seeds might be present, and it is known that this form is more prone to trigger a rapidly progressive disease. Moreover, sample A5 behaves in quite the opposite way, showing the highest PrP^{Sc} deposition, the longest survival time and nearly the longest preclinical incubation time among intracranially infected animals [155], supporting the above mentioned hypothesis.

When coming to validate the microarray data with RT-qPCR, the first evidence we noticed was a considerable variability among samples, both within controls and infected groups. A reason for this inhomogeneity could be that, unlike other common animal models, non-human primates involved in this study were not inbred. Therefore, different genomic backgrounds may have substantially contributed to the inter-individual variations among the animals, leading to a remarkable variation in time of disease onset [155] and in gene expression within the same group. Curiously, for some of the most strongly regulated genes (*APOC1, HBB, HBA2*) the variability resulted even more prominent within the control group than within infected group. One possible explanation might be that BSE infection plays such a dramatic influence on the host organism that the normal biological differences in gene expression within healthy animals are somehow flattened toward up- or down-regulation in diseased ones, as a consequence of the powerful effect of the

pathology. In addition, infected and control animals were kept in different animal facilities, leading to possible differences in diet and/or housing conditions that may have contributed to these diversities.

Concerning the orally infected sample (B6), we observed a peculiar dysregulation pattern for a number of genes, which displayed a completely opposite trend compared to intracranially infected animals (Figure 15). Even though we have no data for PrP^{Sc} deposition in any tissue of this animal, the significantly longer incubation period (1950 days vs 1100 days) could indicate a correlation between the gene expression profile and the route of infection [183]. Of particular interest, *HBB* seemed to be expressed at a higher level in the orally infected animal compared to intracranially infected ones, both in the array platform and in RT-qPCR (FC≈+6 in B6, FC ≈ -6 in A1-A6 animals). This might give some clues on a possible protective role of hemoglobin in prion infection, which may lead to a slower progressing disease and maybe even to a milder phenotype. This model of oral transmission of BSE is particularly reliable since the old-world monkeys, besides being MM homozygous at 129 codon of *PRNP*, show a digestive physiology similar to that of human beings [119, 120, 156]. Of course, we should have had some gene expression data about the preclinical phase of these monkeys in order to conclude that the higher level of *HBB* found in B6 is due to the root of infection and not to a pre-existing higher expression of hemoglobin of the animal itself. Also, the different age at euthanasia should be taken into account while considering this different transcription pattern; the orally infected animal was almost 10 years old while, on average, intracranially infected animals were around 7 years old. Clearly, we are aware that one single sample is not enough to make any conclusion, however this striking difference is anyhow interesting.

Several of our DEGs were already found to be somehow associated with neurodegenerative diseases. Regarding hemoglobin (Hb), some years ago it was unexpectedly found to be expressed in mesencephalic dopaminergic neurons of different mouse strains, as well as in rats and humans. Later, its presence was also confirmed in substantia nigra (SN) of human Parkinson's disease (PD) postmortem brains and in multiple sclerosis (MS) postmortem brains, suggesting the intriguing hypothesis of a role for Hb in brain physiology and PD pathogenesis, presumably related to the respiration processes [213-215].

It has been already established that Hb expression decreases in neurons of PD, Alzheimer's disease (AD), argyrophilic grain disease (AGD) and dementia with Lewy bodies (DLB) brains [171] and that it can be regulated by both histone acetylation and CpG methylation of regulatory regions in erythroid cells [216, 217]. Furthermore, one interesting study suggests that *HBB* gene transcription is susceptible to (down-) regulation by histone deacetylase (HDAC) inhibition in the cortex of thricostatin (TSA)-treated mice, providing evidence for epigenetic mechanisms in the regulation of hemoglobin expression in neurons as well [218]. Substantial evidence already exists for hemoglobin and Hb-related proteins' involvement in neurodegenerative disorders in different animal models. Hba-a1 and Hbb-y were found to be down-regulated both in the preclinical and clinical phase in the CNS of scrapie-infected mice [137, 138] confirming the importance of these genes as pre-clinical neurodegeneration markers.

Interestingly, haptoglobin (Hpt), an Hb-binding protein involved in hemoglobin catabolism, exhibited late up-regulation (45 mpi) in the medulla of orally BSE-infected cattle [27]. In addition, an antioxidant role for Hpt has been proposed in human CSF [219]. Haptoglobin precursor has been found to be up-regulated also in the medulla oblongata of symptomatic naturally infected scrapie sheep [19]. Furthermore, since

hemoglobin is the most abundant source of peripheral iron in humans, one clear implication of its dysregulation would be iron homeostasis alteration.

An expanding body of evidence exists about iron dysregulation in the brain of many neurodegenerative disease affected patients: iron accumulation in AD brains [220], iron deposition in CNS and SN in PD patients [221, 222], and iron imbalance in prion disease affected brains [223]. Moreover, a possible iron-dependent translational control of human α-synuclein mRNA [224]. Also, in regards to AD, it is well known that hypoxic conditions, which may be present as a consequence of hemoglobin down-regulation, up-regulate APP mRNA and protein expression. In addition, it has been shown that Hb is able to bind to Aβ enhancing its aggregation and this in turn co-localizes in amyloid plaques in AD brains [225]. Therefore, if we envision a similar mechanism for prion diseases in which Hb interacts with β-rich PrP^{Sc} isoforms, we could hypothesize that down-regulated Hb fails to promote aggregation of the prion protein, determining an increased presence of toxic species such as oligomers [226]. In addition, the decrease in Hb would determine an increased amount of free iron which is highly toxic due to its ability to generate reactive oxygen species via the Fenton and Haber-Weiss reactions [227]. This released iron would be bound by ferritin, creating a redox-active and cytotoxic complex with PrP^{Sc}, ultimately lead to iron imbalance (deficiency phenotype) and to an increase of PrP^{Sc} toxic species [227], supporting the progression of the disease. This hypothesis is supported by the finding of redox-active iron in association with PrP^{Sc} plaques in vCJD brains [228], α-synuclein aggregates in Lewy bodies in PD brains [229] as well as an increase of total iron coupled with a paradoxical iron deficiency in CJD brains [230]. Furthermore, in PD it has been proposed that Hb may act as storage molecule for oxygen which, if necessary, could be released from oligodendrocytes to neighboring neurons in order to counteract hypoxia conditions and maintain the aerobic metabolism [213, 214].

Therefore, if down-regulated, Hb could not exert this function and neuronal functionality would be impaired by defective oxygen homeostasis.

In our study, we show a consistent down-regulation of both *HBB* and *HBA*, either in late-stage BSE-infected macaques or in post-mortem sCJD and neurodegenerative affected patients. The robustness of the assay was proved through a stringent analysis that excluded any relevant influence of potential blood contamination: small traces of erythrocyte-specific markers were inevitably detected in some samples; however, this negligible blood presence was homogeneously distributed among healthy and diseased groups. These results provide compelling evidence for a common role of Hb and iron dysregulation in neurodegeneration, possibly related to an alteration of O_2 homeostasis and oxidative metabolism [193]. These pathways seem to be shared among different diseases and species, reinforcing the emerging hypothesis of a prion-like mechanism for most –if not all- neurodegenerative disorders [55]. Additional investigations are needed to assess whether this down-regulation occurs as an early/late consequence of the disease, or if it represents a pre-existing condition that may act as a susceptibility factor for the onset of the pathology. One possible explanation for this Hb mRNA down-regulation could reside in a more general alteration of brain energy metabolism due to extensive neurodegeneration occurring in late/end stage disease, when our samples were collected. However, it is known that the specific region we selected for our analysis – superior frontal gyrus- is only moderately affected by CJD-related neurodegenerative processes. This would allow us to identify gene expression alterations which are directly related to early/moderately advanced changes occurring in CJD, and not to secondary effects of cell death occurring with disease progression.

Furthermore, given that our study was performed on whole frontal cortex tissue, we cannot discriminate if this down-regulation occurs in neurons or in glial cells.

However, as discussed previously, array data about some glial markers such as *GFAP* and *CD68* does not suggest any relevant deregulation in this cell population.

One other molecule that appears to be central in neurodegeneration, *APOC1*, was found to be significantly up-regulated in BSE-infected macaques as well in iCJD and sCJD patients. *APOC1* is part of the APOE/C-I/C-IV/C-II gene cluster and codes for apolipoprotein C-I (apoC-I), a small 6.6 kDa apolipoprotein component of lipoproteins (mainly HDL) that is known to inhibit receptor-mediated lipoprotein clearance, in particular particles containing apoE, via direct blockade of the low density lipoprotein (LDL) and VLDL receptors and LDL receptor-related protein [231]. Increasing evidence indicates a role for this gene in neurodegenerative disorders, especially AD and MS. APOC1 has been previously found to be in linkage disequilibrium with APOE 4 in AD [232]. In particular, the H2 allele of APOC1 is a susceptibility factor for LOAD [233] and its mRNA was found to be down-regulated in the frontal cortex – similar to what we found in our NEG samples- especially in H2-allelic individuals [208]. Moreover, its AA genotype has been shown to determine a younger age-of-onset in African American female multiple sclerosis patients, together with a higher progression index and MS severity score [234]. Impairment in lipid metabolism and signaling is one of the early alterations present in many neurodegenerative diseases, including prion diseases [210, 235]. Several studies focus on cholesterol metabolites with the aim of identifying early biomarkers for neurodegenerative disorders [236-238]. A number of genes involved in cholesterol metabolism and lipid biosynthesis have been found to be up-regulated in preclinical scrapie-infected mice [201]. ApoCI, together with ApoE and ApoAI, able to activate cholesterol esterification via lecithin-cholesterol acyltransferase (LCAT) [239], a pathway that contributes to excessive cholesterol elimination from the brain [219]. Indeed, brain cholesterol is mostly converted into an oxysterol (24S-hydroxycholesterol) that can freely diffuse to blood

but, upon esterification, it can also be exported to the liver embedded within lipoproteins throughout circulation [240]. Under normal conditions, this second pathway could be of minor relevance in regulating the efflux of cholesterol from the brain [241], but it could play an important role in triggering the increase of cholesterol accumulation – and particularly the consequent increase of the neurotoxic oxysterol- within neuronal cells upon prion infection [207]. If we add to this scenario the fact that Hpt, an above-mentioned hemoglobin-binding protein, has shown to be able to bind also ApoE and ApoAI [219] and that ApoAI has been found to interact with ApoCI [242], we can try to put together in the same pathway both the up-regulation of *APOC1* and the down-regulation of Hb. As already mentioned, it is known that prion infection reduces cholesterol efflux from neuronal cells leading to an increase in cellular cholesterol [207, 236], the main component of lipid rafts where PrP^{C} conversion into PrP^{Sc} is thought to occur [243, 244]. With this mechanism, prions might promote an increase of cellular cholesterol content in order to have more favorable environment to allow/enhance their conversion [207]. This increase in cholesterol would lead to a simultaneous activation of Hpt that in case of oxidative stress -presumably triggered by increased oxysterol- is expected to work in the CNS [245] preventing oxidative injuries to ApoE and ApoAI, thus saving their esterification function [246]. This Hpt-ApoAI complex could in turn stimulate ApoCI, further raising the esterification of cholesterol in order to increment its displacement from the brain toward the liver, where cholesterol is then catabolized into bile acids [219]. In addition, to increase Hpt available sites to bind apoliproteins, Hb is down-regulated (or due to a negative feedback because Hpt binds less Hb and therefore free Hb levels increase). This decrease in Hb would result in an increase in free iron that, upon binding to ferritin, stimulates the formation of a toxic ferritin-PrP^{Sc} complex which ultimately leads to iron deficiency and increase in PrP^{Sc} toxic species [227].

Consistent with this hypothesis, some *in vitro* studies have shown that depletion of cellular cholesterol reduces the conversion of PrP^{C} to PrP^{Sc} [243]. Taken together, these data suggest that both Hb and ApoCI could represent extremely powerful drug targets as well as potentially useful biomarkers to assess the efficacy of possible therapies.

Another gene that we found highly up-regulated in BSE-infected monkeys -as well as in vCJD, iCJD and sCJD patients- is *SERPINA3*, a serpin peptidase inhibitor extensively reported to be regulated in several neurodegenerative disease models. The encoded protein is involved in acute phase response pathways and it is well known for its interaction with APP in promoting amyloid plaque formation —a hallmark of AD [247]. Indeed, increased levels of SERPINA3 protein have been found in the brain and peripheral blood of AD patients [248], mainly due to persistent inflammation [249]. Furthermore, a polymorphism in its gene promoter has been identified as a disease modifier both for AD and PD: the TT genotype resulted as a risk factor for EOAD [250], while the AA genotype has been suggested to play a modest protective role against early-onset PD in women, especially in the Taiwanese population [251]. In prion disease models, SERPINA3 was increased in urine and cerebrospinal fluid of CJD patients and also in brains of scrapie-infected mice [235, 252]. Moreover, it is up-regulated after 10 weeks post inoculation (prior to clinical sign manifestation) in mice infected with RML prion strain, probably due to activation of astrocytes and microglia [253]. Being an acute phase protein, its up-regulation is generally explained by the onset of an inflammation condition, particularly as a response of the innate immunity to infection [254]. However, inflammation and immune system activation seem not to be a hallmark of prion diseases themselves, and is more likely an eventual consequence of massive late-stage neuronal degeneration [209]; therefore, an alternative role for SERPINA3 in prion disorder

should be considered. Of particular interest, two β-sheets of SERPINA3 exhibit a polymorphism mimicking changes in the serpin structure that normally occur during the formation of its stable complex with the target proteinase. In this conformation, SERPINA3 can bind Aβ, thus imposing a β-strand conformation that upon dissociation leads to a faster formation of fibrils [247]. Therefore, an intriguing hypothesis may be proposed in which PrP conversion into β-sheet conformation can be assisted by the “chaperone” SERPINA3, which would then accelerate the formation of toxic species like PrP oligomers. In addition, *SERPINA3* expression in the brain can be regulated *in vivo* by ApoE [255]. Also, some *in vitro* studies indicated that SERPINA3 is able to bind cholesterol [256]. Therefore we hypothesize that abnormal cholesterol levels might trigger *SERPINA3* up-regulation as a supplementary reinforcement for cholesterol binding and transport when ApoE and other lipoproteins are saturated and therefore no longer available. Nevertheless, due to its presumable capability to bind β-sheet enriched PrP^{Sc}, the SERPINA3 increase would lead to a sustained conversion of the prion protein, therefore supporting the disease progression. Despite SERPINA3 protein has been found up-regulated in several neurodegenerative disease, in addition to CJD, we did not observe up-regulation at the mRNA level in non-CJD affected patients. Therefore, we suggest that transcriptional regulation is a unique mechanism occurring in CJD disorder and that, as well as *APOC1*, represents a specific prion disease marker that could be considered as a potential diagnostic and therapeutic tool.

In the same pathway of acute phase response, also the transthyretin gene was up-regulated in our BSE-infected macaques, even though we were not able to confirm the statistical significance with the more specific TaqMan assay. Nevertheless, we found similar results also in human samples; indeed, both sCJD and especially iCJD patients showed an upregulation for *TTR*. TTR is a prealbumin, best known as a

carrier of the thyroid hormone thyroxine (T4) in serum and CSF. Also, when associated with retinol-binding protein (RBP) in the serum, it can transport retinol as well. TTR is associated with systemic amyloidosis characterized by deposition of aggregated protein in various tissues, but it has been also associated with an anti-amyloidogenic effect in regard to Aβ. Like SERPINA3, TTR binds to beta amyloid, but in this case the binding seems to prevent Aβ deposition. In fact, TTR not only inhibits Aβ fibril formation, but also neutralizes the toxicity of pre-formed oligomers by promoting their further assembly into larger aggregates, as shown in neuroblastoma cells and primary rat neurons [257]. Moreover, increased mRNA and protein levels have been reported in neurons from the AD mouse model 'APP23' and in human AD brain. This suggests that TTR transcription and synthesis may be up-regulated and sustained by the increased production of Aβ or its precursors. The subsequent interaction between TTR and Aβ and the formation of TTR- Aβ complexes with reduction of toxic aggregates may be a protective mechanism in response to AD [258]. Furthermore, silencing the endogenous *TTR* gene accelerated the disease pathogenesis in the well validated AD mouse model APP23, and TTR overexpression suppressed the behavioral symptoms of AD [76], confirming the neuroprotective role of this protein. Even in prion models TTR levels have been found strongly increased in the cortex of scrapie-infected mice [139]. Our study now provides evidence that upregulation of *TTR* is also found in BSE-infected macaques and CJD affected patients, further expanding the view that this is an important player in human neurodegeneration. If we hypothesize a common mechanism in AD and TSEs, we can speculate a possible up-regulation of TTR, promoted by the presence of PrP toxic oligomeric species, as a "protective" mechanism that would facilitate the formation of larger non-toxic PrP aggregates. Taken together, the data on *SERPINA3* and *TTR* suggest an implication of innate immune system activation and

inflammatory response, as suggested by some authors [259, 260]. Fratini *et al*. also reported a clear increase of seven proteins all belonging to the acute phase response processes in a study of plasma samples from sporadic CJD patients [261]. This suggests not only a localized inflammatory condition at brain level, but also a possible generalized systemic inflammation in sCJD. However, analysis of our microarray data did not reveal any relevant deregulation of other genes typically involved in neuroinflammation and/or immune response. Indeed, cytokines and other mediators such as IL6, TNFα, GFAP and CD68 showed FC < |2|, indicating that inflammatory responses seem not be of particular relevance in this prion model or in the area of the CNS that was examined. However, since we found a trend of down-regulation of *TTR* in non-prion neurodegenerative diseases -for which involvement of inflammation has been proposed [247, 262, 263]- we can consider that the *TTR* dysregulation in this case may be actually related to activation of inflammatory responses. It is known that as soon as the inflammation process starts, the synthesis of the negative acute phase proteins, such as TTR, decrease in order to provide more amino acids for the synthesis of positive acute phase ones. Nevertheless, we could suggest a different explanation for *TTR* involvement in neurodegeneration that regards, again, cholesterol. It has been reported that TTR is able to bind membrane lipids via electrostatic interactions [264] and this binding appears to be influenced by the concentration of cholesterol and the lipid composition of the membrane. This membrane binding is also correlated with the cytotoxic effect of TTR oligomers [265]. Therefore, we could hypothesize that TTR in neurodegenerative diseases behaves to some extent similarly to PrP in prion disorders, binding preferentially to lipid rafts in the plasma membrane where it promotes the formation of toxic oligomers that ultimately lead to neuronal degeneration.

Concerning the other genes we analyzed, microarray and RT-qPCR platforms indicated a concordant expression trend. Some of these genes, e.g. *NR4A2* and *IRF3*, have been previously reported in association with prion infection and other neurodegenerative disorders. Our data showed down-regulation for *NR4A2* and slight up-regulation for *IRF3* and, even though we did not obtain statistically significant results, they are in line with the findings of these reports [144, 185, 266-268].

One further interesting point that remains to be elucidated regards the expression of the prion protein gene itself in the different diseases models we studied. In literature, some contradictory results are present; indeed, while some studies reported no *PRNP* alterations during BSE infection in cattle [191], in a recent work Llorens and colleagues found that sCJD MM1 patients displayed a significant slight decrease in *PRNP* mRNA levels which was not found in sCJD VV2 patients [259]. Due to shortage of macaque cDNA, we were not able to investigate *PRNP* levels in BSE-infected samples; nevertheless, our microarray data suggested that, at least at the mRNA level, no changes occur between control and infected animals. However, in humans we were able to analyze *PRNP* mRNA levels across the different groups. Also in this case, no significant alterations were observed between controls and CJD affected patients. Given that genetic analysis was available only for a limited number of the analyzed patients, we were not able to discriminate the influence of the codon 129 genotype and/or the PrP^{Sc} type on the *PRNP* mRNA levels. However, we were able to highlight a difference between the two acquired CJD groups. Indeed, vCJD patients showed a significantly higher level of *PRNP* mRNA levels in comparison with iCJD ones. In light of these findings, we could hypothesize that the route of infection might somehow influence the mRNA levels of PrP. As regards cellular prion protein, its levels have been investigated little due to the concurrent presence of PrP^{Sc}, which

is often present in molar excess and complicates the analysis. Reduced levels of total prion protein has been detected in the CSF of a number of neurodegenerative diseases, including CJD, AD, DLB, PD and MS [269]. However, by using velocity gradient centrifugation and CDI, Safar and colleagues recently highlighted a down-regulation of PrP^{C} in end stage WT mice infected with scrapie, CJD and CWD prion strains. They also found this down-regulation in preclinical WT mice infected with RML, suggesting the occurrence of proteostasis as a host protective response triggered by the presence of PrP^{Sc} [270].

Summarizing, our results suggest that while hemoglobin seems to be involved in unspecific pathways shared among many different neurodegenerative diseases, *APOC1*, *TTR* and particularly *SERPINA3* seem to represent specific CJD alterations. Interestingly, for *TTR*, *APOC1* and *PRNP* we observed a significantly different behavior between vCJD and iCJD patients, indicating that the route of infection plays a major role in the regulation of these genes and presumably also of the related pathways.

One other main consequence of these results is that these genes, in particular *APOC1* and *SERPINA3*, upon further validation, could be exploited as potential biomarkers for both diagnostic purposes and also as promising targets for therapy. All together, these data strongly suggest the crucial role of impaired cholesterol metabolism in prion disease onset and progression, as well as iron imbalance in general neurodegeneration processes.

CONCLUSIONS

As far as we know, this is the first genome-wide expression study in the frontal cortex of cynomolgus macaques inoculated with BSE. In our work we used both microarray

and RT-qPCR technologies that allowed us to identify a gene signature able to distinguish BSE-infected macaques from control animals. The identified genes are involved in oxygen transport and iron metabolism (*HBB, HBA2*), cholesterol metabolism and lipid transport (*APOC1, SERPINA3)* as well as acute phase response (*SERPINA3, TTR*).

Importantly, the dysregulation of four of these genes (*HBA2, APOC1, TTR, SERPINA3)* have been validated with consistent FC values also in CJD affected human samples, confirming the reliability of our previous analysis in BSE-infected monkeys and providing important hints on some prion-specific alterations in CJD disease. These results could be extremely helpful in understanding the mechanism underlying the progression of the disease, possibly leading to the identification of some key players which, even if not the cause of onset, could be some of the target genes affected by the disease. In addition, the two genes related to hemoglobin were found similarly (down-)regulated also in non-CJD neurodegenerative disorders, shedding some light on common pathways underlying neurodegeneration. Therefore, some of our findings support the hypothesis of a potential shared mechanism underlying the onset and the development of all neurodegenerative disorders. This is in concordance with very recent data supporting the idea of a unifying role of prions in these diseases in general and maybe a prion-like behavior for most neurodegenerative disorder [68].

Moreover, all the DEGs we validated were also expressed also in blood. It is reasonable to believe that the genome is equivalent in sequence and structure in all cells and tissues of the same organism [271]. Indeed, in most instances the genome observed in peripheral blood is highly similar to that in the brain – with an overlapping of about 70-80% [272-274]-, allowing for investigation of transcriptional alterations in blood that would reflect brain disorders. Therefore, validating their consistent

dysregulation in blood, would open the interesting possibility to employ these transcripts as "readily available" biomarkers for both diagnostic and therapeutic purposes. Even more important, this could allow to investigate the gene expression pattern of these biomarkers also in earlier stages of the disease, providing an invaluable insight about the pathogenic mechanism underlying the onset of these disorders and, therefore, also a potential tool for early diagnosis and eventual therapy monitoring.

In conclusion, our data suggest that, in order to identify diagnostic and/or therapeutic approaches for prion diseases and other neurodegenerative disorders, a combination of various pathways has to be targeted, including oxygen and iron homeostasis, inflammation response and in particular cholesterol and lipid metabolism.

APPENDIX

	Probe ID	Gene Symbol	Gene name	RefSeq Transcript ID	P-value	FC
1	Mmu.6048.1.S1_s_at	---	---	---	1.47E-09	394.064
2	MmuSTS.2150.1.S1_at	LOC574106	alpha-1-antichymotrypsin	XM_001096947	2.76E-03	16.002
3	Mmu.10083.1.S1_s_at	LOC574106	alpha-1-antichymotrypsin	XM_001096947	4.30E-03	10.108
4	MmuSTS.1168.1.S1_at	LOC703401	similar to chitinase 3-like 1	XM_001103739	2.44E-03	3.875
5	MmugDNA.25842.1.S1_at	---	---	---	2.64E-04	3.820
6	MmugDNA.31051.1.S1_at	---	---	---	1.00E-05	3.477
7	MmugDNA.28171.1.S1_at	---	---	---	3.79E-03	3.385
8	MmugDNA.14064.1.S1_at	---	---	---	9.17E-04	3.198
9	MmugDNA.23791.1.S1_s_at	PROSC	Proline synthetase co-transcribed homolog	XM_001089087	7.65E-04	3.044
10	MmugDNA.13972.1.S1_at	---	---	---	1.26E-03	2.949
11	Mmu.2091.1.S1_x_at	MAMU-AG	major histocompatibility complex, class I, AG	NM_001134230	3.96E-04	2.699
12	MmugDNA.651.1.S1_at	---	---	---	2.80E-03	2.617
13	MmuSTS.1024.1.S1_at	LILRBB	Leukocyte immunoglobulin-like receptor, subfamily B, member b	---	6.20E-04	2.560
14	MmugDNA.15540.1.S1_at	PAPLN	papilin, proteoglycan-like sulfated glycoprotein	XM_001088864	1.95E-03	2.399
15	MmugDNA.26476.1.S1_at	---	---	---	2.00E-03	2.369
16	MmuSTS.242.1.S1_at	LOC710534	hypothetical protein LOC710534	XM_001099170	4.61E-04	2.288
17	MmugDNA.26095.1.S1_at	---	---	---	4.07E-03	2.280
18	Mmu.13692.1.S1_at	---	---	---	1.67E-03	2.244
19	MmugDNA.19355.1.S1_at	---	---	---	5.19E-04	2.161
20	MmugDNA.5017.1.S1_at	LOC694227	similar to msh homeobox 2	XM_001082405	2.30E-03	2.151
21	MmugDNA.42101.1.S1_at	LOC709549	hypothetical protein LOC709549	XM_001110840	9.04E-04	2.146
22	MmugDNA.39745.1.S1_at	LOC712270	Similar to TBC1 domain family, member 10C	XM_001106367 /// XM_001106431	2.28E-04	2.146
23	Mmu.5468.1.S1_at	IRF3	interferon regulatory factor 3	NM_001135797 /// XM_001115379	1.26E-03	2.109
24	MmugDNA.6086.1.S1_at	PLEKHA8	pleckstrin homology domain containing, family A (phosphoinositide binding specif	XM_001086047 /// XM_001086163 /// XM_001086395	1.33E-04	2.108
25	Mmu.2066.1.A1_at	---	---	---	2.33E-03	2.079
26	MmugDNA.38248.1.S1_at	---	---	---	2.82E-03	2.073
27	MmugDNA.15190.1.S1_at	---	---	---	8.00E-04	2.058
28	Mmu.6867.3.S1_s_at	---	---	---	1.20E-03	2.045
29	MmugDNA.1315.1.S1_at	---	---	---	1.60E-03	2.034
30	MmuSTS.242.1.S1_x_at	LOC710534	hypothetical protein LOC710534	XM_001099170	6.68E-04	2.030
31	MmugDNA.21023.1.S1_at	IRF3	interferon regulatory factor 3	NM_001135797 /// XM_001115379	2.58E-04	2.015
32	MmugDNA.29834.1.S1_at	---	---	---	1.58E-05	2.013
33	MmugDNA.13998.1.S1_at	---	---	---	5.50E-05	2.007
34	MmuSTS.1253.1.S1_at	---	---	---	4.26E-03	2.005
35	MmugDNA.42687.1.S1_at	LOC714858	similar to ribosomal protein L35a	XM_001103775 /// XM_001103861	2.12E-03	2.002
36	MmugDNA.24820.1.S1_at	CSNK1G3	casein kinase 1, gamma 3	XM_001093600 /// XM_001093723 /// XM_001093838 /// XM_001093954	4.27E-03	-2.027
37	MmugDNA.2165.1.S1_at	LOC701418	similar to small nuclear ribonucleoprotein E	XM_001099502 /// XM_001099697	9.82E-04	-2.040
38	MmugDNA.27879.1.S1_at	---	---	---	4.90E-03	-2.063
39	MmugDNA.33232.1.S1_at	---	---	---	1.26E-03	-2.079
40	MmugDNA.23281.1.S1_at	---	---	---	2.83E-03	-2.089
41	MmugDNA.36827.1.S1_at	ACVR1C	activin A receptor, type IC	XM_001088259 /// XM_001088355 /// XM_001088467 /// XM_001088578	4.84E-03	-2.119
42	MmunewRS.391.1.S1_at	LOC711550	similar to UDP-GalNAc:betaGlcNAc beta 1,3-galactosaminyltransferase, polypeptide	XM_001101191	2.64E-03	-2.149
43	MmugDNA.2696.1.S1_at	TXNL4A	Thioredoxin-like 4A	XM_001089626	3.97E-03	-2.150
44	MmugDNA.7163.1.S1_at	---	---	---	4.23E-03	-2.163
45	MmuMitochon.12.1.S1_s_at	---	---	---	3.45E-04	-2.163
46	MmugDNA.5156.1.S1_at	FLVCR	feline leukemia virus subgroup C cellular receptor	XM_001107314	5.05E-04	-2.181
47	MmugDNA.42527.1.S1_at	---	---	---	1.92E-03	-2.189
48	MmuSTS.2949.1.S1_at	KPNA6	karyopherin alpha 6	XM_001101656 /// XM_001101838 /// XM_001102023 /// XM_001102113 /// XM_001102197	5.93E-04	-2.189
49	MmugDNA.5766.1.S1_at	TM7SF3	transmembrane 7 superfamily member 3	XM_001099269	4.47E-04	-2.211
50	MmugDNA.9234.1.S1_at	---	---	---	2.34E-03	-2.217
51	MmugDNA.23612.1.S1_at	---	---	---	2.89E-03	-2.218
52	MmugDNA.8176.1.S1_at	---	---	---	1.41E-03	-2.238

53	MmugDNA.34611.1.S1_at	---	---	---	1.12E-03	-2.270
54	MmugDNA.41713.1.S1_at	---	---	---	1.70E-04	-2.309
55	MmugDNA.22094.1.S1_at	PMM2	Phosphomannomutase 2	XM_001102327	3.60E-03	-2.319
56	MmuSTS.1753.1.S1_at	---	---	---	3.86E-03	-2.324
57	MmugDNA.15864.1.S1_at	---	---	---	3.28E-03	-2.335
58	MmugDNA.9027.1.S1_at	RIOK2	RIO kinase 2 (yeast)	XM_001095785	2.20E-04	-2.344
59	MmugDNA.5351.1.S1_at	---	---	---	4.00E-03	-2.413
60	MmugDNA.1268.1.S1_at	---	---	---	1.58E-05	-2.444
61	MmugDNA.34998.1.S1_s_at	LOC720089	similar to CG16989-PA	XM_001115127	1.74E-04	-2.459
62	MmugDNA.24219.1.S1_at	---	---	---	3.51E-03	-2.466
63	MmugDNA.21409.1.S1_at	---	---	---	4.81E-05	-2.472
64	MmugDNA.23359.1.S1_x_at	---	---	---	4.79E-03	-2.506
65	MmuSTS.3838.1.S1_at	SLCO1A2	solute carrier organic anion transporter family, member 1A2	XM_001097798 /// XM_001097901 /// XM_001097987 /// XM_001098080	3.17E-03	-2.518
66	MmugDNA.3753.1.S1_at	SAP18	Sin3A-associated protein, 18kDa	XM_001085227 /// XM_001085342	1.44E-03	-2.602
67	MmugDNA.12750.1.S1_at	---	---	---	3.65E-04	-2.704
68	MmugDNA.2556.1.S1_at	STX16	syntaxin 16	XM_001084489 /// XM_001084615 /// XM_001084730	6.39E-04	-2.728
69	MmugDNA.2127.1.S1_at	SMARCC1	SWI/SNF-related matrix-associated actin-dependent regulator of chromatin c1	XR_012360	2.69E-03	-2.735
70	MmuMitochon.4.1.S1_at	---	---	---	4.17E-05	-2.801
71	MmugDNA.24987.1.S1_at	---	---	---	2.29E-04	-2.895
72	MmugDNA.24269.1.S1_at	---	---	---	4.18E-04	-2.923
73	MmugDNA.1402.1.S1_at	---	---	---	8.07E-04	-2.935
74	MmugDNA.41331.1.S1_at	---	---	---	3.77E-03	-2.959
75	MmugDNA.12544.1.S1_at	LOC703458	Similar to Histidine acid phosphatase domain containing 1	XM_001097844 /// XM_001098229 /// XM_001098433 /// XM_001098530	3.11E-03	-3.102
76	MmugDNA.6830.1.S1_at	ZNF397	zinc finger protein 397	XR_013079	3.65E-03	-3.113
77	Mmu.10780.1.S1_at	SERPINA1	Serpin peptidase inhibitor, clade A (alpha-1 antiproteinase, antitrypsin), membe	XM_001098533 /// XM_001098837 /// XM_001098941 /// XM_001099044 /// XM_001099150	1.21E-03	-3.289
78	MmugDNA.39622.1.S1_at	---	---	---	5.51E-04	-3.498
79	MmugDNA.15556.1.S1_at	---	---	---	6.24E-04	-3.558
80	MmugDNA.32444.1.S1_at	GALNTL2	similar to UDP-N-acetyl-alpha-D-galactosamine:polypeptide	XM_001083446	8.93E-05	-3.746
81	MmuSTS.944.1.S1_at	TM7SF3	transmembrane 7 superfamily member 3	XM_001099269	1.59E-04	-3.922
82	MmugDNA.32138.1.S1_at	LOC712125	similar to zinc transporter like 2	XM_001108032 /// XM_001108096 /// XM_001108147 /// XM_001108199	2.35E-07	-4.922
83	MmugDNA.30314.1.S1_at	---	---	---	6.21E-05	-5.067
84	MmugDNA.23886.1.S1_at	LOC718977	similar to dynein, cytoplasmic, heavy polypeptide 1	XM_001112424	1.41E-07	-5.109
85	MmugDNA.22310.1.S1_at	---	---	---	5.67E-04	-6.042
86	MmuAffx.78.1.S1_s_at	---	---	---	2.77E-08	-21.150

Additional table 1. List of 86 differentially expressed probe sets with *p* values ≤ 0.005 and FC ≥ |2|. Probe ID, Gene Symbol, Gene Name and RefSeq Transcript IDs annotation as of release 29 of the Affymetrix® Rhesus Annotation library (01/July/09). P-values and fold changes are reported for all 86 probe sets.

	Probe ID	Previous gene symbol	Current gene symbol	Gene name	RefSeq Transcript ID	P-value	FC
	FC ≥ |2.5|, p≤0.005 (36 rows)						
1	MmuAffx.78.1.S1_s_at	---	MT-CYB-201	MT:14741-15881(1)	---	2.77E-08	-21.150
2	Mmu.6048.1.S1_s_at	---	ND4	NADH dehydrogenase subunit 4 (mitochondrion)	JN709966.1	1.47E-09	394.064
3	MmugDNA.23886.1.S1_at	LOC718977	DYNC1H1-201	similar to dynein, cytoplasmic, heavy polypeptide 1	XM_001112424	1.41E-07	-5.109
4	MmugDNA.32138.1.S1_at	LOC712125	SLC30A7	solute carrier family 30 (zinc transporter), member 7	NM_001266184.1	2.35E-07	-4.922
5	MmugDNA.31051.1.S1_at	---	---	8:119157054-119157347(-1)	---	1.00E-05	3.477
6	MmuMitochon.4.1.S1_at	---	COXI-201/COXII-201	cytochrome c oxidase subunit II (mitochondrion)	AY972676.1 [Source:RefSeq peptide;Acc:YP_026107]	4.17E-05	-2.801
7	MmugDNA.30314.1.S1_at	---	---	2:27904497-27904521(1)	---	6.21E-05	-5.067
8	MmugDNA.32444.1.S1_at	GALNTL2	GALNTL2	similar to UDP-N-acetyl-alpha-D-galactosamine:polypeptide	---	8.93E-05	-3.746
9	MmuSTS.944.1.S1_at	TM7SF3	TM7SF3	transmembrane 7 superfamily member 3	XM_001099269.2	1.59E-04	-3.922
10	MmugDNA.24987.1.S1_at	---	---	1:165875041-165875065(-1)	---	2.29E-04	-2.895
11	MmugDNA.25842.1.S1_at	---	RPL27A_hu	Homo sapiens ribosomal protein L27a	---	2.64E-04	3.820
12	MmugDNA.12750.1.S1_at	---	---	7:130441604-130441628(-1)	---	3.65E-04	-2.704
13	Mmu.2091.1.S1_x_at	MAMU-AG	---	10992147263 97:214-2416(1)	Uncharacterized protein [Source:UniProtKB/TrEMBL;Acc:H9H4X3]	3.96E-04	2.699
14	MmugDNA.24269.1.S1_at	---	---	10:89173266-89173290(1)	---	4.18E-04	-2.923
15	MmugDNA.39622.1.S1_at	---	---	X:22370278-22370302(1)	---	5.51E-04	-3.498
16	MmugDNA.22310.1.S1_at	---	NUP50_hu	Homo sapiens nucleoporin 50kDa	---	5.67E-04	-6.042
17	MmuSTS.1024.1.S1_at	LILRBB	NEDD4L-205	neural precursor cell expressed, developmentally down-regulated 4-like	[Source:UniProtKB/TrEMBL;Acc:F7AXT7]	6.20E-04	2.560
18	MmugDNA.15556.1.S1_at	---	PLEKHA3-201	pleckstrin homology domain containing, family A (phosphoinositide binding specific) member 3	[Source:UniProtKB/TrEMBL;Acc:F6WME3]	6.24E-04	-3.558
19	MmugDNA.2556.1.S1_at	STX16	STX16	syntaxin 16	XM_001084489 /// XM_001084615 /// XM_001084730	6.39E-04	-2.728
20	MmugDNA.23791.1.S1_s_at	PROSC	---	18:39890353-39890377(-1)	---	7.65E-04	3.044
21	MmugDNA.1402.1.S1_at	---	---	2:74621205-74621229(-1)	---	8.07E-04	-2.935
22	MmugDNA.14064.1.S1_at	---	---	3:75751313-75751337(1)	---	9.17E-04	3.198
23	Mmu.10780.1.S1_at	SERPINA1	ABCD3-201	ATP-binding cassette sub-family D member 3-like	Uncharacterized protein [Source:UniProtKB/TrEMBL;Acc:F6QHX4]	1.21E-03	-3.289
24	MmugDNA.13972.1.S1_at	---	---	13:80841373-80841397(1)	---	1.26E-03	2.949
25	MmugDNA.3753.1.S1_at	SAP18	SAP18	histone deacetylase complex subunit SAP18	NM_001261034.1	1.44E-03	-2.602
26	MmuSTS.1168.1.S1_at	LOC703401	CHI3L1-201	chitinase-3-like protein 1 precursor	NM_001265920.1	2.44E-03	3.875
27	MmugDNA.2127.1.S1_at	SMARCC1	MMU.10107-202	2:88839715-88936168(1)	Uncharacterized protein [Source:UniProtKB/TrEMBL;Acc:F7HJG9]	2.69E-03	-2.735
28	MmuSTS.2150.1.S1_at	LOC574106	SERPINA3	serpin peptidase inhibitor, clade A (alpha-1 antiproteinase, antitrypsin), member 3 precursor	NM_001195350.1 [Source:RefSeq peptide;Acc:NP_001182279]	2.76E-03	16.002
29	MmugDNA.651.1.S1_at	---	---	16:47032713-47032737(1)	---	2.80E-03	2.617
30	MmugDNA.12544.1.S1_at	LOC703458	ACSL3-201	acyl-CoA synthetase long-chain family member 3	Uncharacterized protein [Source:UniProtKB/TrEMBL;Acc:F7GUH7]	3.11E-03	-3.102
31	MmuSTS.3838.1.S1_at	SLCO1A2	SLCO1A2	solute carrier organic anion transporter family, member 1A2	XM_001097798 /// XM_001097901 /// XM_001097987 /// XM_001098080	3.17E-03	-2.518
32	MmugDNA.6830.1.S1_at	ZNF397	ZNF397	zinc finger protein 397	XR_013079	3.65E-03	-3.113
33	MmugDNA.41331.1.S1_at	---	---	13:86724520-86724544(1)	---	3.77E-03	-2.959
34	MmugDNA.28171.1.S1_at	---	---	14:9000414-9000438(-1)	---	3.79E-03	3.385
35	Mmu.10083.1.S1_s_at	LOC574106	SERPINA3	serpin peptidase inhibitor, clade A (alpha-1 antiproteinase, antitrypsin), member 3 precursor	NM_001195350.1 [Source:RefSeq peptide;Acc:NP_001182279]	4.30E-03	10.108
36	MmugDNA.23359.1.S1_x_at	---	---	---		4.79E-03	-2.506
	FC ≥ |2.5|, 0.005≤p≤0.05 (29 rows)						
37	MmugDNA.43301.1.S1_at	---	---	2:27907866-27907890(1)	---	5.12E-03	-3.093
38	MmugDNA.23664.1.S1_at	SGCB	---	4:26168443-26168467(1)	---	5.46E-03	-3.523
39	MmugDNA.18153.1.S1_at	---	---	2: 96,954,542-96,954,566	---	5.56E-03	-2.543
40	MmugDNA.11249.1.S1_at	---	---	---	---	6.25E-03	2.513
41	MmugDNA.35181.1.S1_s_at	---	MTRNR2L1_hu	Homo sapiens MT-RNR2-like 1	---	6.29E-03	-8.751
42	MmugDNA.8255.1.S1_at	---	---	16:73401096-73401120(-1)	---	6.35E-03	-2.728
43	Mmu.1942.1.S1_at	SLC26A2	---	6:146464760-146464784(1)	---	7.07E-03	-3.483
44	MmugDNA.454.1.S1_at	CLIC4	CLIC4	chloride intracellular channel protein 4	XM_001106291 /// XM_001106424 /// XM_001106485	7.51E-03	-2.576
45	MmugDNA.10294.1.S1_at	LOC712063	---	2:138477793-138477817(1)	---	9.84E-03	-2.824
46	MmugDNA.15322.1.S1_at	---	---	9:112213128-112213152(1)	---	1.05E-02	-2.733
47	MmuAffx.161.1.S1_at	---	DNAH2-201	dynein, axonemal, heavy chain 2	Uncharacterized protein [Source:UniProtKB/TrEMBL;Acc:F7EE86]	1.15E-02	2.675
48	MmugDNA.17327.1.S1_at	LOC700825	MMU.13505-201	TIA1 cytotoxic granule-associated RNA binding protein	[Source:RefSeq peptide;Acc:NP_001248687]	1.22E-02	-2.864
49	Mmu.12003.1.S1_s_at	---	---	5:12449924-12449948(1)	---	1.28E-02	-3.417
50	MmugDNA.14890.1.S1_at	TNFSF10	TNFSF10	tumor necrosis factor (ligand) superfamily, member 10	NM_001266034.1	1.39E-02	-2.726

51	MmugDNA.30129.1.S1_at	---	---	14:39186783-39186807(-1)	---	1.46E-02	-2.765
52	MmugDNA.6026.1.S1_at	---	ZBTB33-201	transcriptional regulator Kaiso	[Source:RefSeq peptide;Acc:NP_001253879]	1.50E-02	-3.084
53	MmugDNA.42515.1.S1_at	---	RICTOR-201	RPTOR independent companion of MTOR, complex 2	Uncharacterized protein [Source:UniProtKB/TrEMBL;Acc:F7GUW7]	1.71E-02	2.865
54	MmugDNA.37382.1.S1_s_at	LOC696955	MYBPC1	myosin binding protein C, slow type isoform 1	XM_001091952.1	1.90E-02	2.503
55	MmugDNA.27998.1.S1_at	---	---	5: 77,332,249-77,332,273	---	1.98E-02	-3.780
56	MmugDNA.36174.1.S1_s_at	LOC698803	---	2:96954542-96954566(-1)	---	2.11E-02	-3.144
57	MmugDNA.21587.1.S1_at	---	---	16:73399355-73399379(-1)	---	2.36E-02	-2.769
58	MmugDNA.1587.1.S1_at	LOC706963	PIK3R3-201	phosphoinositide-3-kinase, regulatory subunit 3 (gamma)	---	3.43E-02	4.697
59	Mmu.12263.1.S1_at	NGFR	MRPL42-201	mitochondrial ribosomal protein L42	---	3.70E-02	4.006
60	MmugDNA.32666.1.S1_s_at	LOC706963	APOC1	apolipoprotein C-I	AK240617.1	4.19E-02	4.326
61	MmugDNA.28692.1.S1_at	NCAM1	NCAM1	neural cell adhesion molecule 1	XM_001083697.2	4.34E-02	2.501
62	MmugDNA.11141.1.S1_at	---	---	12:41239625-41239649(-1)	---	4.41E-02	-3.359
63	MmugDNA.28863.1.S1_at	LOC715676	MRPL42-201	similar to Mitochondrial 28S ribosomal protein S32 (S32mt) (MRP-S32)	XM_001106011	4.47E-02	-2.778
64	MmugDNA.39988.1.S1_at	LOC710110	---	11:46397739-46401158(1)	Uncharacterized protein [Source:UniProtKB/TrEMBL;Acc:F7DXF0]	4.71E-02	2.917
65	MmugDNA.27963.1.S1_at	PIK3R3	PIK3R3	phosphoinositide-3-kinase, regulatory subunit 3 (gamma)	NM_001266826.1	4.81E-02	-2.712
	FC ≥ |2.5|, p>0.05 (24 rows)						
66	MmugDNA.19449.1.S1_at	LOC713498	---	17:10740623-10740647(1)	---	5.49E-02	-3.017
67	MmugDNA.40194.1.S1_at	DCLRE1A	USP16	ubiquitin carboxyl-terminal hydrolase 16	NM_001260999.2	6.25E-02	-5.477
68	MmugDNA.22629.1.S1_at	---	LRRC8B_hu	Homo sapiens leucine rich repeat containing 8 family, member B	---	6.61E-02	-5.313
69	MmugDNA.2186.1.S1_at	LOC711628	COMMD7-202	similar to COMM domain containing 7	XR_013448	6.75E-02	-2.651
70	MmugDNA.33730.1.S1_at	---	---	7:151376049-151376073(-1)	---	8.23E-02	-2.522
71	MmuSTS.2380.1.S1_at	LOC707772	MMU.18647-204	similar to nucleolar protein 4	XM_001101858 /// XM_001102048 /// XM_001102225 /// XM_001102410 /// XM_001102505	8.39E-02	-2.513
72	MmugDNA.18446.1.S1_s_at	KDELR2	AKR1C1	aldo-keto reductase family 1, member C1 (dihydrodiol dehydrogenase 1; 20-alpha (3-alpha)-hydroxysteroid dehydrogenase)	NM_001195574.1	8.82E-02	2.917
73	MmugDNA.35992.1.S1_at	---	---	11:96705943-96705967(1)	---	9.93E-02	2.572
74	MmuSTS.2185.1.S1_at	LOC703879	CBLB-201	Cbl proto-oncogene B, E3 ubiquitin protein ligase	Uncharacterized protein [Source:UniProtKB/TrEMBL;Acc:F6T053]	9.97E-02	2.605
75	Mmu.586.2.S1_at	---	EFR3A-201	EFR3 homolog A (S. cerevisiae)	[Source:UniProtKB/TrEMBL;Acc:F6YPW8]	1.30E-01	-3.490
76	MmugDNA.2571.1.S1_s_at	USP14	HBB	globin, beta	NM_001164428.1	1.37E-01	-2.601
77	MmugDNA.2571.1.S1_x_at	HBB	HBB	globin, beta	NM_001164428.1	1.38E-01	-2.551
78	MmugDNA.36491.1.S1_s_at	KDELR2	AKR1C1	aldo-keto reductase family 1, member C1 (dihydrodiol dehydrogenase 1; 20-alpha (3-alpha)-hydroxysteroid dehydrogenase)	NM_001195574.1	1.42E-01	2.514
79	MmuAffx.2181.1.S1_s_at	GNRH1	GNRH1	gonadotropin-releasing hormone 1 (luteinizing-releasing hormone)	NM_001195436.1	1.61E-01	-2.506
80	MmuSTS.2937.1.S1_at	---	KCNS1_hu	Homo sapiens potassium voltage-gated channel, delayed-rectifier, subfamily S, member 1	---	1.77E-01	4.059
81	MmugDNA.35031.1.S1_at	LOC694086	---	6:155104908-155104932(-1)	---	1.88E-01	-2.551
82	MmuSTS.4627.1.S1_at	TWIST1	TWIST1	twist homolog 1 (Drosophila)	XM_001103003	2.07E-01	2.796
83	MmugDNA.36621.1.S1_s_at	LOC709936	TTR	transthyretin	NM_001261679.1	2.28E-01	3.096
84	MmugDNA.33249.1.S1_at	---	---	16:65362929-65362953(1)	---	2.36E-01	-2.614
85	MmugDNA.20093.1.S1_at	LOC704597	MMU.19037-201	thymocyte expressed, positive selection associated 1	Source:RefSeq peptide;Acc:NP_001180892]	2.47E-01	3.516
86	MmugDNA.41313.1.S1_at	LOC697541	OXT-201	oxytocin, prepropeptide	Uncharacterized protein [Source:UniProtKB/TrEMBL;Acc:F7AXI7]	2.66E-01	-3.671
87	MmuSTS.2987.1.S1_at	MEF2C	MEF2C	myocyte enhancer factor 2C	XM_001086062 /// XM_001086412 /// XM_001086519 /// XM_001086651 /// XM_001086773	2.72E-01	2.680
88	MmugDNA.34254.1.S1_at	LOC709882	TNNT2-205	similar to Troponin T, cardiac muscle (TnTc) (Cardiac muscle troponin T) (cTnT)	XM_001098451	3.47E-01	2.704
89	MmugDNA.11820.1.S1_at	DNAJC12	DNAJC12	DnaJ (Hsp40) homolog, subfamily C, member 12	XM_001088102 /// XM_001088215	3.92E-01	-2.800
	FC 1 probe ≥ |2.0| (7 rows)						
90	MmugDNA.16474.1.S1_at	LXN	LXN	latexin	NM_001266988.1	1.34E-02	-2.224
91	MmugDNA.21023.1.S1_at	IRF3	IRF3	interferon regulatory factor 3	NM_001135797	2.58E-04	2.015
92	MmugDNA.5766.1.S1_at	TM7SF3	TM7SF3	transmembrane 7 superfamily member 3	XM_001099269.2	4.47E-04	-2.211
93	Mmu.5468.1.S1_at	IRF3	IRF3	interferon regulatory factor 3	NM_001135798	1.26E-03	2.109
94	MmugDNA.25397.1.S1_at	DACH1	DACH1	dachshund homolog 1 (Drosophila)	XM_001082371.2	5.79E-03	-2.197
95	MmugDNA.23169.1.S1_at	NR4A2	NR4A2	nuclear receptor subfamily 4, group A, member 2	NM_001266910.2	8.35E-02	-2.073
96	MmugDNA.41067.1.S1_at	HINT1	CALB1	Histidine triad nucleotide binding protein 1	XM_001085269.2	3.31E-01	-2.059
	Relevant from literature (1 row)						
97	MmugDNA.32562.1.S1_s_at	HBQ1	HBA2	hemoglobin, alpha 2	NM_001044724.1	2.76E-01	-1.446

Additional table 2. List of 97 differentially expressed probe sets selected as RT-qPCR candidates. Probe IDs and Previous Gene Symbol annotation as of release 29 of the Affymetrix® Rhesus Annotation library (01/July/09). Current Gene Symbol annotation as of the latest Affymetrix®

Rhesus Annotation library (release 32 - 09/June/11). Gene Name and RefSeq Transcript IDs as of Ensembl release 72 (June 2013). Annotation using alignment with the human genome has been performed (as stated in the gene name column) for the most highly regulated probe sets with unknown macaque annotation. P-values and fold changes are reported for all genes.

Bibliography

1. *Good health adds life to years*, W.H. Organization, Editor. 2012. p. 28.
2. Peggion, C., M.C. Sorgato, and A. Bertoli, *Prions and prion-like pathogens in neurodegenerative disorders.* Pathogens, 2014. **3**(1): p. 149-63.
3. Walker, L.C. and M. Jucker, *Neurodegenerative Diseases: Expanding the Prion Concept.* Annu Rev Neurosci, 2015.
4. Heilbronner, G., et al., *Seeded strain-like transmission of beta-amyloid morphotypes in APP transgenic mice.* EMBO Rep, 2013. **14**(11): p. 1017-22.
5. Kretzschmar, H.A., et al., *Molecular cloning of a human prion protein cDNA.* DNA, 1986. **5**(4): p. 315-24.
6. Vey, M., et al., *Subcellular colocalization of the cellular and scrapie prion proteins in caveolae-like membranous domains.* Proc Natl Acad Sci U S A, 1996. **93**(25): p. 14945-9.
7. Acevedo-Morantes, C.Y. and H. Wille, *The structure of human prions: from biology to structural models-considerations and pitfalls.* Viruses, 2014. **6**(10): p. 3875-92.
8. Benetti, F. and G. Legname, *New insights into structural determinants of prion protein folding and stability.* Prion, 2015. **9**(2): p. 119-24.
9. Wiseman, F.K., et al., *The glycosylation status of PrPC is a key factor in determining transmissible spongiform encephalopathy transmission between species.* J Virol, 2015. **89**(9): p. 4738-47.
10. Higashino, A., et al., *Whole-genome sequencing and analysis of the Malaysian cynomolgus macaque (Macaca fascicularis) genome.* Genome Biol, 2012. **13**(7): p. R58.
11. Smith, D.G., J.W. McDonough, and D.A. George, *Mitochondrial DNA variation within and among regional populations of longtail macaques (Macaca fascicularis) in relation to other species of the fascicularis group of macaques.* Am J Primatol, 2007. **69**(2): p. 182-98.
12. Meade-White, K., et al., *Resistance to chronic wasting disease in transgenic mice expressing a naturally occurring allelic variant of deer prion protein.* J Virol, 2007. **81**(9): p. 4533-9.
13. Cosseddu, G.M., et al., *Ultra-efficient PrP(Sc) amplification highlights potentialities and pitfalls of PMCA technology.* PLoS Pathog, 2011. **7**(11): p. e1002370.
14. Nemecek, J., et al., *Red-backed vole brain promotes highly efficient in vitro amplification of abnormal prion protein from macaque and human brains infected with variant Creutzfeldt-Jakob disease agent.* PLoS One, 2013. **8**(10): p. e78710.
15. Hu, W., R.N. Rosenberg, and O. Stuve, *Prion proteins: a biological role beyond prion diseases.* Acta Neurol Scand, 2007. **116**(2): p. 75-82.
16. Glier, H., et al., *Expression of the cellular prion protein affects posttransfusion recovery and survival of red blood cells in mice.* Transfusion, 2015.
17. Chen, S., et al., *Prion protein as trans-interacting partner for neurons is involved in neurite outgrowth and neuronal survival.* Mol Cell Neurosci, 2003. **22**(2): p. 227-33.
18. Kuwahara, C., et al., *Prions prevent neuronal cell-line death.* Nature, 1999. **400**(6741): p. 225-6.
19. Marciano, P.G., et al., *Neuron-specific mRNA complexity responses during hippocampal apoptosis after traumatic brain injury.* J Neurosci, 2004. **24**(12): p. 2866-76.

20. Race, R.E., et al., *Neuron-specific expression of a hamster prion protein minigene in transgenic mice induces susceptibility to hamster scrapie agent.* Neuron, 1995. **15**(5): p. 1183-91.
21. Pan, K.M., et al., *Conversion of alpha-helices into beta-sheets features in the formation of the scrapie prion proteins.* Proc Natl Acad Sci U S A, 1993. **90**(23): p. 10962-6.
22. Prusiner, S.B., *Biology and genetics of prions causing neurodegeneration.* Annu Rev Genet, 2013. **47**: p. 601-23.
23. Moore, R.A., I. Vorberg, and S.A. Priola, *Species barriers in prion diseases--brief review.* Arch Virol Suppl, 2005(19): p. 187-202.
24. Kretzschmar, H. and J. Tatzelt, *Prion disease: a tale of folds and strains.* Brain Pathol, 2013. **23**(3): p. 321-32.
25. Barria, M.A., et al., *Molecular barriers to zoonotic transmission of prions.* Emerg Infect Dis, 2014. **20**(1): p. 88-97.
26. Basu, U., L. Guan le, and S.S. Moore, *Functional genomics approach for identification of molecular processes underlying neurodegenerative disorders in prion diseases.* Curr Genomics, 2012. **13**(5): p. 369-78.
27. Almeida, L.M., et al., *Gene expression in the medulla following oral infection of cattle with bovine spongiform encephalopathy.* J Toxicol Environ Health A, 2011. **74**(2-4): p. 110-26.
28. Panelli, S., et al., *Analysis of gene expression in white blood cells of cattle orally challenged with bovine amyloidotic spongiform encephalopathy.* J Toxicol Environ Health A, 2011. **74**(2-4): p. 96-102.
29. Comoy, E.E., et al., *Atypical BSE (BASE) transmitted from asymptomatic aging cattle to a primate.* PLoS One, 2008. **3**(8): p. e3017.
30. Ono, F., et al., *Atypical L-type bovine spongiform encephalopathy (L-BSE) transmission to cynomolgus macaques, a non-human primate.* Jpn J Infect Dis, 2011. **64**(1): p. 81-4.
31. Beringue, V., et al., *Transmission of atypical bovine prions to mice transgenic for human prion protein.* Emerg Infect Dis, 2008. **14**(12): p. 1898-901.
32. Bradford, B.M., et al., *Human prion diseases and the risk of their transmission during anatomical dissection.* Clin Anat, 2014. **27**(6): p. 821-32.
33. Kong, Q., et al., *Chronic wasting disease of elk: transmissibility to humans examined by transgenic mouse models.* J Neurosci, 2005. **25**(35): p. 7944-9.
34. Sandberg, M.K., et al., *Chronic wasting disease prions are not transmissible to transgenic mice overexpressing human prion protein.* J Gen Virol, 2010. **91**(Pt 10): p. 2651-7.
35. Tamguney, G., et al., *Transmission of elk and deer prions to transgenic mice.* J Virol, 2006. **80**(18): p. 9104-14.
36. Marsh, R.F., et al., *Interspecies transmission of chronic wasting disease prions to squirrel monkeys (Saimiri sciureus).* J Virol, 2005. **79**(21): p. 13794-6.
37. Race, B., et al., *Susceptibilities of nonhuman primates to chronic wasting disease.* Emerg Infect Dis, 2009. **15**(9): p. 1366-76.
38. Head, M.W. and J.W. Ironside, *Review: Creutzfeldt-Jakob disease: prion protein type, disease phenotype and agent strain.* Neuropathol Appl Neurobiol, 2012. **38**(4): p. 296-310.
39. Gambetti, P., et al., *Sporadic and familial CJD: classification and characterisation.* Br Med Bull, 2003. **66**: p. 213-39.
40. Ironside, J.W., *Variant Creutzfeldt-Jakob disease.* Haemophilia, 2010. **16 Suppl 5**: p. 175-80.

41. Kobayashi, A., et al., *The influence of PRNP polymorphisms on human prion disease susceptibility: an update.* Acta Neuropathol, 2015.
42. Kovacs, G.G., et al., *Mutations of the prion protein gene phenotypic spectrum.* J Neurol, 2002. **249**(11): p. 1567-82.
43. Mastrianni, J.A., *Genetic Prion Diseases*, in *GeneReviews(R)*, R. Pagon, et al., Editors. 2003 Mar 27 (Updated 2014 Jan 2), University of Washington, Seattle: Seattle (WA).
44. DeArmond, S.J. and S.B. Prusiner, *Prion diseases*, in *Greensfield's Neuropathology*, P. Lantos and D. Graham, Editors. 1997, Edward Arnold: London, UK. p. 235-80.
45. Revesz, T., et al., *Genetics and molecular pathogenesis of sporadic and hereditary cerebral amyloid angiopathies.* Acta Neuropathol, 2009. **118**(1): p. 115-30.
46. Ghetti, B., et al., *Vascular variant of prion protein cerebral amyloidosis with tau-positive neurofibrillary tangles: the phenotype of the stop codon 145 mutation in PRNP.* Proc Natl Acad Sci U S A, 1996. **93**(2): p. 744-8.
47. Kim, M.O. and M.D. Geschwind, *Clinical update of Jakob-Creutzfeldt disease.* Curr Opin Neurol, 2015. **28**(3): p. 302-10.
48. Safar, J.G., et al., *Structural determinants of phenotypic diversity and replication rate of human prions.* PLoS Pathog, 2015. **11**(4): p. e1004832.
49. Peden, A.H., et al., *The prion protein protease sensitivity, stability and seeding activity in variably protease sensitive prionopathy brain tissue suggests molecular overlaps with sporadic Creutzfeldt-Jakob disease.* Acta Neuropathol Commun, 2014. **2**: p. 152.
50. Zou, W.Q., et al., *Variably protease-sensitive prionopathy: a new sporadic disease of the prion protein.* Ann Neurol, 2010. **68**(2): p. 162-72.
51. Mackay, G.A., R.S. Knight, and J.W. Ironside, *The molecular epidemiology of variant CJD.* Int J Mol Epidemiol Genet, 2011. **2**(3): p. 217-27.
52. Kaski, D., et al., *Variant CJD in an individual heterozygous for PRNP codon 129.* Lancet, 2009. **374**(9707): p. 2128.
53. Lasmezas, C.I., et al., *Adaptation of the bovine spongiform encephalopathy agent to primates and comparison with Creutzfeldt-- Jakob disease: implications for human health.* Proc Natl Acad Sci U S A, 2001. **98**(7): p. 4142-7.
54. Peden, A., et al., *Variant CJD infection in the spleen of a neurologically asymptomatic UK adult patient with haemophilia.* Haemophilia, 2010. **16**(2): p. 296-304.
55. Mead, S., et al., *Variant Creutzfeldt-Jakob disease with extremely low lymphoreticular deposition of prion protein.* JAMA Neurol, 2014. **71**(3): p. 340-3.
56. Gill, O.N., et al., *Prevalent abnormal prion protein in human appendixes after bovine spongiform encephalopathy epizootic: large scale survey.* BMJ, 2013. **347**: p. f5675.
57. Garske, T. and A.C. Ghani, *Uncertainty in the tail of the variant Creutzfeldt-Jakob disease epidemic in the UK.* PLoS One, 2010. **5**(12): p. e15626.
58. Heath, C.A., et al., *Validation of diagnostic criteria for variant Creutzfeldt-Jakob disease.* Ann Neurol, 2010. **67**(6): p. 761-70.
59. Bruce, M.E., et al., *Transmissions to mice indicate that 'new variant' CJD is caused by the BSE agent.* Nature, 1997. **389**(6650): p. 498-501.
60. St Rose, S.G., et al., *Comparative evidence for a link between Peyer's patch development and susceptibility to transmissible spongiform encephalopathies.* BMC Infect Dis, 2006. **6**: p. 5.
61. Mead, S., et al., *A novel protective prion protein variant that colocalizes with kuru exposure.* N Engl J Med, 2009. **361**(21): p. 2056-65.

62. Atkins, K.E., et al., *Epidemiological mechanisms of genetic resistance to kuru.* J R Soc Interface, 2013. **10**(85): p. 20130331.
63. Asante, E.A., et al., *A naturally occurring variant of the human prion protein completely prevents prion disease.* Nature, 2015.
64. Duffy, P., et al., *Letter: Possible person-to-person transmission of Creutzfeldt-Jakob disease.* N Engl J Med, 1974. **290**(12): p. 692-3.
65. Thadani, V., et al., *Creutzfeldt-Jakob disease probably acquired from a cadaveric dura mater graft. Case report.* J Neurosurg, 1988. **69**(5): p. 766-9.
66. Xiao, X., et al., *Comparative Study of Prions in Iatrogenic and Sporadic Creutzfeldt-Jakob Disease.* J Clin Cell Immunol, 2014. **5**(4).
67. Prusiner, S.B., *Scrapie prions.* Annu Rev Microbiol, 1989. **43**: p. 345-74.
68. Prusiner, S.B., *Cell biology. A unifying role for prions in neurodegenerative diseases.* Science, 2012. **336**(6088): p. 1511-3.
69. Castilla, J. and J.R. Requena, *Prion-like diseases: Looking for their niche in the realm of infectious diseases.* Virus Res, 2015. **207**: p. 1-4.
70. Fernandez-Borges, N., et al., *Infectivity versus Seeding in Neurodegenerative Diseases Sharing a Prion-Like Mechanism.* Int J Cell Biol, 2013. **2013**: p. 583498.
71. Aguzzi, A. and L. Rajendran, *The transcellular spread of cytosolic amyloids, prions, and prionoids.* Neuron, 2009. **64**(6): p. 783-90.
72. Westermark, G.T. and P. Westermark, *Serum amyloid A and protein AA: molecular mechanisms of a transmissible amyloidosis.* FEBS Lett, 2009. **583**(16): p. 2685-90.
73. Lundmark, K., et al., *Transmissibility of systemic amyloidosis by a prion-like mechanism.* Proc Natl Acad Sci U S A, 2002. **99**(10): p. 6979-84.
74. Pecho-Vrieseling, E., et al., *Transneuronal propagation of mutant huntingtin contributes to non-cell autonomous pathology in neurons.* Nat Neurosci, 2014. **17**(8): p. 1064-72.
75. Ren, P.H., et al., *Cytoplasmic penetration and persistent infection of mammalian cells by polyglutamine aggregates.* Nat Cell Biol, 2009. **11**(2): p. 219-25.
76. Chiti, F. and C.M. Dobson, *Protein misfolding, functional amyloid, and human disease.* Annu Rev Biochem, 2006. **75**: p. 333-66.
77. Goedert, M., *NEURODEGENERATION. Alzheimer's and Parkinson's diseases: The prion concept in relation to assembled Abeta, tau, and alpha-synuclein.* Science, 2015. **349**(6248): p. 1255555.
78. Watts, J.C., et al., *Serial propagation of distinct strains of Abeta prions from Alzheimer's disease patients.* Proc Natl Acad Sci U S A, 2014. **111**(28): p. 10323-8.
79. Ridley, R.M., et al., *Very long term studies of the seeding of beta-amyloidosis in primates.* J Neural Transm, 2006. **113**(9): p. 1243-51.
80. Meyer-Luehmann, M., et al., *Exogenous induction of cerebral beta-amyloidogenesis is governed by agent and host.* Science, 2006. **313**(5794): p. 1781-4.
81. Morales, R., et al., *De novo induction of amyloid-beta deposition in vivo.* Mol Psychiatry, 2012. **17**(12): p. 1347-53.
82. Rosen, R.F., et al., *Exogenous seeding of cerebral beta-amyloid deposition in betaAPP-transgenic rats.* J Neurochem, 2012. **120**(5): p. 660-6.
83. Stohr, J., et al., *Purified and synthetic Alzheimer's amyloid beta (Abeta) prions.* Proc Natl Acad Sci U S A, 2012. **109**(27): p. 11025-30.
84. Petkova, A.T., et al., *Self-propagating, molecular-level polymorphism in Alzheimer's beta-amyloid fibrils.* Science, 2005. **307**(5707): p. 262-5.
85. Jenner, P., et al., *Parkinson's disease--the debate on the clinical phenomenology, aetiology, pathology and pathogenesis.* J Parkinsons Dis, 2013. **3**(1): p. 1-11.

86. Olanow, C.W. and S.B. Prusiner, *Is Parkinson's disease a prion disorder?* Proc Natl Acad Sci U S A, 2009. **106**(31): p. 12571-2.
87. Conway, K.A., J.D. Harper, and P.T. Lansbury, *Accelerated in vitro fibril formation by a mutant alpha-synuclein linked to early-onset Parkinson disease.* Nat Med, 1998. **4**(11): p. 1318-20.
88. Aulic, S., et al., *Defined alpha-synuclein prion-like molecular assemblies spreading in cell culture.* BMC Neurosci, 2014. **15**: p. 69.
89. Li, J.Y., et al., *Lewy bodies in grafted neurons in subjects with Parkinson's disease suggest host-to-graft disease propagation.* Nat Med, 2008. **14**(5): p. 501-3.
90. Masuda-Suzukake, M., et al., *Prion-like spreading of pathological alpha-synuclein in brain.* Brain, 2013. **136**(Pt 4): p. 1128-38.
91. Luk, K.C., et al., *Intracerebral inoculation of pathological alpha-synuclein initiates a rapidly progressive neurodegenerative alpha-synucleinopathy in mice.* J Exp Med, 2012. **209**(5): p. 975-86.
92. Recasens, A., et al., *Lewy body extracts from Parkinson disease brains trigger alpha-synuclein pathology and neurodegeneration in mice and monkeys.* Ann Neurol, 2014. **75**(3): p. 351-62.
93. Watts, J.C., et al., *Transmission of multiple system atrophy prions to transgenic mice.* Proc Natl Acad Sci U S A, 2013. **110**(48): p. 19555-60.
94. Guo, J.L., et al., *Distinct alpha-synuclein strains differentially promote tau inclusions in neurons.* Cell, 2013. **154**(1): p. 103-17.
95. Strong, M. and J. Rosenfeld, *Amyotrophic lateral sclerosis: a review of current concepts.* Amyotroph Lateral Scler Other Motor Neuron Disord, 2003. **4**(3): p. 136-43.
96. Grad, L.I., S.M. Fernando, and N.R. Cashman, *From molecule to molecule and cell to cell: prion-like mechanisms in amyotrophic lateral sclerosis.* Neurobiol Dis, 2015. **77**: p. 257-65.
97. Kato, S., et al., *New consensus research on neuropathological aspects of familial amyotrophic lateral sclerosis with superoxide dismutase 1 (SOD1) gene mutations: inclusions containing SOD1 in neurons and astrocytes.* Amyotroph Lateral Scler Other Motor Neuron Disord, 2000. **1**(3): p. 163-84.
98. Forsberg, K., et al., *Novel antibodies reveal inclusions containing non-native SOD1 in sporadic ALS patients.* PLoS One, 2010. **5**(7): p. e11552.
99. Neumann, M., et al., *Ubiquitinated TDP-43 in frontotemporal lobar degeneration and amyotrophic lateral sclerosis.* Science, 2006. **314**(5796): p. 130-3.
100. Matias-Guiu, J., et al., *Superoxide dismutase: the cause of all amyotrophic lateral sclerosis?* Ann Neurol, 2008. **64**(3): p. 356-7; author reply 358.
101. Synofzik, M., et al., *Mutant superoxide dismutase-1 indistinguishable from wild-type causes ALS.* Hum Mol Genet, 2012. **21**(16): p. 3568-74.
102. Munch, C., J. O'Brien, and A. Bertolotti, *Prion-like propagation of mutant superoxide dismutase-1 misfolding in neuronal cells.* Proc Natl Acad Sci U S A, 2011. **108**(9): p. 3548-53.
103. Grad, L.I., et al., *Intermolecular transmission of superoxide dismutase 1 misfolding in living cells.* Proc Natl Acad Sci U S A, 2011. **108**(39): p. 16398-403.
104. Arai, T., et al., *TDP-43 is a component of ubiquitin-positive tau-negative inclusions in frontotemporal lobar degeneration and amyotrophic lateral sclerosis.* Biochem Biophys Res Commun, 2006. **351**(3): p. 602-11.
105. Johnson, B.S., et al., *A yeast TDP-43 proteinopathy model: Exploring the molecular determinants of TDP-43 aggregation and cellular toxicity.* Proc Natl Acad Sci U S A, 2008. **105**(17): p. 6439-44.

106. Furukawa, Y., et al., *A seeding reaction recapitulates intracellular formation of Sarkosyl-insoluble transactivation response element (TAR) DNA-binding protein-43 inclusions.* J Biol Chem, 2011. **286**(21): p. 18664-72.
107. Nonaka, T., et al., *Prion-like properties of pathological TDP-43 aggregates from diseased brains.* Cell Rep, 2013. **4**(1): p. 124-34.
108. Clavaguera, F., et al., *Transmission and spreading of tauopathy in transgenic mouse brain.* Nat Cell Biol, 2009. **11**(7): p. 909-13.
109. Clavaguera, F., et al., *Brain homogenates from human tauopathies induce tau inclusions in mouse brain.* Proc Natl Acad Sci U S A, 2013. **110**(23): p. 9535-40.
110. Lasagna-Reeves, C.A., et al., *Alzheimer brain-derived tau oligomers propagate pathology from endogenous tau.* Sci Rep, 2012. **2**: p. 700.
111. Fernandez-Borges, N., et al., *Animal models for prion-like diseases.* Virus Res, 2015.
112. Gajdusek, D.C., C.J. Gibbs, and M. Alpers, *Experimental transmission of a Kuru-like syndrome to chimpanzees.* Nature, 1966. **209**(5025): p. 794-6.
113. Gibbs, C.J., Jr., et al., *Creutzfeldt-Jakob disease (spongiform encephalopathy): transmission to the chimpanzee.* Science, 1968. **161**(3839): p. 388-9.
114. Gibbs, C.J., Jr., et al., *Oral transmission of kuru, Creutzfeldt-Jakob disease, and scrapie to nonhuman primates.* J Infect Dis, 1980. **142**(2): p. 205-8.
115. Krasemann, S., et al., *Non-human primates in prion research.* Folia Neuropathol, 2012. **50**(1): p. 57-67.
116. Ducrot, C., et al., *Review on the epidemiology and dynamics of BSE epidemics.* Vet Res, 2008. **39**(4): p. 15.
117. Wadman, M., *Lab bred chimps despite ban.* Nature, 2011. **479**(7374): p. 453-4.
118. Glatzel, M., et al., *Analysis of the prion protein in primates reveals a new polymorphism in codon 226 (Y226F).* Biol Chem, 2002. **383**(6): p. 1021-5.
119. Lasmezas, C.I., et al., *BSE transmission to macaques.* Nature, 1996. **381**(6585): p. 743-4.
120. Lasmezas, C.I., et al., *Risk of oral infection with bovine spongiform encephalopathy agent in primates.* Lancet, 2005. **365**(9461): p. 781-3.
121. Mestre-Frances, N., et al., *Oral transmission of L-type bovine spongiform encephalopathy in primate model.* Emerg Infect Dis, 2012. **18**(1): p. 142-5.
122. Takada, L.T. and M.D. Geschwind, *Prion diseases.* Semin Neurol, 2013. **33**(4): p. 348-56.
123. Steinhoff, B.J., et al., *Diagnostic value of periodic complexes in Creutzfeldt-Jakob disease.* Ann Neurol, 2004. **56**(5): p. 702-8.
124. Kovacs, G.G., et al., *Genetic prion disease: the EUROCJD experience.* Hum Genet, 2005. **118**(2): p. 166-74.
125. McGuire, L.I., et al., *Real time quaking-induced conversion analysis of cerebrospinal fluid in sporadic Creutzfeldt-Jakob disease.* Ann Neurol, 2012. **72**(2): p. 278-85.
126. Sano, K., et al., *Early detection of abnormal prion protein in genetic human prion diseases now possible using real-time QUIC assay.* PLoS One, 2013. **8**(1): p. e54915.
127. Orru, C.D., et al., *A test for Creutzfeldt-Jakob disease using nasal brushings.* N Engl J Med, 2014. **371**(6): p. 519-29.
128. Collie, D.A., et al., *Diagnosing variant Creutzfeldt-Jakob disease with the pulvinar sign: MR imaging findings in 86 neuropathologically confirmed cases.* AJNR Am J Neuroradiol, 2003. **24**(8): p. 1560-9.
129. Jackson, G.S., et al., *Population screening for variant Creutzfeldt-Jakob disease using a novel blood test: diagnostic accuracy and feasibility study.* JAMA Neurol, 2014. **71**(4): p. 421-8.

130. Moda, F., et al., *Prions in the urine of patients with variant Creutzfeldt-Jakob disease.* N Engl J Med, 2014. **371**(6): p. 530-9.
131. Paterson, R.W., L.T. Takada, and M.D. Geschwind, *Diagnosis and treatment of rapidly progressive dementias.* Neurol Clin Pract, 2012. **2**(3): p. 187-200.
132. Haik, S., et al., *Doxycycline in Creutzfeldt-Jakob disease: a phase 2, randomised, double-blind, placebo-controlled trial.* Lancet Neurol, 2014. **13**(2): p. 150-8.
133. Geschwind, M.D., et al., *Quinacrine treatment trial for sporadic Creutzfeldt-Jakob disease.* Neurology, 2013. **81**(23): p. 2015-23.
134. Guo, J.L. and V.M. Lee, *Cell-to-cell transmission of pathogenic proteins in neurodegenerative diseases.* Nat Med, 2014. **20**(2): p. 130-8.
135. Benetti, F., S. Gustincich, and G. Legname, *Gene expression profiling and therapeutic interventions in neurodegenerative diseases: a comprehensive study on potentiality and limits.* Expert Opin Drug Discov, 2012. **7**(3): p. 245-59.
136. Benetti, F., et al., *Gene expression profiling to identify druggable targets in prion diseases.* Expert Opin Drug Discov, 2010. **5**(2): p. 177-202.
137. Booth, S., et al., *Identification of central nervous system genes involved in the host response to the scrapie agent during preclinical and clinical infection.* J Gen Virol, 2004. **85**(Pt 11): p. 3459-71.
138. Kim, H.O., et al., *Prion disease induced alterations in gene expression in spleen and brain prior to clinical symptoms.* Adv Appl Bioinform Chem, 2008. **1**: p. 29-50.
139. Riemer, C., et al., *Gene expression profiling of scrapie-infected brain tissue.* Biochem Biophys Res Commun, 2004. **323**(2): p. 556-64.
140. Xiang, W., et al., *Identification of differentially expressed genes in scrapie-infected mouse brains by using global gene expression technology.* J Virol, 2004. **78**(20): p. 11051-60.
141. Sorensen, G., et al., *Comprehensive transcriptional profiling of prion infection in mouse models reveals networks of responsive genes.* BMC Genomics, 2008. **9**: p. 114.
142. Skinner, P.J., et al., *Gene expression alterations in brains of mice infected with three strains of scrapie.* BMC Genomics, 2006. **7**: p. 114.
143. Filali, H., et al., *Gene and protein patterns of potential prion-related markers in the central nervous system of clinical and preclinical infected sheep.* Vet Res, 2013. **44**(1): p. 14.
144. Filali, H., et al., *Gene expression profiling and association with prion-related lesions in the medulla oblongata of symptomatic natural scrapie animals.* PLoS One, 2011. **6**(5): p. e19909.
145. Hedman, C., et al., *Differential gene expression and apoptosis markers in presymptomatic scrapie affected sheep.* Vet Microbiol, 2012. **159**(1-2): p. 23-32.
146. Filali, H., et al., *Medulla oblongata transcriptome changes during presymptomatic natural scrapie and their association with prion-related lesions.* BMC Genomics, 2012. **13**: p. 399.
147. Filali, H., et al., *Gene expression profiling of mesenteric lymph nodes from sheep with natural scrapie.* BMC Genomics, 2014. **15**: p. 59.
148. Khaniya, B., et al., *Microarray analysis of differentially expressed genes from Peyer's patches of cattle orally challenged with bovine spongiform encephalopathy.* J Toxicol Environ Health A, 2009. **72**(17-18): p. 1008-13.
149. Almeida, L.M., et al., *Microarray analysis in caudal medulla of cattle orally challenged with bovine spongiform encephalopathy.* Genet Mol Res, 2011. **10**(4): p. 3948-62.

150. Tang, Y., et al., *Transcriptional analysis implicates endoplasmic reticulum stress in bovine spongiform encephalopathy.* PLoS One, 2010. **5**(12): p. e14207.
151. Basu, U., et al., *Transcriptome analysis of the medulla tissue from cattle in response to bovine spongiform encephalopathy using digital gene expression tag profiling.* J Toxicol Environ Health A, 2011. **74**(2-4): p. 127-37.
152. Greenwood, A.D., et al., *Bovine spongiform encephalopathy infection alters endogenous retrovirus expression in distinct brain regions of cynomolgus macaques (Macaca fascicularis).* Mol Neurodegener, 2011. **6**(1): p. 44.
153. Montag, J., et al., *Upregulation of miRNA hsa-miR-342-3p in experimental and idiopathic prion disease.* Mol Neurodegener, 2009. **4**: p. 36.
154. Herzog, C., et al., *PrPTSE distribution in a primate model of variant, sporadic, and iatrogenic Creutzfeldt-Jakob disease.* J Virol, 2005. **79**(22): p. 14339-45.
155. Montag, J., et al., *Asynchronous Onset of Clinical Disease in BSE-Infected Macaques.* Emerg Infect Dis, 2013. **19**(7): p. 1125-7.
156. Lasmézas, C.I., et al., *Risk of oral infection with bovine spongiform encephalopathy agent in primates.* The Lancet, 2005. **365**(9461): p. 781-783.
157. Holznagel, E., et al., *Foodborne transmission of bovine spongiform encephalopathy to nonhuman primates.* Emerg Infect Dis, 2013. **19**(5): p. 712-20.
158. Yutzy, B., et al., *Time-course studies of 14-3-3 protein isoforms in cerebrospinal fluid and brain of primates after oral or intracerebral infection with bovine spongiform encephalopathy agent.* J Gen Virol, 2007. **88**(Pt 12): p. 3469-78.
159. Smyth, G.K., *Linear models and empirical bayes methods for assessing differential expression in microarray experiments.* Stat Appl Genet Mol Biol, 2004. **3**: p. Article3.
160. Gentleman, R.C., et al., *Bioconductor: open software development for computational biology and bioinformatics.* Genome Biol, 2004. **5**(10): p. R80.
161. Irizarry, R.A., et al., *Exploration, normalization, and summaries of high density oligonucleotide array probe level data.* Biostatistics, 2003. **4**(2): p. 249-64.
162. Edgar, R., M. Domrachev, and A.E. Lash, *Gene Expression Omnibus: NCBI gene expression and hybridization array data repository.* Nucleic Acids Res, 2002. **30**(1): p. 207-10.
163. Benjamini, Y. and Y. Hochberg, *Controlling the False Discovery Rate: A Practical and Powerful Approach to Multiple Testing.* Journal of the Royal Statistical Society. Series B (Methodological), 1995. **57**(1): p. 289-300.
164. Winer, J., et al., *Development and validation of real-time quantitative reverse transcriptase-polymerase chain reaction for monitoring gene expression in cardiac myocytes in vitro.* Anal Biochem, 1999. **270**(1): p. 41-9.
165. Cali, I., et al., *Co-existence of scrapie prion protein types 1 and 2 in sporadic Creutzfeldt-Jakob disease: its effect on the phenotype and prion-type characteristics.* Brain, 2009. **132**(Pt 10): p. 2643-58.
166. Parchi, P., et al., *Molecular basis of phenotypic variability in sporadic Creutzfeldt-Jakob disease.* Ann Neurol, 1996. **39**(6): p. 767-78.
167. Antonell, A., et al., *A preliminary study of the whole-genome expression profile of sporadic and monogenic early-onset Alzheimer's disease.* Neurobiol Aging, 2013. **34**(7): p. 1772-8.
168. Osada, N., et al., *Ancient genome-wide admixture extends beyond the current hybrid zone between Macaca fascicularis and M. mulatta.* Mol Ecol, 2010. **19**(14): p. 2884-95.

169. Osada, N., et al., *Large-scale analysis of Macaca fascicularis transcripts and inference of genetic divergence between M. fascicularis and M. mulatta.* BMC Genomics, 2008. **9**: p. 90.
170. Zhang, Y., et al., *Characterization of a human 20alpha-hydroxysteroid dehydrogenase.* J Mol Endocrinol, 2000. **25**(2): p. 221-8.
171. Ferrer, I., et al., *Neuronal hemoglobin is reduced in Alzheimer's disease, argyrophilic grain disease, Parkinson's disease, and dementia with Lewy bodies.* J Alzheimers Dis, 2011. **23**(3): p. 537-50.
172. Schmitt-Ulms, G., et al., *Binding of neural cell adhesion molecules (N-CAMs) to the cellular prion protein.* J Mol Biol, 2001. **314**(5): p. 1209-25.
173. Le, W.D., et al., *Mutations in NR4A2 associated with familial Parkinson disease.* Nat Genet, 2003. **33**(1): p. 85-9.
174. Shanbhag, N.M., et al., *ATM-dependent chromatin changes silence transcription in cis to DNA double-strand breaks.* Cell, 2010. **141**(6): p. 970-81.
175. Soontornniyomkij, V., et al., *Hippocampal calbindin-1 immunoreactivity correlate of recognition memory performance in aged mice.* Neurosci Lett, 2012. **516**(1): p. 161-5.
176. Backman, M., et al., *Targeted disruption of mouse Dach1 results in postnatal lethality.* Dev Dyn, 2003. **226**(1): p. 139-44.
177. Liu, Q., et al., *Cloning, tissue expression pattern and genomic organization of latexin, a human homologue of rat carboxypeptidase A inhibitor.* Mol Biol Rep, 2000. **27**(4): p. 241-6.
178. Silver, M., et al., *Identification of gene pathways implicated in Alzheimer's disease using longitudinal imaging phenotypes with sparse regression.* Neuroimage, 2012. **63**(3): p. 1681-94.
179. Liang, W.S., et al., *Altered neuronal gene expression in brain regions differentially affected by Alzheimer's disease: a reference data set.* Physiol Genomics, 2008. **33**(2): p. 240-56.
180. Guttula, S.V., A. Allam, and R.S. Gumpeny, *Analyzing microarray data of Alzheimer's using cluster analysis to identify the biomarker genes.* Int J Alzheimers Dis, 2012. **2012**: p. 649456.
181. Saetre, P., et al., *Inflammation-related genes up-regulated in schizophrenia brains.* BMC Psychiatry, 2007. **7**: p. 46.
182. Kamboh, M.I., et al., *Alpha-1-antichymotrypsin (ACT or SERPINA3) polymorphism may affect age-at-onset and disease duration of Alzheimer's disease.* Neurobiol Aging, 2006. **27**(10): p. 1435-9.
183. Mc Guire, C., R. Beyaert, and G. van Loo, *Death receptor signalling in central nervous system inflammation and demyelination.* Trends Neurosci, 2011. **34**(12): p. 619-28.
184. Stevenson, T.J., et al., *Gonadotropin-releasing hormone plasticity: a comparative perspective.* Front Neuroendocrinol, 2012. **33**(3): p. 287-300.
185. Ishibashi, D., et al., *Protective role of interferon regulatory factor 3-mediated signaling against prion infection.* J Virol, 2012. **86**(9): p. 4947-55.
186. Lucatelli, J.F., et al., *Genetic influences on Alzheimer's disease: evidence of interactions between the genes APOE, APOC1 and ACE in a sample population from the South of Brazil.* Neurochem Res, 2011. **36**(8): p. 1533-9.
187. Li, X. and J.N. Buxbaum, *Transthyretin and the brain re-visited: is neuronal synthesis of transthyretin protective in Alzheimer's disease?* Mol Neurodegener, 2011. **6**: p. 79.

188. Noriega, N.C., S.G. Kohama, and H.F. Urbanski, *Microarray analysis of relative gene expression stability for selection of internal reference genes in the rhesus macaque brain.* BMC Mol Biol, 2010. **11**: p. 47.
189. Kabanova, S., et al., *Gene expression analysis of human red blood cells.* Int J Med Sci, 2009. **6**(4): p. 156-9.
190. Llorens, F., et al., *Subtype and regional-specific neuroinflammation in sporadic creutzfeldt-jakob disease.* Front Aging Neurosci, 2014. **6**: p. 198.
191. Tang, Y., et al., *Transcriptional changes in the brains of cattle orally infected with the bovine spongiform encephalopathy agent precede detection of infectivity.* J Virol, 2009. **83**(18): p. 9464-73.
192. Spuhler, J.N., *Evolution of mitochondrial DNA in monkeys, apes, and humans.* American Journal of Physical Anthropology, 1988. **31**(Supplement 9): p. 15-48.
193. Wang, Q., et al., *Stability of endogenous reference genes in postmortem human brains for normalization of quantitative real-time PCR data: comprehensive evaluation using geNorm, NormFinder, and BestKeeper.* Int J Legal Med, 2012. **126**(6): p. 943-52.
194. Stan, A.D., et al., *Human postmortem tissue: what quality markers matter?* Brain Res, 2006. **1123**(1): p. 1-11.
195. Schoor, O., et al., *Moderate degradation does not preclude microarray analysis of small amounts of RNA.* Biotechniques, 2003. **35**(6): p. 1192-6, 1198-201.
196. Koppelkamm, A., et al., *RNA integrity in post-mortem samples: influencing parameters and implications on RT-qPCR assays.* Int J Legal Med, 2011. **125**(4): p. 573-80.
197. Fleige, S. and M.W. Pfaffl, *RNA integrity and the effect on the real-time qRT-PCR performance.* Mol Aspects Med, 2006. **27**(2-3): p. 126-39.
198. Weis, S., et al., *Quality control for microarray analysis of human brain samples: The impact of postmortem factors, RNA characteristics, and histopathology.* J Neurosci Methods, 2007. **165**(2): p. 198-209.
199. Penna, I., et al., *Selection of candidate housekeeping genes for normalization in human postmortem brain samples.* Int J Mol Sci, 2011. **12**(9): p. 5461-70.
200. Bojesen, S.E., et al., *Multiple independent variants at the TERT locus are associated with telomere length and risks of breast and ovarian cancer.* Nat Genet, 2013. **45**(4): p. 371-84, 384e1-2.
201. Brown, A.R., et al., *Gene expression profiling of the preclinical scrapie-infected hippocampus.* Biochem Biophys Res Commun, 2005. **334**(1): p. 86-95.
202. Koechlin, E. and A. Hyafil, *Anterior prefrontal function and the limits of human decision-making.* Science, 2007. **318**(5850): p. 594-8.
203. Mutch, D.M., et al., *Microarray data analysis: a practical approach for selecting differentially expressed genes.* Genome Biol, 2001. **2**(12): p. PREPRINT0009.
204. Ding, L., et al., *Coordinated Actions of FXR and LXR in Metabolism: From Pathogenesis to Pharmacological Targets for Type 2 Diabetes.* Int J Endocrinol, 2014. **2014**: p. 751859.
205. Patel, N.V. and B.M. Forman, *Linking lipids, Alzheimer's and LXRs?* Nucl Recept Signal, 2004. **2**: p. e001.
206. Safar, J.G., et al., *Human prions and plasma lipoproteins.* Proc Natl Acad Sci U S A, 2006. **103**(30): p. 11312-7.
207. Cui, H.L., et al., *Prion infection impairs cholesterol metabolism in neuronal cells.* J Biol Chem, 2014. **289**(2): p. 789-802.
208. Petit-Turcotte, C., et al., *Apolipoprotein C-I expression in the brain in Alzheimer's disease.* Neurobiol Dis, 2001. **8**(6): p. 953-63.

209. Cunningham, C., et al., *Comparison of inflammatory and acute-phase responses in the brain and peripheral organs of the ME7 model of prion disease.* J Virol, 2005. **79**(8): p. 5174-84.
210. Katsel, P., C. Li, and V. Haroutunian, *Gene expression alterations in the sphingolipid metabolism pathways during progression of dementia and Alzheimer's disease: a shift toward ceramide accumulation at the earliest recognizable stages of Alzheimer's disease?* Neurochem Res, 2007. **32**(4-5): p. 845-56.
211. De Pablos V, B.C., Yuste-Jiménez JE, Ros-Bernal F, Carrillo-de Sauvage MA, Fernández-Villalba E, Herrero MT *Acute Phase Protein's Levels as Potential Biomarkers for Early Diagnosis of Neurodegenerative Diseases*, in *Acute Phase Proteins as Early Non-Specific Biomarkers of Human and Veterinary Diseases*, P.F. Veas, Editor. 2011.
212. Mead, S., et al., *Genome-wide association study in multiple human prion diseases suggests genetic risk factors additional to PRNP.* Hum Mol Genet, 2012. **21**(8): p. 1897-906.
213. Biagioli, M., et al., *Unexpected expression of alpha- and beta-globin in mesencephalic dopaminergic neurons and glial cells.* Proc Natl Acad Sci U S A, 2009. **106**(36): p. 15454-9.
214. Richter, F., et al., *Neurons express hemoglobin alpha- and beta-chains in rat and human brains.* J Comp Neurol, 2009. **515**(5): p. 538-47.
215. Broadwater, L., et al., *Analysis of the mitochondrial proteome in multiple sclerosis cortex.* Biochim Biophys Acta, 2011. **1812**(5): p. 630-41.
216. Fathallah, H., G. Portnoy, and G.F. Atweh, *Epigenetic analysis of the human α- and β-globin gene clusters.* Blood Cells, Molecules, and Diseases, 2008. **40**(2): p. 166-173.
217. Lathrop, M.J., et al., *Developmentally regulated extended domains of DNA hypomethylation encompass highly transcribed genes of the human β-globin locus.* Experimental Hematology, 2009. **37**(7): p. 807-813.e2.
218. Vadnal, J., et al., *Transcriptional signatures mediated by acetylation overlap with early-stage Alzheimer's disease.* Exp Brain Res, 2012. **221**(3): p. 287-97.
219. Salvatore, A., et al., *Haptoglobin binds apolipoprotein E and influences cholesterol esterification in the cerebrospinal fluid.* J Neurochem, 2009. **110**(1): p. 255-63.
220. Bush, A.I., *The metal theory of Alzheimer's disease.* J Alzheimers Dis, 2013. **33 Suppl 1**: p. S277-81.
221. Olivieri, S., et al., *Ceruloplasmin oxidation, a feature of Parkinson's disease CSF, inhibits ferroxidase activity and promotes cellular iron retention.* J Neurosci, 2011. **31**(50): p. 18568-77.
222. Ayton, S., et al., *Ceruloplasmin dysfunction and therapeutic potential for parkinson disease.* Ann Neurol, 2012.
223. Singh, A., et al., *Change in the characteristics of ferritin induces iron imbalance in prion disease affected brains.* Neurobiol Dis, 2012. **45**(3): p. 930-8.
224. Febbraro, F., et al., *alpha-Synuclein expression is modulated at the translational level by iron.* Neuroreport, 2012. **23**(9): p. 576-80.
225. Johnson, V.E., W. Stewart, and D.H. Smith, *Traumatic brain injury and amyloid-beta pathology: a link to Alzheimer's disease?* Nat Rev Neurosci, 2010. **11**(5): p. 361-70.
226. Wu, C.W., et al., *Hemoglobin promotes Abeta oligomer formation and localizes in neurons and amyloid deposits.* Neurobiol Dis, 2004. **17**(3): p. 367-77.

227. Singh, N., et al., *Iron in neurodegenerative disorders of protein misfolding: a case of prion disorders and Parkinson's disease.* Antioxid Redox Signal, 2014. **21**(3): p. 471-84.
228. Petersen, R.B., et al., *Redox metals and oxidative abnormalities in human prion diseases.* Acta Neuropathol, 2005. **110**(3): p. 232-8.
229. Castellani, R.J., et al., *Sequestration of iron by Lewy bodies in Parkinson's disease.* Acta Neuropathol, 2000. **100**(2): p. 111-4.
230. Singh, A., et al., *Abnormal brain iron homeostasis in human and animal prion disorders.* PLoS Pathog, 2009. **5**(3): p. e1000336.
231. Cudaback, E., et al., *Apolipoprotein C-I is an APOE genotype-dependent suppressor of glial activation.* J Neuroinflammation, 2012. **9**: p. 192.
232. Poduslo, S.E., et al., *The apolipoprotein CI A allele as a risk factor for Alzheimer's disease.* Neurochem Res, 1998. **23**(3): p. 361-7.
233. Ki, C.S., et al., *Genetic association of an apolipoprotein C-I (APOC1) gene polymorphism with late-onset Alzheimer's disease.* Neurosci Lett, 2002. **319**(2): p. 75-8.
234. Huang, R., et al., *APOE genotypes in African American female multiple sclerosis patients.* Neurosci Lett, 2007. **414**(1): p. 51-6.
235. Xiang, W., et al., *Transcriptome analysis reveals altered cholesterol metabolism during the neurodegeneration in mouse scrapie model.* J Neurochem, 2007. **102**(3): p. 834-47.
236. Bach, C., et al., *Prion-induced activation of cholesterogenic gene expression by Srebp2 in neuronal cells.* J Biol Chem, 2009. **284**(45): p. 31260-9.
237. Gilch, S., et al., *Inhibition of cholesterol recycling impairs cellular PrP(Sc) propagation.* Cell Mol Life Sci, 2009. **66**(24): p. 3979-91.
238. Leoni, V., et al., *Are the CSF levels of 24S-hydroxycholesterol a sensitive biomarker for mild cognitive impairment?* Neurosci Lett, 2006. **397**(1-2): p. 83-7.
239. Jong, M.C., M.H. Hofker, and L.M. Havekes, *Role of ApoCs in lipoprotein metabolism: functional differences between ApoC1, ApoC2, and ApoC3.* Arterioscler Thromb Vasc Biol, 1999. **19**(3): p. 472-84.
240. Vega, G.L. and M.F. Weiner, *Plasma 24S hydroxycholesterol response to statins in Alzheimer's disease patients: effects of gender, CYP46, and ApoE polymorphisms.* J Mol Neurosci, 2007. **33**(1): p. 51-5.
241. Bjorkhem, I., *Do oxysterols control cholesterol homeostasis?* J Clin Invest, 2002. **110**(6): p. 725-30.
242. Ritter, M., et al., *Cloning and characterization of a novel apolipoprotein A-I binding protein, AI-BP, secreted by cells of the kidney proximal tubules in response to HDL or ApoA-I.* Genomics, 2002. **79**(5): p. 693-702.
243. Taraboulos, A., et al., *Cholesterol depletion and modification of COOH-terminal targeting sequence of the prion protein inhibit formation of the scrapie isoform.* J Cell Biol, 1995. **129**(1): p. 121-32.
244. Baron, G.S., et al., *Conversion of raft associated prion protein to the protease-resistant state requires insertion of PrP-res (PrP(Sc)) into contiguous membranes.* EMBO J, 2002. **21**(5): p. 1031-40.
245. Lee, M.Y., et al., *Upregulation of haptoglobin in reactive astrocytes after transient forebrain ischemia in rats.* J Cereb Blood Flow Metab, 2002. **22**(10): p. 1176-80.
246. Bovio, G., et al., *Energy balance in haemodialysis and peritoneal dialysis patients assessed by a 7-day weighed food diary and a portable armband device.* J Hum Nutr Diet, 2013. **26**(3): p. 276-85.

247. Janciauskiene, S. and H.T. Wright, *Inflammation, antichymotrypsin, and lipid metabolism: autogenic etiology of Alzheimer's disease.* Bioessays, 1998. **20**(12): p. 1039-46.
248. Matsubara, E., et al., *Alpha 1-antichymotrypsin as a possible biochemical marker for Alzheimer-type dementia.* Ann Neurol, 1990. **28**(4): p. 561-7.
249. Akiyama, H., et al., *Inflammation and Alzheimer's disease.* Neurobiol Aging, 2000. **21**(3): p. 383-421.
250. Licastro, F., et al., *A new promoter polymorphism in the alpha-1-antichymotrypsin gene is a disease modifier of Alzheimer's disease.* Neurobiol Aging, 2005. **26**(4): p. 449-53.
251. Lin, J.J., et al., *The homozygote AA genotype of the alpha1-antichymotrypsin gene may confer protection against early-onset Parkinson's disease in women.* Parkinsonism Relat Disord, 2004. **10**(8): p. 469-73.
252. Miele, G., et al., *Urinary alpha1-antichymotrypsin: a biomarker of prion infection.* PLoS One, 2008. **3**(12): p. e3870.
253. Hwang, D., et al., *A systems approach to prion disease.* Mol Syst Biol, 2009. **5**: p. 252.
254. Cray, C., J. Zaias, and N.H. Altman, *Acute phase response in animals: a review.* Comp Med, 2009. **59**(6): p. 517-26.
255. Licastro, F., et al., *A role for apoE in regulating the levels of alpha-1-antichymotrypsin in the aging mouse brain and in Alzheimer's disease.* Am J Pathol, 1999. **155**(3): p. 869-75.
256. Janciauskiene, S. and S. Eriksson, *In vitro complex formation between cholesterol and alpha 1-proteinase inhibitor.* FEBS Lett, 1993. **316**(3): p. 269-72.
257. Cascella, R., et al., *Transthyretin suppresses the toxicity of oligomers formed by misfolded proteins in vitro.* Biochim Biophys Acta, 2013. **1832**(12): p. 2302-14.
258. Li, X., et al., *Neuronal production of transthyretin in human and murine Alzheimer's disease: is it protective?* J Neurosci, 2011. **31**(35): p. 12483-90.
259. Llorens, F., et al., *PrP mRNA and protein expression in brain and PrP(c) in CSF in Creutzfeldt-Jakob disease MM1 and VV2.* Prion, 2013. **7**(5): p. 383-93.
260. McGeer, P.L. and E.G. McGeer, *History of innate immunity in neurodegenerative disorders.* Front Pharmacol, 2011. **2**: p. 77.
261. Fratini, F., et al., *Increased levels of acute-phase inflammatory proteins in plasma of patients with sporadic CJD.* Neurology, 2012. **79**(10): p. 1012-8.
262. McGeer, P.L. and E.G. McGeer, *The inflammatory response system of brain: implications for therapy of Alzheimer and other neurodegenerative diseases.* Brain Res Brain Res Rev, 1995. **21**(2): p. 195-218.
263. McGeer, P.L. and E.G. McGeer, *Inflammation and the degenerative diseases of aging.* Ann N Y Acad Sci, 2004. **1035**: p. 104-16.
264. Hou, Y., et al., *Increased opioid receptor binding and G protein coupling in the accumbens and ventral tegmental area of postnatal day 2 rats.* Neurosci Lett, 2006. **395**(3): p. 244-8.
265. Hou, X., et al., *Cholesterol and anionic phospholipids increase the binding of amyloidogenic transthyretin to lipid membranes.* Biochim Biophys Acta, 2008. **1778**(1): p. 198-205.
266. Perlmann, T. and A. Wallen-Mackenzie, *Nurr1, an orphan nuclear receptor with essential functions in developing dopamine cells.* Cell Tissue Res, 2004. **318**(1): p. 45-52.

267. Baptista, M.J., et al., *Co-ordinate transcriptional regulation of dopamine synthesis genes by alpha-synuclein in human neuroblastoma cell lines.* J Neurochem, 2003. **85**(4): p. 957-68.
268. Chu, Y., et al., *Nurr1 in Parkinson's disease and related disorders.* J Comp Neurol, 2006. **494**(3): p. 495-514.
269. Meyne, F., et al., *Total prion protein levels in the cerebrospinal fluid are reduced in patients with various neurological disorders.* J Alzheimers Dis, 2009. **17**(4): p. 863-73.
270. Mays, C.E., et al., *Prion disease tempo determined by host-dependent substrate reduction.* J Clin Invest, 2014. **124**(2): p. 847-58.
271. Tylee, D.S., D.M. Kawaguchi, and S.J. Glatt, *On the outside, looking in: a review and evaluation of the comparability of blood and brain "-omes".* Am J Med Genet B Neuropsychiatr Genet, 2013. **162B**(7): p. 595-603.
272. Borovecki, F., et al., *Genome-wide expression profiling of human blood reveals biomarkers for Huntington's disease.* Proc Natl Acad Sci U S A, 2005. **102**(31): p. 11023-8.
273. Liew, C.C., et al., *The peripheral blood transcriptome dynamically reflects system wide biology: a potential diagnostic tool.* J Lab Clin Med, 2006. **147**(3): p. 126-32.
274. Sullivan, P.F., C. Fan, and C.M. Perou, *Evaluating the comparability of gene expression in blood and brain.* Am J Med Genet B Neuropsychiatr Genet, 2006. **141B**(3): p. 261-8.

ACKNOWLEDGEMENTS

In these four years spent as PhD student in SISSA, I had the great opportunity of working in the Prion Biology Lab of Giuseppe Legname. I am really grateful to him for having introduced me to the world of prions with all its fascinating aspect of molecular and cellular biology, which has been the source of my motivation over the years. The encouragement, reassurance and the active support I received from Prof. Legname have been important in establishing my confidence and persistency in carrying out my research work. Grazie GL!!

I would like to express my sincere thanks to Dr. Maura Barbisin who has worked with me step-by-step in these years. Her knowledge, patience and attention to the even smallest details have been an invaluable help in addressing every practical and technical issue of this work. The results of this thesis would have not been achieved without the uncountable days she spent working with me and without the precious advices she gave me.

I would like to give my true appreciation to Dr. Fabio Moda and Prof. Fabrizio Tagliavini from the “Istituto Neurologico Carlo Besta” in Milan for hosting me on several occasions in the Institute’s in order to carry out the human part of this work. It has been a great experience for me to enter a BSL3 lab and learn how to work with human brain samples.

In addition, I would like to thank Prof. Jason Bartz and Prof. Isidro Ferrer for their very useful comments and suggestions for the improvement of this thesis.

I want to thank Prof. Gianluigi Zanusso for providing human control samples and the DPZ for providing macaque samples and initial analysis.

A sincere thank also to Helena Krmac for her help in analyzing hundreds of RNA and to Dr. Paolo Vatta, Dr. Raffaella Calligaris and Prof. Gustincich for the useful discussions we had and for kindly sharing with me their knowledge.

I want to thank also all the SISSA technicians, in particular Jessica Franzot and Andrea Tomicich, for being always available every time I got lost in the lab looking for reagents or for internet connectivity ☺

A huge thank to all my present and past colleagues of Legname's lab who were always ready to help me when I had questions or problems… or even existential doubts! In particular I want to thank the "seniors" Gabriele, Diana and Lisa for their advices and for the time they spent training me in my first steps inside the lab.
Also, I have to thank a lot Suzana, Ludovica and Marcella for supporting me in the "obscure" world of proteins… a lot of endless WB and ELISA would have been a real nightmare without you all!

I wish to thank Elena for so many reasons that I would need to write another thesis… but I can sum up all of these just saying thank you for being a real friend. I definitely can say you're one of the best people I've ever met.

Many thanks also go to Ilenia, Anna and Marika for their much-needed support in this last year of work... and life. I will never forget you ladies!! :*

Last but not least, a big thank to my parents, who always believed in me and pushed me to not get discouraged by difficulties and bad experiments ☺

Barbisin et al. BMC Genomics 2014, 15:434
http://www.biomedcentral.com/1471-2164/15/434

BMC Genomics

RESEARCH ARTICLE Open Access

Gene expression profiling of brains from bovine spongiform encephalopathy (BSE)-infected cynomolgus macaques

Maura Barbisin[1†], Silvia Vanni[1†], Ann-Christin Schmädicke[2], Judith Montag[2,4], Dirk Motzkus[2], Lennart Opitz[3], Gabriela Salinas-Riester[3] and Giuseppe Legname[1*]

Abstract

Background: Prion diseases are fatal neurodegenerative disorders whose pathogenesis mechanisms are not fully understood. In this context, the analysis of gene expression alterations occurring in prion-infected animals represents a powerful tool that may contribute to unravel the molecular basis of prion diseases and therefore discover novel potential targets for diagnosis and therapeutics. Here we present the first large-scale transcriptional profiling of brains from BSE-infected cynomolgus macaques, which are an excellent model for human prion disorders.

Results: The study was conducted using the GeneChip® Rhesus Macaque Genome Array and revealed 300 transcripts with expression changes greater than twofold. Among these, the bioinformatics analysis identified 86 genes with known functions, most of which are involved in cellular development, cell death and survival, lipid homeostasis, and acute phase response signaling. RT-qPCR was performed on selected gene transcripts in order to validate the differential expression in infected animals versus controls. The results obtained with the microarray technology were confirmed and a gene signature was identified. In brief, *HBB* and *HBA2* were down-regulated in infected macaques, whereas *TTR*, *APOC1* and *SERPINA3* were up-regulated.

Conclusions: Some genes involved in oxygen or lipid transport and in innate immunity were found to be dysregulated in prion infected macaques. These genes are known to be involved in other neurodegenerative disorders such as Alzheimer's and Parkinson's diseases. Our results may facilitate the identification of potential disease biomarkers for many neurodegenerative diseases.

Keywords: Prion diseases, BSE, Non-human primates, Neurodegeneration, Transcriptome, Microarray, RT-qPCR, Biomarker, Serpina3, Hemoglobin

Background

Prion diseases, or transmissible spongiform encephalopathies (TSEs), are incurable and fatal neurodegenerative disorders that affect both humans and animals; their origin may be sporadic, acquired or genetic [1,2]. TSEs include Creutzfeldt-Jakob Disease (CJD), Gerstmann-Sträussler-Scheinker syndrome (GSS), kuru and fatal familial insomnia (FFI) in humans [2], bovine spongiform encephalopathy (BSE) in cattle [3], scrapie in sheep and goats [4], chronic wasting disease (CWD) in cervids [5], transmissible mink encephalopathy, and feline spongiform encephalopathy (FSE) [6].

A major event that leads to the development of prion diseases is the conversion of the cellular form of the prion protein (PrP^{C}) into an abnormally folded, β-sheet enriched and protease resistant isoform (PrP^{Sc}). PrP^{Sc} is prone to accumulate and aggregate in the brain of affected individuals [1,2,4] leading to neuronal loss, spongiosis and astrogliosis, which are hallmarks of neurodegeneration. The underlying conversion mechanism of PrP^{C} into PrP^{Sc} is poorly understood and it is further complicated by the existence of several different strains characterized by distinct

* Correspondence: legname@sissa.it
†Equal contributors
[1]Department of Neuroscience, Scuola Internazionale Superiore di Studi Avanzati (SISSA), Via Bonomea 265, 34136 Trieste, Italy
Full list of author information is available at the end of the article

tertiary and quaternary structures as well as different clinical patterns [7,8]. Several hypotheses exist about the contribution of unknown molecules other than PrP to prion propagation [9-11]. To address this issue, several animal studies have investigated the host response to prion infection of different origin and strain. The differential transcription profile after prion infection has been extensively explored (reviewed in [6,12]); however, most of the studies involved animal models such as mice [13-18], sheep [4,19-22] and cattle [23-28], all not closely related to humans. Some expression analyses have been conducted in non-human primates focusing mainly on the susceptibility to the infection and the variety of clinical symptoms [29-33], but none has investigated large-scale transcriptome changes due to prion infection. All these investigations suggest that besides the PrP-encoding gene (*PRNP* in humans), other genes are key players and contribute to the genetic susceptibility to acquired TSEs [6,34]. The main genes identified so far are related to oxidative stress, mitochondrial apoptotic pathways, endosome/lysosome function, immunity, synapse function, metal ion binding, activated cholesterol biosynthesis, immune and inflammatory response, protease inhibitors, calcium binding proteins, regulation of the actin cytoskeleton, ion transport, cell adhesion, and transcription processes [6]. Dysregulation of these genes seems to cause increased oxidative stress that in turn determines oxidation of proteins, lipids and DNA as well as mitochondrial dysfunction and ER stress [6]. Apart from TSEs, transcriptional changes of these genes are common to other neurodegenerative pathologies [12] and, together with functional proteomics data, may help to identify novel selective biomarkers of prion diseases and neurodegeneration in general.

To accomplish that, we performed a large-scale transcriptional profiling in BSE-infected cynomolgus macaques (*Macaca fascicularis*). They are known to be an excellent model for studying human acquired prion diseases [32,33,35-37], as shown by BSE transmission via the intracranial and oral routes, which lead to a disease pattern comparable to that of human maladies in terms of preclinical incubation time, clinical symptoms and pathophysiology [35]. The objective of this study was to identify genes that are differentially expressed in brain tissue of intracranially infected monkeys compared to non-infected ones using an unbiased genomic approach such as expression microarrays with subsequent data validation by RT-qPCR. Our study aims at revealing biological processes that are relevant to the pathogenesis of human prion diseases using a systematic approach that connects the identified DEGs into potential networks of interacting pathways. This may allow us to discover novel selective markers as potential targets for diagnostic and therapeutic strategies.

Results

PrP^{Sc} content in brain tissue

The relative amount of PrP^{Sc} in brain homogenate of 6 BSE-infected macaques was examined by Western Blot. Densitometric analysis of the monoglycosylated band revealed that the relative amount of PrP^{Sc} strongly differed between the individual macaques. We wondered whether this discrepancy might be due to the preclinical incubation time or rather correspond to the gradual accumulation of PrP^{Sc} during the clinical phase of disease as reported for sCJD [38,39]. As anticipated, we found a significant correlation between PrP^{Sc} content and the duration of the symptomatic phase (Figure 1). The correlation analysis includes only the 6 intracranially inoculated macaques. Since these animals were housed in one social group, environmental factors, which may influence the disease course and duration, are identical. Such factors can be different for the orally inoculated animal, which was therefore omitted from the analysis. The infected animals were at an advanced stage of prion disease and the details of their clinical course have been previously described [33]. Briefly, animal A1 showed the shortest duration of disease (17 days) and a short pre-clinical incubation time (931 days) together with the lowest PrP^{Sc} content, while animal A5 showed the longest survival period (143 days), compared to an average clinical phase of about 90 days, together with the highest PrP^{Sc} content and the second longest pre-clinical phase (1340 days).

Microarray analysis of brain gene expression in cynomolgus macaques

To investigate differential mRNA expression in BSE-infected macaques we used brain samples from 6 animals that were intracranially challenged [33]. One macaque that

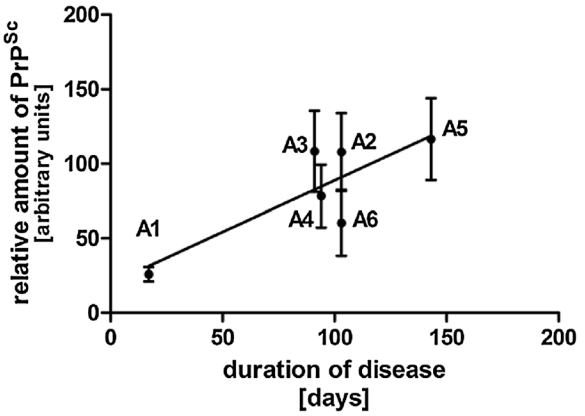

Figure 1 Correlation between PrP^{Sc} content and duration of clinical phase. Western Blot analysis from PK-treated homogenates of brain samples derived from BSE-infected macaques was performed. The monoglycosylated bands of PrP^{Sc} were analyzed densitometrically. Relative amounts of PrP^{Sc} from brain homogenates were averaged and correlated to the disease duration.

was orally infected with 50 mg BSE-homogenate was also included in our study. For comparison purposes, we used 5 brain samples derived from non-infected age- and sex-matched control macaques.

RNA was isolated from the *gyrus frontalis superior* of all animals and checked for quality by nano-scale electrophoresis, which resulted in an overall RNA Integrity Number (RIN) of about 6. This value is indicative of at least partially degraded RNA within the sample; one possible reason for the reduced RNA integrity may be the procedure utilized to remove the *gyrus frontalis superior* region from the frozen tissue slide. The biopsy stamp was plugged into a cordless screwdriver that was used to drill a borehole in the frozen tissue block of +/− 1 cm height. This method was chosen to ensure that the material did not thaw; however, the local heat induced by the rotating biopsy stamp may have led to substantial degradation of the RNA. Nonetheless, human brain material exhibiting a comparable RIN value was successfully used for similar studies [40]. All samples were analyzed using the GeneChip® Rhesus Macaque Genome Array (Affymetrix®) that contains 52,024 rhesus probe sets to enable gene expression studies of *Macaca mulatta* transcriptome interrogating more than 47,000 transcripts. The genomes of *M. mulatta* and *M. fascicularis* exhibit a small genetic divergence of approximately 0.4% [41,42] that presumably allows for the detection of homologue transcripts with high specificity.

Raw data were quality checked and analyzed using Affymetrix® proprietary analysis tools, a hierarchical clustering was performed and a heat map was generated. Then the signals were aligned to the annotation library and a spreadsheet containing gene symbols, p-values and expression fold changes was created. Microarray data were submitted to Gene Expression Omnibus (GEO). The bioinformatics analysis identified 300 probe sets that were up- or down-regulated about twofold (≥ |1.95|). Because among them no candidate appeared using FDR 0.05, we chose as criteria an unadjusted p-value of ≤ 0.005 together with a fold change ≥ |2.0|. Additional file 1 lists the resulting 86 probe sets that were then used to generate the heat map shown in Figure 2.

Functional classification of differentially expressed genes (DEGs)

We used the Ingenuity Pathways Analysis (IPA®, see section: Availability of supporting data) to annotate genes according to their functional relationships and to determine potential regulatory networks and pathways. Among the 300 differentially expressed (about twofold, (≥ |1.95|) probe sets identified, 105 were associated to mapped IDs; 53 of the latter were identified as network eligible genes, while 86 were identified as function eligible genes. It should be emphasized that the designation of functional class in the present study is neither definitive nor exclusive, as annotation of gene function is incomplete, and

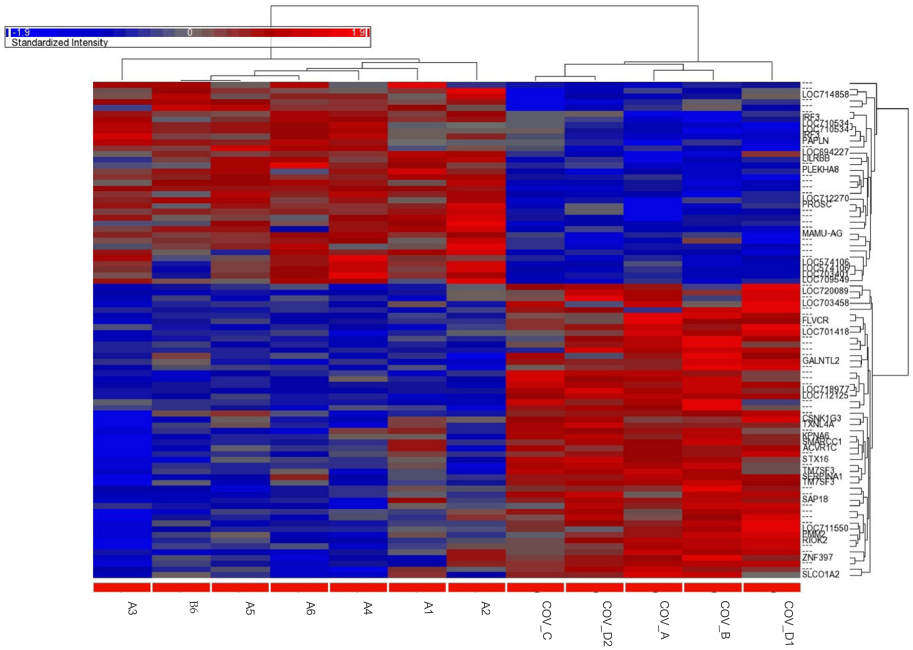

Figure 2 Condition trees of the clustering analysis. The cluster analysis was performed using a hierarchical approach with the average linkage-method (R and Partek® Software, Partek® Inc.): 86 probe sets showed a differential expression with FC ≥ 2. The color represents the level of expression (red: up-regulation, blue: down-regulation) and the sample information is listed across the bottom. The names of the known genes are indicated. More details on all genes are reported in Additional file 1.

multifunctional gene products can be involved in several cellular pathways. First, we identified key biological functions and/or diseases that contain a disproportionately high number of genes from the DEG list compared to the total gene population from the microarray. The analysis was started by identifying the top categories ($p < 0.01$) of DEGs within three main classes. In the "Diseases and Disorders" class the categories were cancer and developmental disorder, while within the "Molecular and Cellular functions" class most genes were involved in cellular development and cell death/survival. The main categories for the "Physiological System Development and Function" class were tissue morphology as well as nervous system development and function. As a second step, genes were clustered in relation to the main pathways they belong to: the top two canonical pathways in our DEG list were LXR/RXR activation, which is associated with lipid metabolism and transport, and acute phase response signaling.

Identification of biologically relevant networks

To further investigate the global expression response to BSE infection and to define interactions among the identified specific pathways containing the regulated genes, potential networks of interacting DEGs were identified using IPA®. All potential networks with score > 9 (a score ≥ 3 was considered significant, $p < 0.001$) are listed in Table 1 with information on network genes, score, focus molecules and top functions associated with the focus genes in each network. The highest ranked network identified by IPA® was associated with tissue morphology (specifically the determination of cell quantity), developmental disorder and biological processes controlling cell death and survival (Figure 3a). This network contained genes that are known to be involved in several neurological diseases and nervous system functions, as shown in Figure 3b.

Validation of differentially expressed genes by RT-qPCR

To further confirm the array results using an independent and more sensitive technique, we decided to perform RT-qPCR for a subset of differentially expressed genes. This subset (Additional file 2) was selected in subsequent steps: first, among the 86 probe sets identified during the microarray analysis (Additional file 1) we selected the top 36 with fold change ≥ |2.5| and $p \leq 0.005$. Then, after realizing that many were not annotated or did not have a known function, we extended the selection to additional 29 probe sets having fold change ≥ |2.5| but $0.005 \leq p \leq 0.05$; for the same reasons stated above, we extended the list of candidates one more time using as criteria fold change ≥ |2.5| and $p > 0.05$ (24 candidates). At this point, having still some cDNA available and only 13 feasible candidate transcripts, we added seven probe sets, corresponding to 5 additional transcripts, selected among the ones with a slightly lower fold change (FC ≥ 2 for at least 1 probe) but possessing an interesting function as revealed by the IPA® analysis or according to the literature. Lastly, *HBA2* was added to the list because of its tight

Table 1 List of 3 Ingenuity networks generated by mapping the focus genes that were differentially expressed between non-infected and BSE-infected samples

ID	Molecules in network	Score	Focus molecules	Top functions
1	ACVR1C, AKR1D1, Alp, AMPK, Ap1, APOC1, Calcineurin protein(s), CARTPT, caspase, CD3, CHI3L1, Creb, cytochrome C, DACH1, DLK1, ERK, ERK1/2, F13A1, Focal adhesion kinase, GNRH1, HBA1/HBA2, HBB, HDL, hemoglobin, HEY2, HINT1, HIPK2, Ikk (family), IL1, IRF3, Jnk, KDELR2, LDL, LGALS1, Mapk, MEF2C, Mek, MET, MT2A, N4BP1, NADPH oxidase, NGFR, NR4A2, OTX2, P38 MAPK, p85 (pik3r), Pdgf (complex), PDGF BB, PI3K (complex), PI3K (family), PIK3R3, Pkc(s), PLC gamma, PON3, Pro-inflammatory Cytokine, Ras, SERPINA1, SERPINA3, Shc, SHOC2, SLCO1A2, Sos, STK4, TCF, TCR, TNFSF10, TTR, TWIST1, Vegf, WSB1	71	35	Tissue Morphology, Cell Death and Survival, Developmental Disorder
2	ABR, ACTL6B, ARMC6, ASB6, C10orf137, C6orf211, CAMKV, CHMP2A, CLIC4, CLPP, CSNK1G3, CTBP2, DCLRE1A, DDX19B, DGKE, ECT2, FHL3, FLVCR1, GALNTL5, GLOD4, HEATR6, HSP90AA1, HSPA12A, ITFG1, KLF3, KPNA6, MCTS1, MEIG1, METTL7B, MRPL44, MXD3, MYBPC1, NCLN, NIPBL, NOL4, OSBPL10, PCBP3, PLEKHA8, PMM2, POLR2J, PPAP2C, PRCP, PROSC, RAI2, SAP18, SCAND1, SEPT6, SGTB, SMARCC1, SMC3, SPATA22, SPSB3, SRPK3, SSU72, STAG1, TATDN1, TESPA1, TM7SF3, TNK1, TNNI3K, TP53BP1, TRAPPC2L, TRIP12, TUFM, TXNL4A, UBC, ZNF131, ZNF235, ZNF397, ZNF420	54	28	Developmental Disorder, Hereditary Disorder, Hematological Disease
3	26 s Proteasome, ADCY, AKR1C1/AKR1C2, Akt, APP, ARL4C, Arntl-Clock, AVP, AVPR1B, CACNA1B, CAMKV, CARTPT, CBLN2, CEACAM6, CLDN10, CLOCK, COX4I2, CTF1, DNAJC12, endocannabinoid, estrogen receptor, FAM46A, FSH, GABRE, GNA15, GPR158, GPX1, GPX2, GSK3A, Histone h3, HMGCR, HNF4A, HSPA12A, Insulin, JPH3, KCNC3, KCNS1, LINGO1, LPAR1, LXN, MGAT2, miR-125b-5p (and other miRNAs w/seed CCCUGAG), Mmp, MST1, NFkB (complex), Npff, OPN1LW, PDX1, PIK3R5, Pka, PKM, PLC, Proinsulin, RAB39A, RAI2, RIOK2, RUFY3, SERPINA3, SMAD5, SMC4, SOX7, SYT17, TCF19, Tnfrsf22/Tnfrsf23, TOR2A, tretinoin, trypsin, TXNL4B, ZBTB44, ZFHX3	36	21	Cellular Development, Neurological Disease, Skeletal and Muscular System Development and Function

Names in lowercase are genes/molecules that are not from the DEG list but are associated with some of them within pathways identified by Ingenuity Pathway Knowledge Base (IPKB).

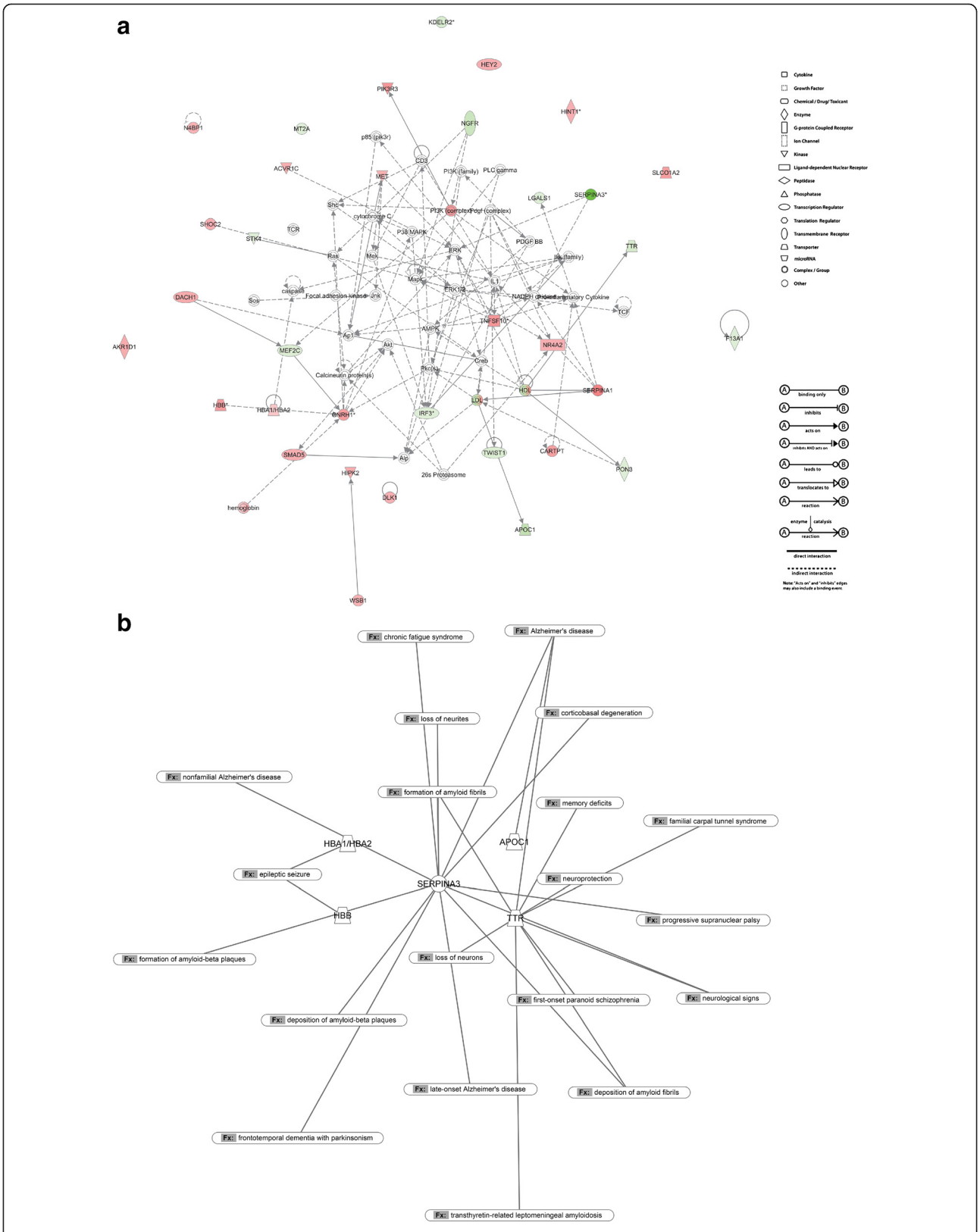

Figure 3 (See legend on next page.)

(See figure on previous page.)
Figure 3 Identification of biologically relevant networks. (a) Top ranking network generated by mapping the focus genes that were differentially expressed in infected animals. Pathway analysis based on the Ingenuity Pathway Knowledge Base (IPKB) is shown. Color shading corresponds to the type of dysregulation: red for up-regulated and green for down-regulated genes according to the microarray fold change calculation method. White open nodes are not from the list of 300 DEGs, but are transcription factors that are associated with the regulation of some of these genes identified by IPKB. The shape of the node indicates the major function of the protein. A line denotes binding of the products of the two genes, while a line with an arrow denotes 'acts on'. A dotted line denotes an indirect interaction. **(b)** Schematic representation of nervous system-related functions for selected DEGs. The most regulated/interesting DEGs were selected and associated to known nervous system-related functions according to the Ingenuity Pathway Knowledge Base (IPKB) software.

relationship with one of the previously selected genes of the hemoglobin complex (*HBB*), as revealed in the top ranking network from the IPA® analysis (Figure 3a). In summary, we designed RT-qPCR assays for 19 genes (Table 2) and most of them were already known to be involved in neurodegenerative disorders or nervous system regulation, even though very few had been implicated in prion diseases. Among these, we were able to successfully analyze only 11 (reported in Table 3 together with 2 housekeeping genes, *ACTB* and *GAPDH*), since the RT-qPCR assays for the remaining 8 genes either showed too low expression (C_T > 35) or amplification of trace amounts of residual gDNA. Furthermore, because several gene names have changed since the first annotation was done, updated names from the latest Affymetrix® annotated library are provided in Additional file 2, together with the old ones.

In order to achieve optimal RT-qPCR conditions we performed titration of template and primers as well as optimization of cycling conditions using human cDNA from SH-SY5Y neuroblastoma cells (macaque cDNA was scarce). To assess the specificity of the chosen oligonucleotides prior to performing the quantitative assays, some reactions were carried out using macaque cDNA obtained from control animals to verify the correct amplicon length. Two housekeeping genes, *GAPDH* and *ACTB* [61], were used as reference genes to normalize RT-qPCR data. Both genes were monitored across samples derived from infected and control macaques in order to evaluate their expression stability, yielding very similar results (Additional file 3).

At this point we performed the quantitative analysis and in general we observed large intra-assay variability for most genes across different samples, both for infected

Table 2 Candidate genes for validation

Gene	Accession number	Known relation with PrP/nervous system	References
AKR1C1	NM_001195574.1	Putative role in myelin formation	[43]
HBB	NM_001164428.1	Putative role in intraneuronal oxygen homeostasis, reduced in Alzheimer's and Parkinson's disease	[44]
NCAM1	XM_001083697.2	PrP/N-CAM complexes found in prion infected N2a cells	[45]
NR4A2	NM_001266910.2	Mutations related to dopaminergic dysfunction, including Parkinson schizophrenia and depression	[46,47]
USP16	NM_001260999.2	Depletion of USP16 prevented ATMi from restoring transcription after DSB induction	[48]
CALB1	XM_001085269.2	Plays a protective role in neurodegenerative disorders (depleted in HD)	[49]
DACH1	XM_001082371.2	Required for normal brain development	[50]
LXN	NM_001266988.1	Marker for the regional specification of the neocortex	[51]
PIK3R3	NM_001266826.1	Linked to β-amyloid plaque formation in AD brain	[52]
SAP18	NM_001261034.1	Possibly related to AD	[53]
SERPINA3	NM_001195350.1	Increased in schizophrenia, SNPs affecting onset and duration of AD	[54,55]
TNFSF10	NM_001266034.1	Implicated in pathogenesis of MS (causing demyelination)	[56]
HBA2	NM_001044724.1	Putative role in intraneuronal oxygen homeostasis, reduced in Alzheimer's and Parkinson's diseases	[44]
GNRH1	NM_001195436.1	Key regulator of the reproductive neuroendocrine system in vertebrates	[57]
IRF3	NM_001135797	Putative protective role against prion infection	[58]
APOC1*	AK240617.1	Binds to ApoE, risk factor for Alzheimer's disease	[59]
TM7SF3	XM_001099269.2	-	-
MYBPC1	XM_001091952.1	-	-
TTR	NM_001261679	Amyloid neuropathies, interaction with Aβ	[60]

List of 19 identified genes selected on the basis of fold change value and known relevance for neurodegeneration. Because of very low signal (*LXN, PIK3R3, TNFSF10, GNRH1*) or lack of reliable sequence data (*CALB1, DACH1, TM7SF3, MYBPC1*), only 11 genes (in bold) were successfully analyzed. **Macaca fascicularis* transcript.

Table 3 Genes analyzed by RT-qPCR

Gene	Chromosome	Primer sequence		Amplicon length (bp)	Accession number
ACTB	3	F:	GTTGCGTTACACCCTTTCTTG	146	NM_001033084.1
		R:	CTGTCACCTTCACCGTTCC		
GAPDH	11	F:	CCTGCACCACCAACTGCTTA	74	NM_001195426.1
		R:	CATGAGTCCTTCCACGATACCA		
AKR1C1	9	F:	CCGCCATATTGATTCTGCTCAT	132	NM_001195574.1
		R:	TGGGAATTGCACCAAAGCTT		
HBB	14	F:	GTCCTCTCCTGATGCTGTTATG	102	NM_001164428.1
		R:	TTGAGGTTGTCCAGGTGATTC		
NCAM1	14	F:	GAGCAAGAGGAAGATGACGAG	150	XM_001083697.2
		R:	GACTTTGAGGTGGATGGTCG		
NR4A2	12	F:	CCAGTGGAGGGTAAACTCATC	145	NM_001266910.2
		R:	AGGAGAAGGCAGAAATGTCG		
USP16	3	F:	GCAGAACTTGTCACAAACACC	146	NM_001260999.2
		R:	CTAAAGTAAGAGGGCCTGGAG		
SAP18	17	F:	GGAAATGTACCGTCCAGCGA	109	NM_001261034.1
		R:	TGCCCTTCTTTCTAGCTTCTGG		
SERPINA3	7	F:	GCTGGGCATTGAGGAAGTCT	123	NM_001195350.1
		R:	GTGCCCTCCTCAGACACATC		
HBA2	20	F:	CGACAAGAGCAACGTCAAGG	126	NM_001044724.1
		R:	TCGAAGTGGGGGAAGTAGGT		
IRF3	19	F:	TGGGTTGTGTTTAGCAGAGG	90	NM_001135797
		R:	GAAAAGTCCCCAACTCCTGAG		
APOC1*	19	F:	TTCTGTCGATGGTCTTGGAAG	138	AK240617.1
		R:	CACTCTGTTTGATGCGGTTG		
TTR	18	F:	TCACTTGGCATCTCCCCATTC	114	NM_001261679
		R:	GGTGGAATAGGAGTAGGGGCT		

Primers (F: forward and R: reverse) used for gene amplification, amplicon length and GenBank® accession numbers of the macaque cDNA sequences used for primer design. All primers were designed according to the genome sequence of *Macaca mulatta*.
*Apolipoprotein C-I (*APOC1*) primers were designed according to the genome sequence of *Macaca fascicularis* because the *Macaca mulatta* mRNA sequence was not annotated (TSA *Macaca mulatta* Mamu_450725, accession number: JV045807.1). Homology between the two sequences was 99%.

(Additional file 4) and for control animals (Additional file 5). Interestingly, we found a completely different expression pattern for B6, the only orally-infected sample, compared to the intracranially infected animals, except for a couple of genes (*AKR1C1*, *NCAM1*), suggesting that the route of infection might play a role in determining the gene expression changes (Additional file 6). Therefore we decided to rerun the microarray clustering analysis excluding this animal in order to verify its influence on the final results. As shown in Additional file 7, the comparison of the clustering analysis with (panel A) and without (panel B) the orally challenged animal B6 does not show marked differences.

Using SYBR® Green-based RT-qPCR we confirmed the statistically significant up-regulation of *TTR* (FC = 7.11), *SERPINA3* (FC = 18.73) and *APOC1* (FC = 6.33) as well as the down-regulation of *HBB* (FC = 0.19) and *HBA2* (FC = 0.22), normalizing the data against *GAPDH* (Figure 4). Similar results were obtained against *ACTB* (Additional file 8). For all the other genes the RT-qPCR results confirmed the regulation trend of the microarrays, but without statistical significance (p-value > 0.05).

In order to confirm the SYBR® Green -based results we performed an additional RT-qPCR analysis using FAM-labeled TaqMan® probes, providing more sensitive and specific detection signals for those genes that showed a significant fold change. Using this approach we confirmed the regulation of *SERPINA3*, *APOC1*, *HBB* and *HBA2*, but not of *TTR*, which showed comparable trends in FC but lost statistical significance (Figure 5). This may be due to higher variability among triplicates, caused by C_T values higher than 35 obtained with the TaqMan® probe chemistry compared to SYBR® Green detection system (Additional file 9).

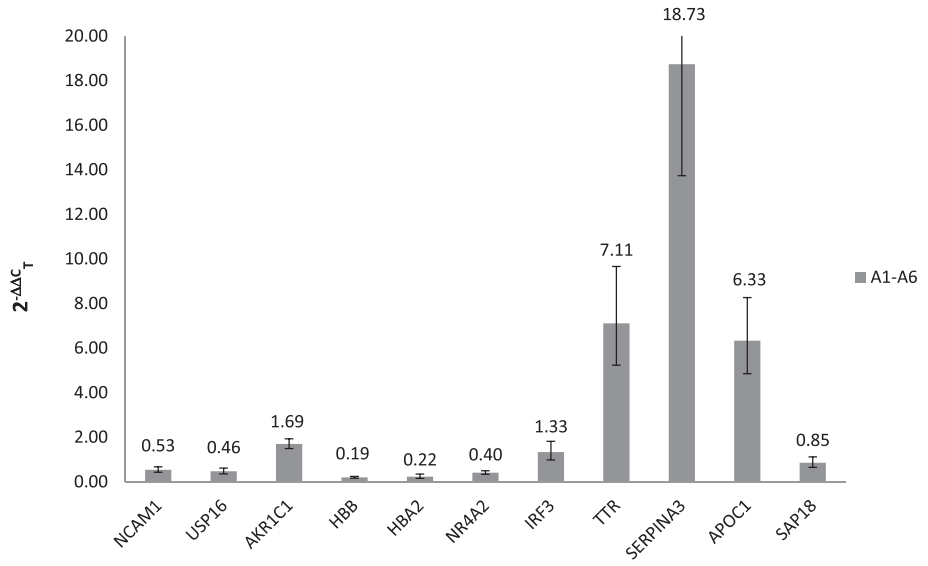

Figure 4 SYBR® Green-based RT-qPCR validation of microarray results. Relative expression levels of 11 genes normalized against *GAPDH* in BSE-infected cynomolgus macaques.

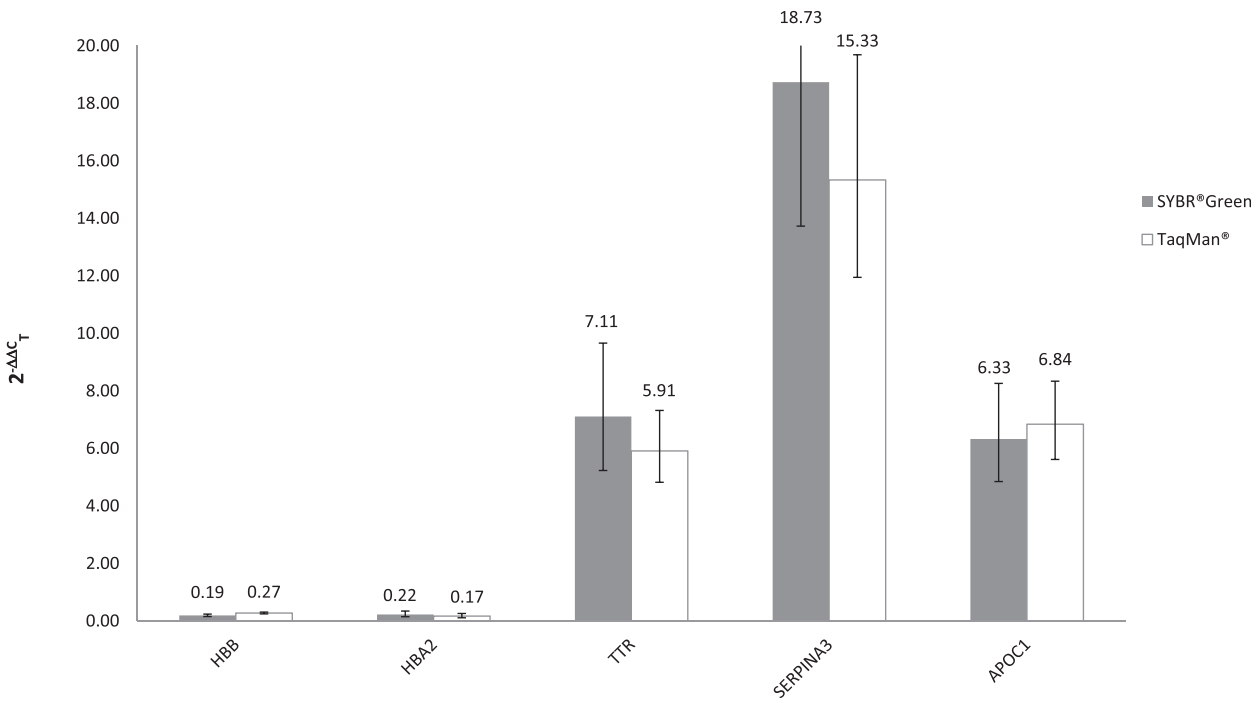

Figure 5 Comparison between SYBR® Green-based and TaqMan® probe-based results. TaqMan® (white) versus SYBR® Green-based (grey) expression levels for each transcript. Both detection systems yielded similar results. Data are normalized against *GAPDH*. Similar results were obtained with normalization against *ACTB* (data not shown).

Table 4 RT-qPCR confirmation of microarray results

Gene symbol	Microarray fold change			RT-qPCR fold change			
				SYBR® Green		TaqMan®	
	Min	Max	Mean	FC	P value	FC	P value
AKR1C1	2.3	2.9	2.5	1.7	0.433	2.4	0.235
HBB	−2.2	−2.6	−2.4	0.2	0.020	0.3	0.021
NCAM1	−1.1	2.5	−0.3	0.5	0.160	-	-
NR4A2	1.1	−2.1	−1.6	0.4	0.248	-	-
USP16	−1.2	−5.5	−2.6	0.5	0.308	-	-
SAP18	−1.2	−2.6	−1.7	0.8	0.393	-	-
SERPINA3	10.0	16.0	13.0	18.7	0.0001	15.3	0.0005
HBA2	-	-	-	0.2	0.041	0.2	0.019
IRF3	2.0	2.1	2.0	1.3	0.123	-	-
APOC1	4.3	-	4.3	6.3	0.047	6.8*	0.028*
TTR	3.1	-	3.1	7.1	0.025	5.9	0.076

Differential expression of selected genes analyzed by microarray and RT-qPCR. For microarray analysis, the lowest (Min), the highest (Max) and the average (Mean) fold change values of all the respective probes are shown. For RT-qPCR analysis, fold change (FC) and statistical significance (p-value) for both SYBR® Green and TaqMan® results are shown. In bold are the genes validated with statistical significance. HBA2 was not present in the array chip.
*Normalization performed vs. *ACTB* only.

In general, we were able to confirm the results of the array platform obtaining consistent fold change values for all genes analyzed, even though we validated with statistical significance using the specific TaqMan® detection system only four of them: *HBB, HBA2, APOC1, SERPINA3* (see Table 4 for details on p-values and FC).

In addition, dealing with animals whose brain material isolation may be susceptible to blood contamination, and as several works in the last few years have shown the presence of active transcription within human red blood cells [62], we decided to analyze the samples also for expression of some erythrocyte markers, such as *ALAS2* and *RHAG*, in order to verify the reliability of the results related to the regulation of both chains of hemoglobin (*HBB* and *HBA2*). Although the array data for these genes suggested a negligible and virtually identical presence of blood in both control and infected samples, RT-qPCR analysis revealed a small blood contamination ($C_T \geq 34$ for *ALAS2*, $C_T \geq 36$ for *RHAG*) within two samples, one control (CovD1) and one infected sample (A4) (Additional file 10 and Additional file 11). In light of these results, we performed an additional gene expression analysis for *HBB* and *HBA2* excluding these two samples. As expected, we obtained slightly different results (FC ~ 0.3 for *HBB* and 0.2 for *HBA2* using TaqMan® probes), but a relevant down-regulation still persisted with statistical significance.

Discussion

The precise mechanisms regulating the molecular processes that lead to neurodegeneration in TSEs remain unknown. Genomic approaches represent unbiased and powerful tools to uncover the molecular basis of these complex mechanisms and they may also contribute to discover new biomarkers for these diseases. Several studies have presented genomic analyses of brain tissues from animal models of TSE; a few of them involved the mRNA profiling of cattle BSE [23,25-27] or ovine scrapie [4,19-22,63] whereas the vast majority was performed on rodent-adapted models of prion disease [13-18,64]. In several of these prion-infected mice, genomic expression profiles revealed the induction of oxidative and endoplasmic reticulum (ER) stress, activated ER and mitochondrial apoptosis pathways as well as activated cholesterol biosynthesis in the CNS of preclinical mice [64].

We report here the first large-scale transcriptome analysis of the superior frontal gyrus of BSE-infected macaques. This region was selected based on its histopathological and functional relevance in the majority of neurodegenerative disorders [65] and because it corresponds to Brodmann areas 10 and 11, known to be involved in strategic processes in memory recall, various executive functions as well as in planning, reasoning, and decision making [66], all processes known to be disturbed by neurodegeneration. In general, RT-qPCR results confirmed the regulation trend seen in the microarray platform for all the 11 genes analyzed with very similar values using either *GAPDH* or *ACTB* for normalization. For five of them (*HBB*, *HBA2*, *TTR*, *SERPINA3*, *APOC1*) we obtained statistical significance with one or both qPCR detection systems utilized in this study (SYBR® Green and TaqMan® probes) and some of them were involved in the top two canonical pathways identified during the functional classification reported in the Results section: *APOC1* and *TTR* are part of the LXR/RXR activation pathway, which is associated with lipid metabolism and transport, whereas *SERPINA3* and *TTR* are involved in the acute phase response signaling pathway. All the other genes seemed to fall in the grey zone of both platforms and therefore their FC values could not be considered reliable.

When validating the array results by RT-qPCR, the first evidence obtained was a marked variability among the samples of the same group, either control or infected animals. Unlike other animal models, nonhuman primates are usually not inbred. Therefore, differences in the genomic background of the animals in our study may have contributed to the variability in the time of disease onset [33] and in gene expression within the same group. Paradoxically, for some genes that resulted strongly regulated (*APOC1*, *HBB*, *HBA2*) the variability resulted even more accentuated within the control group

if compared to that of the infected group. The experimental and control animals were housed in different animal facilities and this may have generated slight differences in diet and/or housing conditions that may have contributed to the above-mentioned effect.

We also reported a peculiar dysregulation pattern of the orally infected sample (B6) for several genes, showing a completely opposite trend compared to intracranially infected animals. Although no data are available for PrP^{Sc} deposition in brain or other tissues of this animal, the significantly longer incubation period (1950 days compared to an average of 1100 days for the other animals) could suggest a correlation between the mRNA expression profile and the route of infection [67]. Nonetheless, this different pattern may be due to the age difference at the time of euthanasia: 7.1 +/− 0.7 years for the intracranially infected macaques versus 9.9 years for the orally infected animal.

Concerning hemoglobin (Hb), a few years ago its expression was unexpectedly discovered in mesencephalic dopaminergic neurons of different mouse strains, as well as in rats and humans affected by Parkinson's disease (PD) and multiple sclerosis (MS) [68-70].

Hb expression is known to decrease in neurons of PD, Alzheimer's disease (AD), argyrophilic grain disease (AGD) and dementia with Lewy bodies (DLB) brains [44] as well as in the CNS of scrapie-infected mice [13,14]. Also, it has been shown that Hb binds to Aβ enhancing its aggregation and co-localizes in amyloid plaques in AD brains [71]. If we consider a possible similar interaction with β-rich PrP^{Sc} isoforms in prion diseases, we can hypothesize that in our animal model down-regulated Hb fails to promote aggregation of the prion protein, thus leading to a higher presence of toxic species like oligomers [72]. Moreover, in PD it has been hypothesized that Hb may act as oxygen storage molecule in oligodendrocytes [68]. Oxygen would be later released to neighboring neurons in hypoxia conditions to maintain the aerobic metabolism [68,69]. When down-regulated, Hb would not be available for this function and cells would be damaged by the defective oxygen homeostasis. Our results indicated a strong down-regulation (about 70-80% lower expression than normal) of both *HBB* and *HBA2* in symptomatic advanced-stage BSE-infected macaques. The data were analyzed with a very stringent procedure after excluding any major effect of potential blood contamination, thus confirming the robustness of the results.

Taken together, all these data indicate a possible general role for hemoglobin in neurodegenerative disorders, possibly related to an alteration of O_2 homeostasis and oxidative metabolism [68]. One point that needs further investigation is whether this alteration (down-regulation) occurs as an early/late consequence of the disease, or may act as a susceptibility factor that influences the onset of the pathology. Furthermore, future studies may investigate the localization of the observed down-regulation in terms of cell population: it could involve neurons as well as astrocytes or microglia.

Another crucial molecule, APOC1, was significantly up-regulated in BSE-infected brains samples compared to controls. Apolipoprotein C-I, whose gene *APOC1* is part of the APOE/C-I/C-IV/C-II gene cluster, (apoC-I) is a small 6.6 kDa component of lipoproteins (mainly HDL) that is known to inhibit receptor-mediated lipoprotein clearance, especially particles containing apoE [73]. Increasing evidence indicates a role for this gene in neurodegenerative disorders, especially in AD and MS [74-76]. A disruption in lipid metabolism and signaling is one of the early alterations apparent in many neurodegenerative diseases, including prion diseases [77,78]; indeed, cholesterol metabolites are investigated by a number of studies aimed at the identification of early biomarkers for neurodegenerative disorders [79-81]. Several genes involved in cholesterol metabolism and lipid biosynthesis have been found to be up-regulated in preclinical scrapie-infected mice [64]. Since APOC1 is able to activate cholesterol esterification via lecithin-cholesterol acyltransferase [75], its up-regulation could lead to an increase in cholesterol biosynthesis, consistent with the concomitant presence of prion disease. In fact, *in vitro* studies have shown that depletion of cellular cholesterol reduces the conversion of PrP^{C} to PrP^{Sc} [82] and evidence exists also in AD, where altered cholesterol metabolism has been found [83]. Hypercholesterolemia has also been shown to influence amyloid precursor protein processing [84]. One explanation for altered cholesterol homeostasis affecting prion disease development could lie in the fact that PrP is localized in cholesterol-rich lipid rafts [85].

SERPINA3, a serpin peptidase inhibitor involved in acute phase response pathways, is another gene that we found highly regulated in our animal model. It is extensively reported to be regulated in other neurodegenerative disease models and in particular it is well known to interact with APP to promote amyloid plaque formation — a hallmark of AD [86]. Indeed, increased levels of SERPINA3 have been found in the brain and peripheral blood of AD patients [87], mainly due to persistent and almost chronic inflammation [88]. In prion disease studies, SERPINA3 was found increased in brains of scrapie-infected mice [77], in mice infected with RML prior to clinical onset [89] as well as in urine and cerebrospinal fluid of CJD patients [90]. Being an acute phase protein, its up-regulation is explained by the onset of an inflammatory condition, particularly as a response of the innate immune system [91]. Interestingly, two β-sheets of SERPINA3 exhibit a polymorphism mimicking changes in

the serpin structure that normally occur during the formation of its stable complex with the target proteinase. In this conformation, SERPINA3 can bind Aβ, thus imposing a β-strand conformation that upon dissociation leads to a faster formation of fibrils [86]. Therefore, an intriguing hypothesis may be envisioned in which PrP conversion into β-sheet conformation can be assisted by SERPINA3, which would accelerate the formation of toxic species like PrP oligomers.

Transthyretin, a protein in the same pathway of acute phase response as SERPINA3, was found to be up-regulated at the transcription level in our BSE-infected macaques according to the SYBR® Green assay. Even though we were not able to confirm the statistical significance using the TaqMan® assay, this gene seems to be of interest. Indeed, TTR, carrier of the thyroid hormone thyroxine (T_4) in serum and CSF, is associated with systemic amyloidosis in humans [92], but also with an anti-amyloidogenic effect preventing Aβ deposition in neuronal cell cultures [93]. Moreover, increased mRNA and protein levels have been shown in neurons from the AD mouse model 'APP23' and in human AD brain with a neuroprotective role [94,95]. Even in prion models *TTR* levels have been found strongly increased in the cortex of scrapie-infected mice [15]. Our study now provides indication that up-regulation of *TTR* may also be found in BSE-infected macaques, further reinforcing the hypothesis of a common mechanism in AD and TSEs. Taken together, these data may suggest innate immune system activation and inflammatory response in these diseases [96], leading to a sustained up-regulation of both *SERPINA3* and *TTR* genes simultaneously: *SERPINA3* as inflammation effect, *TTR* as attempt to neutralize the infectious agent preventing its deposition. However, analysis of the microarray data did not reveal relevant deregulation of other genes typically involved in neuroinflammation and/or immune response, such as cytokines and other mediators. Even though some authors have reported alteration of these pathways [97], in our array IL6, TNFα, GFAP and CD68 showed a fold change < |2|, suggesting that inflammatory responses may not be particularly severe in this model.

One last point that remains to be addressed is the expression of the prion protein gene itself (*PRNP* in humans) upon infection. Because of shortage of cDNA, we were not able to validate its levels in our samples. Nevertheless, our microarray data did not identify any changes between control and infected samples, at least at the mRNA level. This is in agreement with findings reported for BSE-infected cattle [3], but differs from the situation in sporadic CJD patients who show reduced mRNA expression [97]. Whether this disagreement is related to the host or the infectious agent needs to be explored.

Conclusions

To our knowledge, this is the first genome-wide expression study in the *gyrus frontalis superior* region of cynomolgus macaques inoculated with BSE. Using microarray and RT-qPCR technologies we identified a gene signature able to distinguish infected macaques from control animals. These results could be extremely helpful in understanding the progression of the disease, allowing for the identification of some key players which, if not being the cause of the onset, could be some of the target genes affected by the disease. Therefore, after deeper investigations to validate these targets at the protein level and confirm their specificity for prion diseases, they may be exploited as potential biomarkers to set up pre-clinical diagnostic tests.

In particular, our findings support the hypothesis of a potential shared mechanism underlying the onset and the development of all neurodegenerative disorders, as the majority of our DEGs are known to be involved in other diseases such as AD or PD. This is in concordance with very recent data supporting the idea of a unifying role of prions in these diseases in general and maybe a prion-like behavior for most neurodegenerative disorders [98]. Furthermore, some of the DEG transcripts we found are present also in blood (hemoglobin, transthyretin, serpin peptidase inhibitor) and among them hemoglobin exhibited decreased expression throughout the entire course of the infection, including preclinical time points, in mouse models. Therefore, there is the intriguing possibility to employ these "readily available" biomarkers for diagnostic purposes, especially if additional studies will confirm the expression level of the proteins encoded by these DEGs in brain and/or blood tissue.

In general, our results suggest that, in order to identify potential biomarkers and drug targets for prion diseases and other neurodegenerative disorders, a combination of various pathways has to be targeted, including oxygen homeostasis, lipid metabolism and inflammation response.

In summary, large-scale transcriptome analyses of human TSEs are rare [97,99] and primate models are a valid approach to better understand the mechanisms of these fatal diseases. Even with all the limitations discussed above, our BSE-infected macaques are, to our knowledge, the closest available model for human vCJD and these results, obtained with an unbiased methodology as the gene expression microarray technology, are contributing to shed some light on the molecular basis of TSEs as well as neurodegeneration as a whole.

Methods

Ethics statement

Ethics approval for the study was issued by the Lower Saxony Ministry for consumer protection and food safety (509.42502/08/07.98). Animal experimentation

was performed in accordance with section 8 of the German Animal Protection Law in compliance with EC Directive 86/609.

Samples

Samples were derived from six BSE-infected macaques, *Macaca fascicularis* (A1 to A6) that were intracranially inoculated with a single dose of 50 mg brain homogenate (10% wt/vol) [33,37]. One cynomolgus macaque (B6) was orally inoculated with the same material; inoculation was performed *per os*, as single dose.

Brain material from five age- and sex-matched non-infected cynomolgus macaques (CovA, CovB, CovC, CovD1, CovD2) was obtained from Covance Laboratory Münster GmbH and processed in an equivalent manner.

Tissue and RNA extraction

At autopsy of seven BSE-infected cynomolgus macaques at advanced stage of disease and five non-infected control animals, one hemisphere of the brain was sliced dorso-ventrally and snap-frozen on dry-ice plates. The *gyrus frontalis superior* region was macroscopically identified on the frozen tissue and removed via a biopsy stamp. Total RNA (RNA > 200 bases) was isolated by manually homogenizing the material with micro pestles (Kisker Biotech GmbH) in TRIzol (Invitrogen). RNA isolation was performed according to the supplier's instructions. Following RNA isolation, a DNase I digestion was performed using 1 unit of enzyme per μg RNA (Fermentas) for 30 min at 37°C, and heat inactivated for 5 min at 95°C followed by precipitation with Sodium Acetate/Ethanol. RNA was checked for quantity and purity on a Spectrophotometer 2000 (PEQLAB) and for integrity of the 18S and 28S ribosomal bands by capillary electrophoresis using the 2100 Bioanalyzer (Agilent Technologies).

Immunoblot analysis

PK-treated (50 μg/mL for 1 hour at 37°C) and untreated brain homogenates corresponding to 0.7 mg or 0.3 mg brain tissue, respectively, were separated on 12% Bis/Tris Acrylamide gels (NuPAGE, Invitrogen) and transferred to nitrocellulose membranes (Protran, Schleicher & Schüll, Germany). Detection of macaque PrP^{Sc} was performed using the monoclonal anti-PrP antibody 11C6 and a Peroxidase conjugated anti-mouse IgG-antibody (Sigma-Aldrich, Germany). Signal was visualized using a chemiluminescent substrate (Super Signal West Pico, Pierce) and high sensitivity films (Amersham). Densitometric analysis of PrP^{Sc} was performed using the Image J program 1.37v.

Microarray analysis using the GeneChip® Rhesus Macaque genome array

Samples were labeled using the GeneChip® 3'IVT Express Kit (Affymetrix®). Reverse transcription of RNA was performed using 500 ng of total RNA to synthesize first-strand cDNA. This cDNA was then converted into a double-stranded DNA template for transcription. *In vitro* transcription included a linear RNA amplification (aRNA) and the incorporation of a biotin-conjugated nucleotide. The aRNA was then purified to remove unincorporated NTPs, salts, enzymes, and inorganic phosphate. The labeled aRNA of each animal was fragmented (50–100 bp) and hybridized to a GeneChip® Rhesus Macaque Genome Array (Cat N° 900656; Affymetrix®). The degree of fragmentation and the length distribution of the aRNA were checked by capillary electrophoresis using the Agilent 2100 Bioanalyzer (Agilent Technologies).

The hybridization was performed for 16 h at 1 × *g* and 45°C in the GeneChip® Hybridization Oven 640 (Affymetrix®). Washing and staining of the arrays were performed on the Gene Chip® Fluidics Station 450 (Affymetrix®) according to the manufacturer's recommendations. The antibody signal amplification and washing and staining protocol were used to stain the arrays with streptavidin R-phycoerythrin (SAPE; Invitrogen). To amplify staining, SAPE solution was added twice with a biotinylated anti-streptavidin antibody (Vector Laboratories, Burlingame, CA, USA) staining step in-between. Arrays were scanned using the GeneChip® Scanner 3000 7G (Affymetrix®).

Microarray data analysis

Intensity data from the CEL. files were imported to the Partek® software including a quality control based on internal controls. All chips passed the quality control and were analyzed using the Limma package [100] of Bioconductor [101,102] and the Partek® software. The microarray data discussed in this paper were generated conforming to the MIAME guidelines and are deposited in the NCBI's Gene Expression Omnibus (GEO) database [103]. They are accessible through GEO series accession number GSE52436 (see section: Availability of supporting data).

The microarray data analysis consisted of the following steps: 1. quantile method normalization, 2. global clustering and PCA-analysis, 3. fitting the data to a linear model, 4. detection of differential gene expression and 5. over-representation analysis of differentially expressed genes. Quantile-normalization was applied to the log2-transformed intensity values as a method for between-array normalization to ensure that the intensities had similar distributions across arrays.

For cluster analysis, we used a hierarchical approach with the average linkage-method. Distances were measured as 1 - Pearson's Correlation Coefficient. The PCA was performed using the princomp-function in the Partek® software. To estimate the average group values for each gene and assess differential gene expression, a

simple linear model was fitted to the data, and group-value averages and standard deviations for each gene were obtained. To find genes with significant expression changes between groups, empirical Bayes statistics were applied to the data by moderating the standard errors of the estimated values [100].

P-values were obtained from the moderated t-statistic and corrected for multiple testing with the Benjamini–Hochberg method [104]. The p-value adjustment guarantees a smaller number of false positive findings by controlling the false discovery rate (FDR). For each gene, the null hypothesis, that there is no differential expression between degradation levels, was rejected when its FDR was lower than 0.05. Because no candidates appeared using FDR 0.05, we made the selection using another p-value (unadjusted p-value ≤ 0.005) and a fold change ≥ |2|.

Reverse transcription and RT-qPCR

Validation by quantitative reverse transcription real-time PCR (RT-qPCR) was performed using gene-specific primer pairs. cDNA synthesis was accomplished using 100 ng RNA, 10 ng random hexamer primer, 2 mM dNTPs, 0.5 U RNase inhibitor and 5 U reverse transcriptase (Bioline) in 1× reaction buffer. For each sample a negative control was carried along by omission of the reverse transcriptase (–RT control).

The cDNA was diluted 1:10 prior to RT-qPCR. Ten ng RNA equivalent was added to the reaction mix including 2× iQ™ SYBR® Green Supermix (Bio-Rad Laboratories, Inc.), 400 nM of the corresponding forward and reverse primer (Sigma), and quantified in technical triplicates on an iQ5 Multicolor Real-Time PCR Detection System (Bio-Rad Laboratories, Inc.). All primers used for RT-qPCR are listed in Table 3.

After initial denaturation for 3 min at 95°C, 45 cycles were performed at 95°C for 15 sec and 58°C for 1 min. Differential gene expression of candidates was normalized to *GAPDH* and *ACTB* expression. –RT controls were included in the plates for each primer pair and sample. The relative expression ratio was calculated using the $\Delta\Delta C_T$ method [105,106]. Significance was calculated with the unpaired student *t*-test ($p < 0.05$). Melting curve analysis and gel electrophoresis of amplification products were performed for each primer pair to verify that artificial products or primer dimers were not responsible for the signals obtained. Some results were further confirmed using TaqMan® MGB probes and iQ™ Multiplex Powermix (Bio-Rad Laboratories, Inc.). The primer sequences, the reaction setup and the cycling conditions were the same as described above.

The probe sequences used for the detection of specific targets were:

GAPDH: 5'-FAM CTGGCCAAGGTCATCCATGA-3';
ACTB: 5'-FAM-ACAAGATGAGATTGGCATGGC-3';
HBB: 5'-FAM-AAGTGCTTGGTGCCTTTAGTGATGG-3';
HBA2: 5'-FAM-TGGCGAGTATGGTGCGGAGG-3';
SERPINA3: 5'-FAM-TTCCTGGCCCCTGTGATCCC-3';
TTR: 5'-FAM-ATCGTTGGCTGTGAATACCACCTCTG-3';
APOC1: 5'-FAM-TGGAGGACAAGGCTTGGGAAGTG-3'.

Availability of supporting data

The microarray data set supporting the results of this article is available in the Gene Expression Omnibus (GEO) repository, [http://www.ncbi.nlm.nih.gov/geo/query/acc.cgi?token=wnmjowqqhrcpzod&acc=GSE52436].

The DEGs were analyzed for their functions, pathways and networks using Ingenuity Pathways Analysis-IPA® [http://www.ingenuity.com/products/ipa/try-ipa-for-free].

Additional files

Additional file 1: List of 86 differentially expressed probe sets with p values ≤ 0.005 and FC ≥ |2|. Probe ID, Gene Symbol, Gene Name and RefSeq Transcript IDs annotation as of release 29 of the Affymetrix® Rhesus Annotation library (01/July/09). P-values and fold changes are reported for all 86 probe sets.

Additional file 2: List of 97 differentially expressed probe sets selected as RT-qPCR candidates. Probe IDs and Previous Gene Symbol annotation as of release 29 of the Affymetrix® Rhesus Annotation library (01/July/09). Current Gene Symbol annotation as of the latest Affymetrix® Rhesus Annotation library (release 32 - 09/June/11). Gene Name and RefSeq Transcript IDs as of Ensembl release 72 (June 2013). Annotation using alignment with the human genome has been performed (as stated in the gene name column) for the most highly regulated probe sets with unknown macaque annotation. P-values and fold changes are reported for all genes.

Additional file 3: Evaluation of reference gene expression stability across non-infected and BSE-infected samples. For each sample, average values of absolute C_{Ts} (+/−SD) of triplicate wells for *GAPDH* (grey) and *ACTB* (white) are shown.

Additional file 4: ΔC_T values for all genes showing variability among BSE-infected samples. ΔC_T values (+/−SD) normalized against *GAPDH*. Very similar results were obtained with normalization against *ACTB* (data not shown).

Additional file 5: ΔC_T values for all genes showing variability among non-infected samples. ΔC_T values (+/−SD) normalized against *GAPDH*. Very similar results were obtained with normalization against *ACTB* (data not shown).

Additional file 6: $\Delta\Delta C_T$ values of selected genes in the infected samples. $\Delta\Delta C_T$ values (+/−SD) for *HBB*, NR4A2, *NCAM1*, *USP16* and *AKR1C1* normalized against *GAPDH* in the orally-infected animal B6 (white) compared to intracranially infected samples A1-A6 (grey). Only 5 genes were analyzed for animal B6 due to shortage of cDNA.

Additional file 7: Cluster analysis. Cluster analysis was performed using a hierarchical approach with the average linkage-method for all animals (panel A) or excluding the orally infected one, B6 (panel B).

Additional file 8: SYBR® Green-based RT-qPCR validation of microarray results. Relative expression levels of 11 genes in BSE-infected cynomolgus macaques normalized against *ACTB* as reference gene.

Additional file 9: Comparison between SYBR® Green -based and TaqMan® probe-based results for *TTR*. Average values of absolute C_{Ts} (+/− SD) of triplicate wells for *TTR* obtained with SYBR® Green (grey) and TaqMan® probe (white) detection methods in BSE-infected samples are shown.

Additional file 10: RT-qPCR analysis of blood specific marker *RHAG*. C_T values for the erythrocyte marker *RHAG* were monitored across BSE-infected (solid fill) and non-infected (dotted fill) samples. Human blood cDNA was used as positive control (gradient fill). Note that for almost all the samples C_T values were ≥ 35 therefore indicating a very low expression level. Primer sequence (3'-5'): RHAG: F = AGGCAAGCTCAA CATGGTTC, R = GGGTGAATTGCCATATCCGC.

Additional file 11: RT-qPCR analysis of blood specific marker *ALAS2*. C_T values for the erythrocyte marker *ALAS2* were monitored across BSE-infected (solid fill) and non-infected (dotted fill) samples. Human blood cDNA was used as positive control (gradient fill). Note that for almost all the samples C_T values were ≥ 35 therefore indicating a very low expression level. Primer sequence (3'-5'): ALAS2: F = TCCCTTCA TGCTGTCGGAAC, R = GAGCTAGGCAGATCTGTTTTGAA.

Abbreviations

RT-qPCR: Reverse transcriptase quantitative polymerase chain reaction; HBB: Hemoglobin, beta; HBA2: Hemoglobin, alpha 2; TTR: Transthyretin; APOC1: Apolipoprotein C-I; SERPINA3: serpin peptidase inhibitor, clade A (alpha-1 antiproteinase, antitrypsin), member 3; TSE: Transmissible spongiform encephalopathy; CJD: Creutzfeldt-Jakob disease; GSS: Gerstmann-Sträussler-Scheinker syndrome; FFI: Fatal familial insomnia; BSE: Bovine spongiform encephalopathy; CWD: Chronic wasting disease; FSE: Feline spongiform encephalopathy; PrP^{C}: Cellular prion protein; PrP^{Sc}: Scrapie prion protein; PRNP: Prion protein; ER: Endoplasmic reticulum; DEG: Differentially expressed gene; RIN: RNA integrity number; FDR: False discovery rate; IPA: Ingenuity pathways analysis; GAPDH: Glyceraldehyde-3-phosphate dehydrogenase; ACTB: Actin, beta; AKR1C1: Aldo-keto reductase family 1, member C1; NCAM1: Neural cell adhesion molecule 1; USP16: Ubiquitin specific peptidase 16; NR4A2: Nuclear receptor subfamily 4, group A, member 2; ALAS2: Aminolevulinate, delta-, synthase 2; RHAG: Rh-associated glycoprotein; FC: Fold change; Hb: Hemoglobin; SN: Substantia nigra; PD: Parkinson's disease; MS: Multiple sclerosis; AD: Alzheimer's disease; AGD: Argyrophilic grain disease; DLB: Dementia with Lewy bodies; Hpt: Haptoglobin; CNS: Central nervous system; HDAC: Histone deacetylase; APP: Amyloid beta precursor protein; PS1: Presenilin 1; RML: Rocky mountain laboratory; Aβ: Amyloid beta; HDL: High density lipoprotein; LDL: Low density lipoprotein; APOE: Apolipoprotein E; LOAD: Late onset Alzheimer's disease; IRF3: Interferon regulatory factor 3; vCJD: Variant Creutzfeldt-Jakob disease; DNase I: Deoxyribonuclease I; dNTP: 2'-deoxynucleoside 5'-triphosphate; MGB: Minor groove binder; PCA: Principal component analysis; PK: Proteinase K.

Competing interests

The authors declare that they have no competing interests.

Authors' contributions

MB conceived and designed the RT-qPCR validation studies, carried out the initial optimization experiments, supervised all the experiments as well as the data interpretation, and wrote the manuscript. SV carried out the functional classification of the DEGs, performed most of the RT-qPCR experiments with the related statistical analysis, and provided the initial draft of the manuscript. ACS performed RNA isolation and cDNA preparation of BSE-infected and non-infected brain material, and contributed to the drafting of the manuscript. JM performed the immunoblot analysis. DM provided tissues and contributed to the drafting of the manuscript. GSR and LO performed microarrays and primary data analysis. GL conceived and designed the whole project, contributed to the drafting of the manuscript and gave final approval of the version to be published. All authors read and approved the final manuscript.

Acknowledgements

The authors wish to thank Dr. Lisa Gasperini for the RT-qPCR initial technical support, Dr. Paolo Vatta for suggestions on primer design and useful discussions, and Prof. Stefano Gustincich for useful discussions. This work was supported by the European Regional Development Fund, Cross-Border Cooperation Italy–Slovenia, Programme 2007–2013, Strategic Project TRANS2CARE to GL and by the European Community's Seventh Framework Programme (FP7/2007–2013) under grant agreement n° 222887—the PRIORITY project to GL. Samples were derived from an EU study supported by grants QLK1-CT-2002-01096 and BMH4-CT-98-6029.

Author details

[1]Department of Neuroscience, Scuola Internazionale Superiore di Studi Avanzati (SISSA), Via Bonomea 265, 34136 Trieste, Italy. [2]Unit of Infection Models, German Primate Center, Kellnerweg 4, 37077 Göttingen, Germany. [3]Microarray Core Facility, University Medical Center Göttingen, Justus-von-Liebig-Weg 11, 37077 Göttingen, Germany. [4]Molecular and Cell Physiology, Hannover Medical School, Carl-Neuberg Str. 1, D-30625 Hannover, Germany.

Received: 13 January 2014 Accepted: 7 May 2014
Published: 5 June 2014

References

1. Prusiner SB: **Prions.** *Proc Natl Acad Sci U S A* 1998, **95**(23):13363–13383.
2. Colby DW, Prusiner SB: **Prions.** *Cold Spring Harbor Perspect Biol* 2011, **3**(1):a006833.
3. Tang Y, Xiang W, Hawkins SA, Kretzschmar HA, Windl O: **Transcriptional changes in the brains of cattle orally infected with the bovine spongiform encephalopathy agent precede detection of infectivity.** *J Virol* 2009, **83**(1):9464–9473.
4. Filali H, Vidal E, Bolea R, Marquez M, Marco P, Vargas A, Pumarola M, Martin-Burriel I, Badiola JJ: **Gene and protein patterns of potential prion-related markers in the central nervous system of clinical and preclinical infected sheep.** *Vet Res* 2013, **44**(3):14.
5. Basu U, Almeida LM, Dudas S, Graham CE, Czub S, Moore SS, Guan LL: **Gene expression alterations in rocky mountain elk infected with chronic wasting disease.** *Prion* 2012, **6**(3):282–301.
6. Basu U, Guan LL, Moore SS: **Functional genomics approach for identification of molecular processes underlying neurodegenerative disorders in prion diseases.** *Curr Genomics* 2012, **13**(5):369–378.
7. Legname G, Nguyen HO, Peretz D, Cohen FE, DeArmond SJ, Prusiner SB: **Continuum of prion protein structures enciphers a multitude of prion isolate-specified phenotypes.** *Proc Natl Acad Sci U S A* 2006, **103**(50):19105–19110.
8. Collinge J, Clarke AR: **A general model of prion strains and their pathogenicity.** *Science* 2007, **318**(5852):930–936.
9. Deleault NR, Piro JR, Walsh DJ, Wang F, Ma J, Geoghegan JC, Supattapone S: **Isolation of phosphatidylethanolamine as a solitary cofactor for prion formation in the absence of nucleic acids.** *Proc Natl Acad Sci U S A* 2012, **109**(22):8546–8551.
10. Deleault NR, Walsh DJ, Piro JR, Wang F, Wang X, Ma J, Rees JR, Supattapone S: **Cofactor molecules maintain infectious conformation and restrict strain properties in purified prions.** *Proc Natl Acad Sci U S A* 2012, **109**(28):E1938–E1946.
11. Miller MB, Wang DW, Wang F, Noble GP, Ma J, Woods VL Jr, Li S, Supattapone S: **Cofactor molecules induce structural transformation during infectious prion formation.** *Structure* 2013, **21**(11):2061–2068.
12. Benetti F, Gustincich S, Legname G: **Gene expression profiling and therapeutic interventions in neurodegenerative diseases: a comprehensive study on potentiality and limits.** *Expert Opin Drug Discov* 2012, **7**(3):245–259.
13. Booth S, Bowman C, Baumgartner R, Sorensen G, Robertson C, Coulthart M, Phillipson C, Somorjai RL: **Identification of central nervous system genes involved in the host response to the scrapie agent during preclinical and clinical infection.** *J Gen Virol* 2004, **85**(Pt 11):3459–3471.
14. Kim HO, Snyder GP, Blazey TM, Race RE, Chesebro B, Skinner PJ: **Prion disease induced alterations in gene expression in spleen and brain prior to clinical symptoms.** *Adv Appl Bioinform Chem* 2008, **1**:29–50.
15. Riemer C, Neidhold S, Burwinkel M, Schwarz A, Schultz J, Kratzschmar J, Monning U, Baier M: **Gene expression profiling of scrapie-infected brain tissue.** *Biochem Biophys Res Commun* 2004, **323**(2):556–564.
16. Xiang W, Windl O, Wunsch G, Dugas M, Kohlmann A, Dierkes N, Westner IM, Kretzschmar HA: **Identification of differentially expressed genes in scrapie-infected mouse brains by using global gene expression technology.** *J Virol* 2004, **78**(201):11051–11060.
17. Sorensen G, Medina S, Parchaliuk D, Phillipson C, Robertson C, Booth SA: **Comprehensive transcriptional profiling of prion infection in mouse models reveals networks of responsive genes.** *BMC Genomics* 2008, **9**:114.
18. Skinner PJ, Abbassi H, Chesebro B, Race RE, Reilly C, Haase AT: **Gene expression alterations in brains of mice infected with three strains of scrapie.** *BMC Genomics* 2006, **7**:114.

19. Filali H, Martin-Burriel I, Harders F, Varona L, Lyahyai J, Zaragoza P, Pumarola M, Badiola JJ, Bossers A, Bolea R: **Gene expression profiling and association with prion-related lesions in the medulla oblongata of symptomatic natural scrapie animals.** *PLoS One* 2011, **6**(5):e19909.
20. Hedman C, Lyahyai J, Filali H, Marin B, Serrano C, Monleon E, Moreno B, Zaragoza P, Badiola JJ, Martin-Burriel I, Bolea R: **Differential gene expression and apoptosis markers in presymptomatic scrapie affected sheep.** *Vet Microbiol* 2012, **159**(1-2):23–32.
21. Filali H, Martin-Burriel I, Harders F, Varona L, Serrano C, Acin C, Badiola JJ, Bossers A, Bolea R: **Medulla oblongata transcriptome changes during presymptomatic natural scrapie and their association with prion-related lesions.** *BMC Genomics* 2012, **13:**399.
22. Filali H, Martin-Burriel I, Harders F, Varona L, Hedman C, Mediano DR, Monzon M, Bossers A, Badiola JJ, Bolea R: **Gene expression profiling of mesenteric lymph nodes from sheep with natural scrapie.** *BMC Genomics* 2014, **15:**59.
23. Almeida LM, Basu U, Khaniya B, Taniguchi M, Williams JL, Moore SS, Guan LL: **Gene expression in the medulla following oral infection of cattle with bovine spongiform encephalopathy.** *J Toxic Environ Health A* 2011, **74**(2-4):110–126.
24. Khaniya B, Almeida L, Basu U, Taniguchi M, Williams JL, Barreda DR, Moore SS, Guan LL: **Microarray analysis of differentially expressed genes from Peyer's patches of cattle orally challenged with bovine spongiform encephalopathy.** *J Toxic Environ Health A* 2009, **72**(17-18):1008–1013.
25. Almeida LM, Basu U, Williams JL, Moore SS, Guan LL: **Microarray analysis in caudal medulla of cattle orally challenged with bovine spongiform encephalopathy.** *Genet Mol Res* 2011, **10**(4):3948–3962.
26. Tang Y, Xiang W, Terry L, Kretzschmar HA, Windl O: **Transcriptional analysis implicates endoplasmic reticulum stress in bovine spongiform encephalopathy.** *PLoS One* 2010, **5**(12):e14207.
27. Basu U, Almeida L, Olson NE, Meng Y, Williams JL, Moore SS, Guan LL: **Transcriptome analysis of the medulla tissue from cattle in response to bovine spongiform encephalopathy using digital gene expression tag profiling.** *J Toxic Environ Health A* 2011, **74**(2-4):127–137.
28. Panelli S, Strozzi F, Capoferri R, Barbieri I, Martinelli N, Capucci L, Lombardi G, Williams JL: **Analysis of gene expression in white blood cells of cattle orally challenged with bovine amyloidotic spongiform encephalopathy.** *J Toxic Environ Health A* 2011, **74**(2-4):96–102.
29. Race B, Meade-White KD, Miller MW, Barbian KD, Rubenstein R, LaFauci G, Cervenakova L, Favara C, Gardner D, Long D, Parnell M, Striebel J, Priola SA, Ward A, Williams ES, Race R, Chesebro B: **Susceptibilities of nonhuman primates to chronic wasting disease.** *Emerg Infect Dis* 2009, **15**(9):1366–1376.
30. Greenwood AD, Vincendeau M, Schmadicke AC, Montag J, Seifarth W, Motzkus D: **Bovine spongiform encephalopathy infection alters endogenous retrovirus expression in distinct brain regions of cynomolgus macaques (Macaca fascicularis).** *Mol Neurodegener* 2011, **6**(1):44.
31. Montag J, Hitt R, Opitz L, Schulz-Schaeffer WJ, Hunsmann G, Motzkus D: **Upregulation of miRNA hsa-miR-342-3p in experimental and idiopathic prion disease.** *Mol Neurodegener* 2009, **4:**36.
32. Herzog C, Riviere J, Lescoutra-Etchegaray N, Charbonnier A, Leblanc V, Sales N, Deslys JP, Lasmezas CI: **PrPTSE distribution in a primate model of variant, sporadic, and iatrogenic Creutzfeldt-Jakob disease.** *J Virol* 2005, **79**(22):14339–14345.
33. Montag J, Schulz-Schaeffer W, Schrod A, Hunsmann G, Motzkus D: **Asynchronous onset of clinical disease in BSE-infected Macaques.** *Emerg Infect Dis* 2013, **19**(7):1125–1127.
34. Tamguney G, Giles K, Glidden DV, Lessard P, Wille H, Tremblay P, Groth DF, Yehiely F, Korth C, Moore RC, Tatzelt J, Rubinstein E, Boucheix C, Yang X, Stanley P, Lisanti MP, Dwek RA, Rudd PM, Moskovitz J, Epstein CJ, Cruz TD, Kuziel WA, Maeda N, Sap J, Ashe KH, Carlson GA, Tesseur I, Wyss-Coray T, Mucke L, Weisgraber KH, *et al*: **Genes contributing to prion pathogenesis.** *J Gen Virol* 2008, **89**(Pt 7):1777–1788.
35. Lasmézas CI, Comoy E, Hawkins S, Herzog C, Mouthon F, Konold T, Auvré F, Correia E, Lescoutra-Etchegaray N, Salès N, Wells G, Brown P, Deslys J-P: **Risk of oral infection with bovine spongiform encephalopathy agent in primates.** *Lancet* 2005, **365**(9461):781–783.
36. Holznagel E, Yutzy B, Schulz-Schaeffer W, Kruip C, Hahmann U, Bierke P, Torres JM, Kim YS, Thomzig A, Beekes M, Hunsmann G, Loewer J: **Foodborne transmission of bovine spongiform encephalopathy to nonhuman primates.** *Emerg Infect Dis* 2013, **19**(5):712–720.
37. Yutzy B, Holznagel E, Coulibaly C, Stuke A, Hahmann U, Deslys JP, Hunsmann G, Lower J: **Time-course studies of 14-3-3 protein isoforms in cerebrospinal fluid and brain of primates after oral or intracerebral infection with bovine spongiform encephalopathy agent.** *J Gen Virol* 2007, **88**(Pt 22):3469–3478.
38. Cali I, Castellani R, Alshekhlee A, Cohen Y, Blevins J, Yuan J, Langeveld JP, Parchi P, Safar JG, Zou WQ, Gambetti P: **Co-existence of scrapie prion protein types 1 and 2 in sporadic Creutzfeldt-Jakob disease: its effect on the phenotype and prion-type characteristics.** *Brain* 2009, **132**(Pt 10):2643–2658.
39. Parchi P, Castellani R, Capellari S, Ghetti B, Young K, Chen SG, Farlow M, Dickson DW, Sima AA, Trojanowski JQ, Petersen RB, Gambetti P: **Molecular basis of phenotypic variability in sporadic Creutzfeldt-Jakob disease.** *Ann Neurol* 1996, **39**(6):767–778.
40. Antonell A, Llado A, Altirriba J, Botta-Orfila T, Balasa M, Fernandez M, Ferrer I, Sanchez-Valle R, Molinuevo JL: **A preliminary study of the whole-genome expression profile of sporadic and monogenic early-onset Alzheimer's disease.** *Neurobiol Aging* 2013, **34**(7):1772–1778.
41. Osada N, Uno Y, Mineta K, Kameoka Y, Takahashi I, Terao K: **Ancient genome-wide admixture extends beyond the current hybrid zone between Macaca fascicularis and M. mulatta.** *Mol Ecol* 2010, **19**(14):2884–2895.
42. Osada N, Hashimoto K, Kameoka Y, Hirata M, Tanuma R, Uno Y, Inoue I, Hida M, Suzuki Y, Sugano S, Terao K, Kusuda J, Takahashi I: **Large-scale analysis of Macaca fascicularis transcripts and inference of genetic divergence between M. fascicularis and M. mulatta.** *BMC Genomics* 2008, **9:**90.
43. Zhang Y, Dufort I, Rheault P, Luu-The V: **Characterization of a human 20alpha-hydroxysteroid dehydrogenase.** *J Mol Endocrinol* 2000, **25**(2):221–228.
44. Ferrer I, Gomez A, Carmona M, Huesa G, Porta S, Riera-Codina M, Biagioli M, Gustincich S, Aso E: **Neuronal hemoglobin is reduced in Alzheimer's disease, argyrophilic grain disease, Parkinson's disease, and dementia with Lewy bodies.** *J Alzheimers Dis* 2011, **23**(3):537–550.
45. Schmitt-Ulms G, Legname G, Baldwin MA, Ball HL, Bradon N, Bosque PJ, Crossin KL, Edelman GM, DeArmond SJ, Cohen FE, Prusiner SB: **Binding of neural cell adhesion molecules (N-CAMs) to the cellular prion protein.** *J Mol Biol* 2001, **314**(5):1209–1225.
46. Le WD, Xu P, Jankovic J, Jiang H, Appel SH, Smith RG, Vassilatis DK: **Mutations in NR4A2 associated with familial Parkinson disease.** *Nat Genet* 2003, **33**(1):85–89.
47. Xing G, Zhang L, Russell S, Post R: **Reduction of dopamine-related transcription factors Nurr1 and NGFI-B in the prefrontal cortex in schizophrenia and bipolar disorders.** *Schizophr Res* 2006, **84**(1):36–56.
48. Shanbhag NM, Rafalska-Metcalf IU, Balane-Bolivar C, Janicki SM, Greenberg RA: **ATM-dependent chromatin changes silence transcription in cis to DNA double-strand breaks.** *Cell* 2010, **141**(6):970–981.
49. Soontornniyomkij V, Risbrough VB, Young JW, Soontornniyomkij B, Jeste DV, Achim CL: **Hippocampal calbindin-1 immunoreactivity correlate of recognition memory performance in aged mice.** *Neurosci Lett* 2012, **516**(1):161–165.
50. Backman M, Machon O, Van Den Bout CJ, Krauss S: **Targeted disruption of mouse Dach1 results in postnatal lethality.** *Dev Dyn* 2003, **226**(1):139–144.
51. Liu Q, Yu L, Gao J, Fu Q, Zhang J, Zhang P, Chen J, Zhao S: **Cloning, tissue expression pattern and genomic organization of latexin, a human homologue of rat carboxypeptidase A inhibitor.** *Mol Biol Rep* 2000, **27**(4):241–246.
52. Silver M, Janousova E, Hua X, Thompson PM, Montana G, Alzheimer's Disease Neuroimaging I: **Identification of gene pathways implicated in Alzheimer's disease using longitudinal imaging phenotypes with sparse regression.** *NeuroImage* 2012, **63**(3):1681–1694.
53. Guttula SV, Allam A, Gumpeny RS: **Analyzing microarray data of Alzheimer's using cluster analysis to identify the biomarker genes.** *Int J Alzheimers Dis* 2012, **2012:**649456.
54. Saetre P, Emilsson L, Axelsson E, Kreuger J, Lindholm E, Jazin E: **Inflammation-related genes up-regulated in schizophrenia brains.** *BMC Psychiatry* 2007, **7:**46.
55. Kamboh MI, Minster RL, Kenney M, Ozturk A, Desai PP, Kammerer CM, DeKosky ST: **Alpha-1-antichymotrypsin (ACT or SERPINA3) polymorphism may affect age-at-onset and disease duration of Alzheimer's disease.** *Neurobiol Aging* 2006, **27**(10):1435–1439.

56. Mc Guire C, Beyaert R, van Loo G: **Death receptor signalling in central nervous system inflammation and demyelination.** *Trends Neurosci* 2011, **34**(12):619–628.
57. Stevenson TJ, Hahn TP, MacDougall-Shackleton SA, Ball GF: **Gonadotropin-releasing hormone plasticity: a comparative perspective.** *Front Neuroendocrinol* 2012, **33**(3):287–300.
58. Ishibashi D, Atarashi R, Fuse T, Nakagaki T, Yamaguchi N, Satoh K, Honda K, Nishida N: **Protective role of interferon regulatory factor 3-mediated signaling against prion infection.** *J Virol* 2012, **86**(9):4947–4955.
59. Lucatelli JF, Barros AC, Silva VK, Machado Fda S, Constantin PC, Dias AA, Hutz MH, de Andrade FM: **Genetic influences on Alzheimer's disease: evidence of interactions between the genes APOE, APOC1 and ACE in a sample population from the South of Brazil.** *Neurochem Res* 2011, **36**(8):1533–1539.
60. Li X, Buxbaum JN: **Transthyretin and the brain re-visited: is neuronal synthesis of transthyretin protective in Alzheimer's disease?** *Mol Neurodegener* 2011, **6:**79.
61. Noriega NC, Kohama SG, Urbanski HF: **Microarray analysis of relative gene expression stability for selection of internal reference genes in the rhesus macaque brain.** *BMC Mol Biol* 2010, **11:**47.
62. Kabanova S, Kleinbongard P, Volkmer J, Andree B, Kelm M, Jax TW: **Gene expression analysis of human red blood cells.** *Int J Med Sci* 2009, **6**(4):156–159.
63. Cosseddu GM, Andreoletti O, Maestrale C, Robert B, Ligios C, Piumi F, Agrimi U, Vaiman D: **Gene expression profiling on sheep brain reveals differential transcripts in scrapie-affected/not-affected animals.** *Brain Res* 2007, **1142:**217–222.
64. Brown AR, Rebus S, McKimmie CS, Robertson K, Williams A, Fazakerley JK: **Gene expression profiling of the preclinical scrapie-infected hippocampus.** *Biochem Biophys Res Commun* 2005, **334**(1):86–95.
65. Liang WS, Dunckley T, Beach TG, Grover A, Mastroeni D, Ramsey K, Caselli RJ, Kukull WA, McKeel D, Morris JC, Hulette CM, Schmechel D, Reiman EM, Rogers J, Stephan DA: **Altered neuronal gene expression in brain regions differentially affected by Alzheimer's disease: a reference data set.** *Physiol Genomics* 2008, **33**(2):240–256.
66. Koechlin E, Hyafil A: **Anterior prefrontal function and the limits of human decision-making.** *Science* 2007, **318**(5850):594–598.
67. Langevin C, Andreoletti O, Le Dur A, Laude H, Beringue V: **Marked influence of the route of infection on prion strain apparent phenotype in a scrapie transgenic mouse model.** *Neurobiol Dis* 2011, **41**(1):219–225.
68. Biagioli M, Pinto M, Cesselli D, Zaninello M, Lazarevic D, Roncaglia P, Simone R, Vlachouli C, Plessy C, Bertin N, Beltrami A, Kobayashi K, Gallo V, Santoro C, Ferrer I, Rivella S, Beltrami CA, Carninci P, Raviola E, Gustincich S: **Unexpected expression of alpha- and beta-globin in mesencephalic dopaminergic neurons and glial cells.** *Proc Natl Acad Sci U S A* 2009, **106**(36):15454–15459.
69. Richter F, Meurers BH, Zhu C, Medvedeva VP, Chesselet MF: **Neurons express hemoglobin alpha- and beta-chains in rat and human brains.** *J Comp Neurol* 2009, **515**(5):538–547.
70. Broadwater L, Pandit A, Clements R, Azzam S, Vadnal J, Sulak M, Yong VW, Freeman EJ, Gregory RB, McDonough J: **Analysis of the mitochondrial proteome in multiple sclerosis cortex.** *Biochim Biophys Acta* 2011, **1812**(5):630–641.
71. Johnson VE, Stewart W, Smith DH: **Traumatic brain injury and amyloid-beta pathology: a link to Alzheimer's disease?** *Nat Rev Neurosci* 2010, **11**(5):361–370.
72. Wu CW, Liao PC, Yu L, Wang ST, Chen ST, Wu CM, Kuo YM: **Hemoglobin promotes Abeta oligomer formation and localizes in neurons and amyloid deposits.** *Neurobiol Dis* 2004, **17**(3):367–377.
73. Cudaback E, Li X, Yang Y, Yoo T, Montine KS, Craft S, Montine TJ, Keene CD: **Apolipoprotein C-I is an APOE genotype-dependent suppressor of glial activation.** *J Neuroinflammation* 2012, **9:**192.
74. Ki CS, Na DL, Kim DK, Kim HJ, Kim JW: **Genetic association of an apolipoprotein C-I (APOC1) gene polymorphism with late-onset Alzheimer's disease.** *Neurosci Lett* 2002, **319**(2):75–78.
75. Petit-Turcotte C, Stohl SM, Beffert U, Cohn JS, Aumont N, Tremblay M, Dea D, Yang L, Poirier J, Shachter NS: **Apolipoprotein C-I expression in the brain in Alzheimer's disease.** *Neurobiol Dis* 2001, **8**(6):953–963.
76. Huang R, Hughes M, Mobley S, Lanham I, Poduslo SE: **APOE genotypes in African American female multiple sclerosis patients.** *Neurosci Lett* 2007, **414**(1):51–56.
77. Xiang W, Hummel M, Mitteregger G, Pace C, Windl O, Mansmann U, Kretzschmar HA: **Transcriptome analysis reveals altered cholesterol metabolism during the neurodegeneration in mouse scrapie model.** *J Neurochem* 2007, **102**(3):834–847.
78. Katsel P, Li C, Haroutunian V: **Gene expression alterations in the sphingolipid metabolism pathways during progression of dementia and Alzheimer's disease: a shift toward ceramide accumulation at the earliest recognizable stages of Alzheimer's disease?** *Neurochem Res* 2007, **32**(4-5):845–856.
79. Bach C, Gilch S, Rost R, Greenwood AD, Horsch M, Hajj GN, Brodesser S, Facius A, Schadler S, Sandhoff K, Beckers J, Leib-Mosch C, Schatzl HM, Vorberg I: **Prion-induced activation of cholesterogenic gene expression by Srebp2 in neuronal cells.** *J Biol Chem* 2009, **284**(45):31260–31269.
80. Gilch S, Bach C, Lutzny G, Vorberg I, Schatzl HM: **Inhibition of cholesterol recycling impairs cellular PrP(Sc) propagation.** *Cell Mol Life Sci* 2009, **66**(24):3979–3991.
81. Leoni V, Shafaati M, Salomon A, Kivipelto M, Bjorkhem I, Wahlund LO: **Are the CSF levels of 24S-hydroxycholesterol a sensitive biomarker for mild cognitive impairment?** *Neurosci Lett* 2006, **397**(1-2):83–87.
82. Taraboulos A, Scott M, Semenov A, Avrahami D, Laszlo L, Prusiner SB: **Cholesterol depletion and modification of COOH-terminal targeting sequence of the prion protein inhibit formation of the scrapie isoform.** *J Cell Biol* 1995, **129**(1):121–132.
83. Cutler RG, Kelly J, Storie K, Pedersen WA, Tammara A, Hatanpaa K, Troncoso JC, Mattson MP: **Involvement of oxidative stress-induced abnormalities in ceramide and cholesterol metabolism in brain aging and Alzheimer's disease.** *Proc Natl Acad Sci U S A* 2004, **101**(7):2070–2075.
84. Refolo LM, Malester B, LaFrancois J, Bryant-Thomas T, Wang R, Tint GS, Sambamurti K, Duff K, Pappolla MA: **Hypercholesterolemia accelerates the Alzheimer's amyloid pathology in a transgenic mouse model.** *Neurobiol Dis* 2000, **7**(4):321–331.
85. Patel NV, Forman BM: **Linking lipids, Alzheimer's and LXRs?** *Nucl Recept Signal* 2004, **2:**e001.
86. Janciauskiene S, Wright HT: **Inflammation, antichymotrypsin, and lipid metabolism: autogenic etiology of Alzheimer's disease.** *Bioessays* 1998, **20**(12):1039–1046.
87. Matsubara E, Hirai S, Amari M, Shoji M, Yamaguchi H, Okamoto K, Ishiguro K, Harigaya Y, Wakabayashi K: **Alpha 1-antichymotrypsin as a possible biochemical marker for Alzheimer-type dementia.** *Ann Neurol* 1990, **28**(4):561–567.
88. Akiyama H, Barger S, Barnum S, Bradt B, Bauer J, Cole GM, Cooper NR, Eikelenboom P, Emmerling M, Fiebich BL, Finch CE, Frautschy S, Griffin WS, Hampel H, Hull M, Landreth G, Lue L, Mrak R, Mackenzie IR, McGeer PL, O'Banion MK, Pachter J, Pasinetti G, Plata-Salaman C, Rogers J, Rydel R, Shen Y, Streit W, Strohmeyer R, Tooyoma I: **Inflammation and Alzheimer's disease.** *Neurobiol Aging* 2000, **21**(3):383–421.
89. Hwang D, Lee IY, Yoo H, Gehlenborg N, Cho JH, Petritis B, Baxter D, Pitstick R, Young R, Spicer D, Price ND, Hohmann JG, Dearmond SJ, Carlson GA, Hood LE: **A systems approach to prion disease.** *Mol Syst Biol* 2009, **5:**252.
90. Miele G, Seeger H, Marino D, Eberhard R, Heikenwalder M, Stoeck K, Basagni M, Knight R, Green A, Chianini F, Wuthrich RP, Hock C, Zerr I, Aguzzi A: **Urinary alpha1-antichymotrypsin: a biomarker of prion infection.** *PLoS One* 2008, **3**(12):e3870.
91. Cray C, Zaias J, Altman NH: **Acute phase response in animals: a review.** *Comp Med* 2009, **59**(6):517–526.
92. Hanna M: **Novel drugs targeting transthyretin amyloidosis.** *Curr Heart Fail Rep* 2014, **11**(11):50–57.
93. Cascella R, Conti S, Mannini B, Li X, Buxbaum JN, Tiribilli B, Chiti F, Cecchi C: **Transthyretin suppresses the toxicity of oligomers formed by misfolded proteins in vitro.** *Biochim Biophys Acta* 2013, **1832**(12):2302–2314.
94. Li X, Masliah E, Reixach N, Buxbaum JN: **Neuronal production of transthyretin in human and murine Alzheimer's disease: is it protective?** *J Neurosci* 2011, **31**(35):12483–12490.
95. Buxbaum JN, Ye Z, Reixach N, Friske L, Levy C, Das P, Golde T, Masliah E, Roberts AR, Bartfai T: **Transthyretin protects Alzheimer's mice from the behavioral and biochemical effects of Abeta toxicity.** *Proc Natl Acad Sci U S A* 2008, **105**(7):2681–2686.
96. McGeer PL, McGeer EG: **History of innate immunity in neurodegenerative disorders.** *Front Pharmacol* 2011, **2:**77.
97. Llorens F, Ansoleaga B, Garcia-Esparcia P, Zafar S, Grau-Rivera O, Lopez-Gonzalez I, Blanco R, Carmona M, Yague J, Nos C, Del Rio JA, Gelpi E, Zerr I,

Ferrer I: **PrP mRNA and protein expression in brain and PrP(c) in CSF in Creutzfeldt-Jakob disease MM1 and VV2.** *Prion* 2013, **7**(5):383–393.
98. Prusiner SB: **Cell biology. A unifying role for prions in neurodegenerative diseases.** *Science* 2012, **336**(6088):1511–1513.
99. Xiang W, Windl O, Westner IM, Neumann M, Zerr I, Lederer RM, Kretzschmar HA: **Cerebral gene expression profiles in sporadic Creutzfeldt-Jakob disease.** *Ann Neurol* 2005, **58**(2):242–257.
100. Smyth GK: **Linear models and empirical bayes methods for assessing differential expression in microarray experiments.** *Stat Appl Genet Mol Biol* 2004, **3**(1). Article3.
101. Gentleman RC, Carey VJ, Bates DM, Bolstad B, Dettling M, Dudoit S, Ellis B, Gautier L, Ge Y, Gentry J, Hornik K, Hothorn T, Huber W, Iacus S, Irizarry R, Leisch F, Li C, Maechler M, Rossini AJ, Sawitzki G, Smith C, Smyth G, Tierney L, Yang JY, Zhang J: **Bioconductor: open software development for computational biology and bioinformatics.** *Genome Biol* 2004, **5**(10):R80.
102. Irizarry RA, Hobbs B, Collin F, Beazer-Barclay YD, Antonellis KJ, Scherf U, Speed TP: **Exploration, normalization, and summaries of high density oligonucleotide array probe level data.** *Biostatistics* 2003, **4**(2):249–264.
103. Edgar R, Domrachev M, Lash AE: **Gene expression omnibus: NCBI gene expression and hybridization array data repository.** *Nucleic Acids Res* 2002, **30**(1):207–210.
104. Benjamini Y, Hochberg Y: **Controlling the false discovery rate - a practical and powerful approach to multiple testing.** *J Roy Stat Soc B Met* 1995, **57**(1):289–300.
105. Livak KJ, Schmittgen TD: **Analysis of relative gene expression data using real-time quantitative PCR and the 2(−Delta Delta C(T)) Method.** *Methods* 2001, **25**(4):402–408.
106. Winer J, Jung CK, Shackel I, Williams PM: **Development and validation of real-time quantitative reverse transcriptase-polymerase chain reaction for monitoring gene expression in cardiac myocytes in vitro.** *Anal Biochem* 1999, **270**(1):41–49.

doi:10.1186/1471-2164-15-434
Cite this article as: Barbisin *et al.*: Gene expression profiling of brains from bovine spongiform encephalopathy (BSE)-infected cynomolgus macaques. *BMC Genomics* 2014 **15**:434.